IMPACT STRESSES AND DEFORMATIONS IN SPHERICAL SHELLS

Final Report

to

National Aeronautics and Space Administration

(NASA Research Grant NGR-05-018-056)

Prepared by

N.E. Johnson

and

M.P. Bieniek

(Principal Investigator)

Department of Civil Engineering

University of Southern California

Los Angeles California 90007

February 1969

ABSTRACT

This report contains a study of the dynamic response of a spherical shell colliding with our elastic surface. The analysis is based on the membrane theory and the bending theory with transverse shear deformation taken into account. The fundamental properties of the stress waves in spherical shells are investigated. The solution of the impact problem is developed in the form of a natural mode series and by the method of characteristics.

TABLE OF CONTENTS

LIST OF TABLES

LIST OF ILLUSTRATIONS

Figure Page

LIST OF SYMBOLS

$A_n(\tau)$ = tangential displacement time function.

$B_n(\tau)$ = radial displacement time function.

$C_n(\tau)$ = rotation time function.

$c = \sqrt{\dfrac{E}{\rho(1-\nu^2)}}$ = equivalent sound velocity (inches/second).

$D_n(\tau)$ = radial load time function.

$D = \dfrac{Eh^3}{12(1-\nu^2)}$ = bending stiffness parameter (inch-pounds).

$d^*(\phi)$ = geometric relation (inches).

$d(\phi) = d^*/h$ = non-dimensional geometric relation.

$E_n(\tau)$ = tangential load time function.

E = modulus of elasticity (pounds/inch^2).

$F_n(\tau)$ = geometrical relation time function.

$F_i(\tau),\ i = 1,2,3$ = generalized modal expansion time function.

$G = K(1-\nu^2)\left(\dfrac{R}{h}\right)^2$ = non-dimensional impact surface stiffness parameter.

$G_i(\tau),\ i = 1,2,3$ = generalized modal expansion time function.

$G_i(n),\ i = 4, 5, 6$ = frequency constant.

h = shell thickness (inches).

$H_i(\tau),\ i = 1, 2, 3$ = generalized modal expansion time function.

K^* = impact surface stiffness parameter (pounds/inch^3).

$K = \dfrac{K^* h}{E}$ = non-dimensional impact surface stiffness parameter.

$k_s = \dfrac{6}{5}$ = transverse shear stress distribution coefficient.

$K_s = \sqrt{\dfrac{1-\nu}{2k_s}}$.

$L_n(\tau)$ = geometrical relation time function.

$M_n(\tau)$ = geometrical relation time function.

$M_\phi(\phi, t)$ = shell bending moment in ϕ direction (inch-pounds/inch).

$M_\theta(\phi, t)$ = shell bending moment in θ direction (inch-pounds/inch).

$m_\phi(\phi, \tau) = \left(\dfrac{1-\nu^2}{Eh^2}\right) M_\phi$ = non-dimensional shell bending moment in ϕ direction.

$m_\theta(\phi, \tau) = \left(\dfrac{1-\nu^2}{Eh^2}\right) M_\theta$ = non-dimensional shell bending moment in θ direction.

$N_n(\tau)$ = geometrical relation time function.

$N_\phi(\phi, t)$ = shell force in ϕ direction (pounds/

inch).

$N_\theta(\phi, t)$ = shell force in θ direction (pounds/inch).

$n_\phi(\phi,\tau)=\left(\frac{1-\nu^2}{Eh}\right)\left(\frac{R}{h}\right)N_\phi$ = non-dimensional shell force in ϕ direction.

$n_\theta(\phi,\tau)=\left(\frac{1-\nu^2}{Eh}\right)\left(\frac{R}{h}\right)N_\theta$ = non-dimensional shell force in θ direction.

n = mode number.

$p^*(\phi, t)$ = tangential load (pounds/inch^2).

$p(\phi,\tau) = p^*/E$ = non-dimensional tangential load.

$P(\phi,\tau)=(1-\nu^2)\left(\frac{R}{h}\right)^2 p$ = non-dimensional tangential load.

$P_n(x)$ = Legendre polynomial of the first kind.

$P_n^1(x)$ = Associated Legendre polynomial of the first kind.

$q^*(\phi, t)$ = radial load (pounds/inch^2).

$q(\phi,\tau) = q^*/E$ = non-dimensional radial load.

$Q(\phi,\tau)=(1-\nu^2)\left(\frac{R}{h}\right)^2 q$ = non-dimensional radial load.

$Q_\phi(\phi, t)$ = transverse shear force in ϕ direction (pounds/inch).

$q_\phi(\phi,\tau)=\left(\frac{1-\nu^2}{Eh}\right)\left(\frac{R}{h}\right)Q_\phi$ = non-dimensional transverse shear force in ϕ direction.

$Q_n(\tau)$ = tangential displacement time function.

$Q_n(x)$ = Legendre polynomial of the second kind.

$Q_n^1(x)$ = associated Legendre polynomial of the second kind.

$R_n(\tau)$ = radial displacement time function.

R = shell radius (inches).

$S_n(\tau)$ = rotation time function.

t = time (seconds).

$u^*(\phi, t)$ = tangential displacement (inches).

$u(\phi,\tau) = u^*/h$ = non-dimensional tangential displacement.

$U_n(\phi)$ = tangential displacement space function.

V_o = initial vertical velocity (inches/second).

$V_i(\phi,\tau)$, $i = 1, 8$ = non-dimensional variable defined in characteristic direction.

$w^*(\phi, t)$ = radial displacement (inches).

$w(\phi,\tau) = w^*/h$ = non-dimensional radial displacement.

$W_n(\phi)$ = radial displacement space function.

x = $\cos\phi$ (Note: This quantity is used interchangeably with ϕ as the argument of several variables).

$y^*(\phi, t)$ = impact surface displacement in the direction of w^* (inches).

$y(\phi,\tau) = y^*/h$ = non-dimensional impact surface

	displacement in the direction of w.
$Y_i(\phi, \tau),\ i = 1, 5$	= product of physical variables and ctn ϕ.
$\beta = V_o / c$	= non-dimensional initial vertical velocity.
β_ϕ	= rotation angle of shell element (radians).
$\beta_n(\phi)$	= rotation space function.
$\varepsilon = \frac{1}{12}\left(\frac{h}{R}\right)$	
$\eta_n(\tau)$	= radial displacement time function.
$\Theta_n(\tau)$	= rigid body motion time function.
$\lambda_i,\ i = 1, 8$	= function of n.
μ_n	= non-dimensional shell frequency.
ν	= Poisson's ratio.
ρ	= shell density (pound-seconds^2/inch^4).
$\tau = \frac{ct}{R}$	= non-dimensional time.
ϕ	= angle (radians).
$\phi_o^*(\tau)$ and $\phi_o(\tau)$	= angles denoting limits of contact area (radians).
$\Psi_n(\tau)$	= tangential displacement time function.
$\Phi_n(\tau)$	= tangential displacement time function.
$\Omega_n(\tau)$	= radial displacement time function.
ω_n	= non-dimensional shell frequency.

CHAPTER I

INTRODUCTION

General

In this investigation, the response of a complete spherical shell is determined as it impacts a special type of elastic surface. Small, elastic deformations are assumed to occur.

Solutions are obtained both for a shell theory which includes bending, shear, and rotatory inertia effects and for one which considers only extensional (membrane) effects. However, numerical computations are restricted to the membrane theory solutions.

The shell is assumed to have an initial vertical velocity just prior to impact. Since the shell is axisymmetric about the impact point, only axisymmetric loading and deformation parameters need be considered.

The impact surface is assumed to be of the type first introduced by E. Winkler in 1867 (5:1). The reaction forces of this surface are assumed proportional at every point to the radial deflection of the shell at that point.

Considering some practical applications (e.g., a granular medium), the nature of the impacted surface is not known and is probably very complicated. While the assumption used in this work is mathematically by far the simplest that one can make regarding the nature of a supporting elastic surface, the errors introduced are often minimal.

Previous Work in Problem Area

There are a considerable number of published papers on the dynamics of spherical shells. As discussed in a recent review by Kalnins (8), most of them deal with the problem of free vibrations. Of particular interest for this work is the solution to the free vibration membrane problem by Baker (1) and the discussion of spherical shells including shear and rotatory inertia effects by Prasad (12).

The problem of the response of a spherical shell to a harmonic forcing function has been studied by Wilkinson and Kalnins (15).

In a recent paper, Wilkinson, Capelli, and Salzman (16) studied the response of certain shells of revolution as they impacted water surfaces. This work did not consider the effects of stress wave propagation in the shell during impact. Furthermore, the shells studied numerically were shallow in nature and were not complete shells. The problem studied in this paper utilized a pressure-velocity boundary relation and consequently resulted in a solution of a considerably different nature than that studied here. The deflected shape of the shell was not too important in this problem since the water pressure was computed for a flat disc rather than a deformable body.

The problem of wave propagation in spherical shells has been studied in two limited applications. First, using membrane theory, Huth and Cole (6) have considered the waves produced by pressure loads on a spherical shell. Second, Medick (10) has considered the initial response of a shallow spherical shell to a concentrated force at the apex.

No prior solutions are available for the problem of the impact of a deep spherical shell against a rigid or a deformable surface.

Methods of Investigation

The theories used in this investigation assume a shell which is thin, of uniform thickness, and made of an elastic, isotropic, homogeneous material. The normal and tangential components of the inertia forces are considered. Within these assumptions, analyses are performed using membrane theory and bending and transverse shear theory.

Analyses are not performed using classical bending theory since the application of this theory results in stress waves of infinite velocity. Such an analysis would only be appropriate for times long enough after impact such that wave effects could be neglected.

The reason for infinite velocity stress waves when using bending theory can be explained in the following manner. The essential differences between bending and bending-shear theories is the omission of rotatory inertia effects and the assumption of infinite shear rigidity in the bending theory. With these omissions, the equations of the problem are no longer hyperbolic. It has been shown by Courant and Hilbert (3) and others that waves only propagate at finite velocities in systems defined by hyperbolic equations. It is noted that the membrane theory system of equations is hyperbolic (see Chapter IV for derivation).

The equations of the shell theory used in this research are essentially of the Love-Timoshenko type and generally conform to the equations used by Baker (1) and Prasad (12). The notation and development of these equations generally conform to that presented by Naghdi (11).

The most significant contribution of this work to the study of the dynamic behavior of spherical shells is the solution of a new boundary value problem. This problem, the problem of dynamic contact between an elastic spherical shell and an elastic surface, results in a time-dependent coupling between the contact stress and the displacements of both the shell and the impacted surface. The complex nature of the solutions requires the use of numerical methods and digital computer programs.

Solutions have been obtained using both the classical normal mode expansion method and the method of characteristics. The normal mode expansion method is best used to describe the response of the system at relatively long times after impact. To properly describe the behavior of the shell immediately after impact, the modal expansion method requires the use of a large number of normal modes.

The use of the method of characteristics has the advantage of accurately describing the behavior at the wave front within the limitations inherent in the use of numerical integration techniques. Both methods of solution give an identical description of the contact surface as a function of time.

Using membrane theory, both methods have been programmed on a digital computer. As shown later, reasonable correlation exists between the solutions although the computer time with the method of characteristics solution is significantly less.

The characteristics solution considering shear and rotatory inertia effects has been prepared. While this solution has not been programmed, the necessary numerical procedures have been described.

Applications and Possible Extensions

This work has several applications, particularly to the aerospace industry. One such application would lie in the design of a spherical capsule to survive touchdown on either the earth or some other planet when impacted with a high velocity.

Other applications might include the effect of landing impact on the behavior of internally mounted capsule components and the effect of pyrotechnically initiated transient loads on spacecraft components. In some of these applications one might have to come to some additional understanding of the behavior of a stress as it crosses the interface between a spherical shell surface and another structural shape.

A relatively simple extension to this work would be to include the effects of an internal pressure in the shell. With this solution, it might be of some interest to study the behavior of a basketball during the play of a basket-ball game. Perhaps some such study would result in the improvement of either the ball or the playing surface.

The theories developed in this study consider the effects of both radial and tangential shell loading where practical. Because of this, this work could easily be extended to consider the effects of a more refined impact surface. Such a surface might consist of either a different form of a Winkler surface or a surface with continuity (e.g., an elastic or inelastic half-space).

Shells with non-uniform properties could be studied. In fact, the method of characteristics solution as developed here could be applied to a symmetrical, non-uniform shell by making certain minor modifications to its computational procedure. A practical spacecraft capsule would have various components mounted internally to the shell. Such a system might be idealized for analytical purposes by lumping the component masses at various points on the shell.

Many sphèrical landing capsules under current study are not of spherical shape. Thus, a reasonable extension of this work would consider the study of shells of revolution with non-spherical geometries.

Other extensions to this work would consider the use of inelastic materials and finite deformations.

CHAPTER II

EQUATIONS OF THE PROBLEM

Equations of Motion of the Shell

In the following discussion, the equations of motion are presented for the axisymmetric motion of a spherical shell. A complete derivation of these equations and a discussion of the shell theory used is given in Appendix E. The effects of shear, bending, and rotatory inertia are considered in addition to the extensional effects.

The equations are written in the following form using the notation and sign convention shown in Figures 1 and 2.

$$\begin{aligned} N_{\phi,\phi} + (N_\phi - N_\theta)\,\mathrm{ctn}\,\phi + Q_\phi &= \rho h R \frac{\partial^2 u^*}{\partial t^2} - R p^* \\ Q_{\phi,\phi} + Q_\phi\,\mathrm{ctn}\,\phi - (N_\phi + N_\theta) &= \rho h R \frac{\partial^2 w^*}{\partial t^2} - R q^* \qquad (2.1) \\ M_{\phi,\phi} + (M_\phi - M_\theta)\,\mathrm{ctn}\,\phi - R Q_\phi &= \frac{1}{12} \rho h^3 R \frac{\partial^2 \beta_\phi}{\partial t^2} \end{aligned}$$

It is noted that equations 2.1 can be found using those presented by Prasad (12) and others if we assume axial symmetry and $h/R << 1$.

Equations 2.1 can also be found using the general theory developed by Naghdi (11). In this case we must make the additional assumptions that (a) the applied loads act on the middle surface of the shell and (b) the effect of transverse normal stress is neglected.

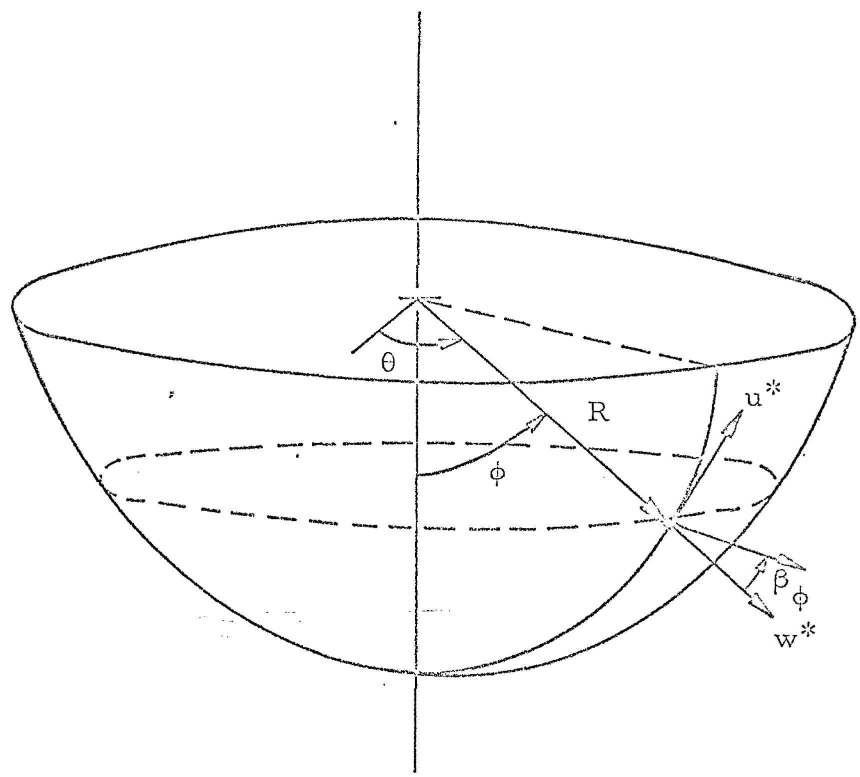

Figure 1. Coordinate System

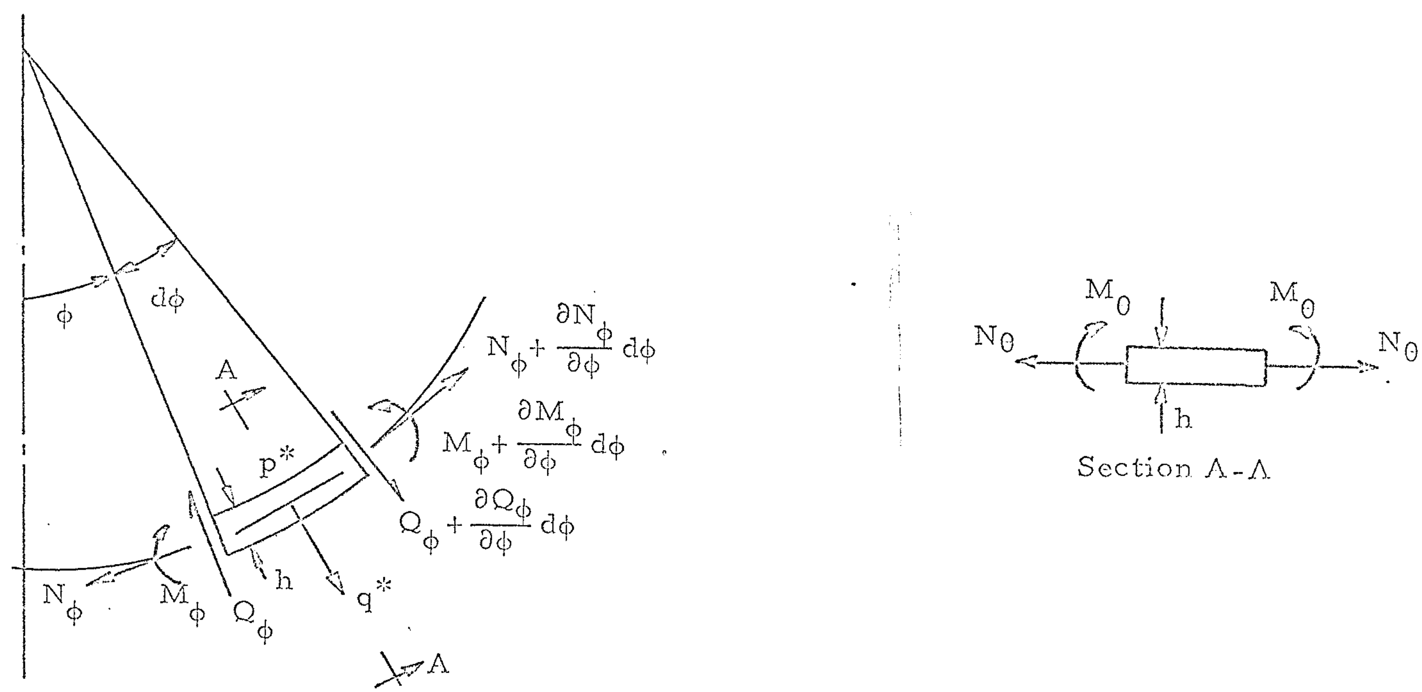

Figure 2. Sign Conventions

In the work which follows, equations 2.1 are generally used in the following non-dimensional form.

$$n_{\phi,\phi} + (n_\phi - n_\theta)\,ctn\,\phi + q_{b\phi} = u_{,\tau\tau} - P$$
$$q_{b\phi,\phi} + q_{b\phi}\,ctn\,\phi - (n_\phi + n_\theta) = w_{,\tau\tau} - Q \qquad (2.2)$$
$$m_{\phi,\phi} + (m_\phi - m_\theta)\,ctn\,\phi - q_b = \epsilon\beta_{\phi,\tau\tau}$$

where
$$m_\phi = \left(\frac{1-\nu^2}{Eh}\right)M_\phi$$
$$m_\theta = \left(\frac{1-\nu^2}{Eh}\right)M_\theta$$
$$n_\phi = \left(\frac{1-\nu^2}{Eh}\right)\left(\frac{R}{h}\right)N_\phi$$
$$n_\theta = \left(\frac{1-\nu^2}{Eh}\right)\left(\frac{R}{h}\right)N_\theta$$
$$q_{b\phi} = \left(\frac{1-\nu^2}{Eh}\right)\left(\frac{R}{h}\right)Q_\phi$$
$$u = u^*/h$$
$$w = w^*/h$$
$$P = (1-\nu^2)\left(\frac{R}{h}\right)^2\left(\frac{p^*}{E}\right)$$
$$Q = (1-\nu^2)\left(\frac{R}{h}\right)^2\left(\frac{q_b^*}{E}\right)$$
$$\tau = \frac{ct}{R}$$
$$\epsilon = \frac{1}{12}\left(\frac{h}{R}\right)$$
$$c^2 = \frac{E}{\rho(1-\nu^2)}$$

Stress-Displacement Relations for the Shell

As with the equations of motion, the stress-displacement or force- and moment-displacement relations for the shell can be either taken from the equations presented by Prasad (12) or developed from Naghdi's theory (11). These equations, which are derived in Appendix E, are written in the following form:

$$N_\phi = \left(\frac{Eh}{1-\nu^2}\right)\left(\frac{1}{R}\right)\left[u^*_{,\phi} + \nu u^* \operatorname{ctn}\phi + (1+\nu)w^*\right]$$

$$N_\theta = \left(\frac{Eh}{1-\nu^2}\right)\left(\frac{1}{R}\right)\left[u^* \operatorname{ctn}\phi + \nu u^*_{,\phi} + (1+\nu)w^*\right]$$

$$M_\phi = \frac{D}{R}\left(\beta_{\phi,\phi} + \nu\beta_\phi \operatorname{ctn}\phi\right) \qquad (2.3)$$

$$M_\theta = \frac{D}{R}\left(\beta_\phi \operatorname{ctn}\phi + \nu\beta_{\phi,\phi}\right)$$

$$Q_\phi = \left[\frac{Eh}{2(1+\nu)k_s}\right]\left(\frac{w^*_{,\phi}}{R} + \beta_\phi\right)$$

where $D = \dfrac{Eh^3}{12(1-\nu^2)}$

The non-dimensional form of equations 2.3 may be written as follows using the parameters previously defined after equations 2.2.

$$n_\phi = u_{,\phi} + \nu u \operatorname{ctn}\phi + (1+\nu)w$$

$$n_\theta = u \operatorname{ctn}\phi + \nu u_{,\phi} + (1+\nu)w$$

$$m_\phi = \varepsilon\left(\beta_{\phi,\phi} + \nu\beta_\phi \operatorname{ctn}\phi\right) \qquad (2.4)$$

$$m_\theta = \varepsilon\left(\beta_\phi \operatorname{ctn}\phi + \nu\beta_{\phi,\phi}\right)$$

$$q_{b\phi} = K_s^2\left[w_{,\phi} + \left(\frac{R}{h}\right)\beta_\phi\right]$$

where $K_s^2 = \dfrac{1-\nu}{2k_s}$

Equations of Motion in Terms of Displacements

Equations 2.2 and 2.4 are presented in a suitable form for a solution using the method of characteristics.

On the other hand the normal mode expansion method requires the use of a set of equations wherein the displacements (and applied loads) are the only variables.

The non-dimensional equations of motion found by combining equations 2.2 and 2.4 may be written in the following form:

$$
\begin{aligned}
& u_{,\phi\phi} + u_{,\phi} \operatorname{ctn}\phi - u(\nu + \operatorname{ctn}^2\phi) + (1+\nu) w_{,\phi} \\
& \qquad + K_s^2 \left[w_{,\phi} + \left(\tfrac{R}{h}\right)\beta_\phi \right] = u_{,\tau\tau} - P \\
& K_s^2 \left\{ w_{,\phi\phi} + \left(\tfrac{R}{h}\right)\beta_{\phi,\phi} + \left[w_{,\phi} + \left(\tfrac{R}{h}\right)\beta_\phi \right] \operatorname{ctn}\phi \right\} \\
& \qquad - (1+\nu)(u_{,\phi} + u \operatorname{ctn}\phi + 2w) = w_{,\tau\tau} - Q \\
& \beta_{\phi,\phi\phi} + \beta_{\phi,\phi} \operatorname{ctn}\phi - \beta_\phi(\nu + \operatorname{ctn}^2\phi) \\
& \qquad - \frac{1}{\varepsilon} K_s^2 \left[w_{,\phi} + \left(\tfrac{R}{h}\right)\beta_\phi \right] = \beta_{\phi,\tau\tau}
\end{aligned}
\tag{2.5}
$$

Membrane Theory

The various equations previously presented can be greatly simplified if we neglect shear, bending, and rotatory inertia effects. To do this we must assume that $m_\phi = q_{\phi\phi} = 0$. This assumption infers that $\varepsilon \approx K_s \approx 0$.

The resulting membrane theory equations are presented below. The equations of motion are taken from equations 2.2 and written

$$
\begin{aligned}
& n_{\phi,\phi} + (n_\phi - n_\theta) \operatorname{ctn}\phi = u_{,\tau\tau} - P \\
& -(n_\phi + n_\theta) = w_{,\tau\tau} - Q
\end{aligned}
\tag{2.6}
$$

The stress-displacement relations are taken from equations 2.4 and written

$$n_\phi = u_{,\phi} + \nu u \operatorname{ctn}\phi + (1+\nu)w$$
$$n_\theta = u \operatorname{ctn}\phi + \nu u_{,\phi} + (1+\nu)w \tag{2.7}$$

Equations 2.6 and 2.7 may be combined to form the following equations of motion in terms of displacements.

$$u_{,\phi\phi} + u_{,\phi}\operatorname{ctn}\phi - u(\nu + \operatorname{ctn}^2\phi) + (1+\nu)w_{,\phi} = u_{,\tau\tau} - P$$
$$-(1+\nu)(u_{,\phi} + u\operatorname{ctn}\phi + 2w) = w_{,\tau\tau} - Q \tag{2.8}$$

Load-Displacement Relation

The impact surface is defined as a surface that deforms under a radial shell load $q^*(\phi, t)$ in such a manner that

$$y^*(\phi, t) = -\frac{q^*(\phi, t)}{K^*} \tag{2.9}$$

where y^* = displacement of impact surface (positive into surface) (inches)

K^* = impact surface stiffness parameter (pounds/inch/square inch)

The surface defined by equations 2.9 is commonly known as a Winkler surface.

Equation 2.9 may also be written in the following non-dimensional form:

$$y = -\frac{q}{K} \tag{2.10}$$

where
$$y = \frac{y^*}{h}$$
$$q_b = \frac{q^*}{E}$$
$$K = \frac{K^* h}{E}$$

The various parameters relating the shell to the impact surface are shown in Figure 3. As seen from this figure, we may write

$$w^*(\phi, t) = y^*(\phi, t) + d^*(\phi) \qquad (2.11)$$

for all points on the shell which are in contact with the impact surface.

The geometrical quantity $d^*(\phi)$ is seen to be of the form:

$$d^*(\phi) = \frac{R}{\cos\phi} - R = R\left(\frac{1-\cos\phi}{\cos\phi}\right) = R\left(\frac{1-x}{x}\right) \qquad (2.12)$$

where $x = \cos\phi$.

Equations 2.11 and 2.12 can be written in the following non-dimensional form:

$$w = y + d \qquad (2.13)$$

$$d = \frac{R}{h}\left(\frac{1-\cos\phi}{\cos\phi}\right) = \frac{R}{h}\left(\frac{1-x}{x}\right) \qquad (2.14)$$

where $d = d^*/h$

Substituting equations 2.10 into equation 2.13, we may write

$$q_b = K(d - w) \qquad (2.15)$$

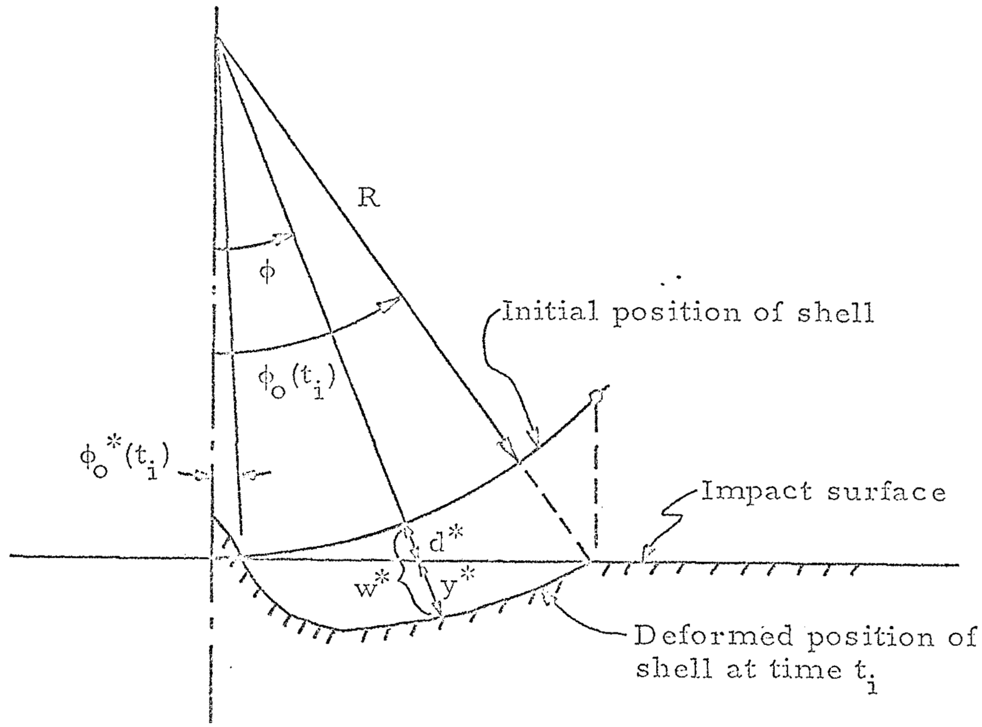

Figure 3. Relations between shell and impact surface

As developed here, this relation is valid over the entire contact area between the shell and the impact surface.

Since the shell load can only occur over that portion of the shell in contact with the impact surface, we see from equation 2.15 that the shell load boundary condition may be expressed in the form

$$q = \begin{cases} K(d-w) & , \ \phi_o^* \leq \phi \leq \phi_o \\ 0 & , \ 0 \leq \phi \leq \phi_o^* , \ \phi_o \leq \phi \leq \pi \end{cases} \tag{2.16}$$

or in the equivalent form

$$Q = \begin{cases} G(d-w) & , \ \phi_o^* \leq \phi \leq \phi_o \\ 0 & , \ 0 \leq \phi \leq \phi_o^* , \ \phi_o \leq \phi \leq \pi \end{cases} \tag{2.17}$$

where $G = K(1-\nu^2)\left(\frac{R}{h}\right)^2$

$\phi_o(\tau)$ = largest angle over which the shell is loaded, and

$\phi_o^*(\tau)$ = smallest angle over which the shell is loaded.

The angle $\phi_o^*(\tau)$ will be found to be zero except for certain times after the apex of the shell has rebounded.

It is noted that the use of the special Winkler surface defined above infers that the tangential load $p^*(\phi,t)$ is zero. Nevertheless the various solutions developed in the succeeding chapters do include this load wherever practical. In this way extensions to the solutions wherein a more complex impact surface is used may be easily developed.

CHAPTER III

NORMAL MODE SOLUTION

Introductory Remarks

One solution to this problem can be developed using the classical normal mode expansion method. The general procedure followed in this solution is described as follows.

First, the eigenvectors or normal modes of the system are developed from the homogeneous or free vibration solution to the displacement form of the equations of motion. Only the space dependence of these normal modes is determined although the procedure is described for obtaining the complete modes. Each of the displacement and applied load variables are then defined as an infinite series expansion of the product of the appropriate eigen-vector parameters of the system and an arbitrary time dependent function.

A conventional forced vibration solution to the problem now leads to a solution for the displacements in terms of an unknown load distribution and an unknown shell-impact surface contact area. These unknown quantities are determined by an appropriate application of the load-displacement boundary condition described in Chapter II and the vertical equilibrium of the shell at each point in time.

The solution which is initially developed incorporates bending, shear, and rotatory inertia effects. However, the final normal mode determination and the numerical computations are carried out for a solution that considers only membrane theory.

Free Vibration Solution

The eigenvectors or normal modes of the system may be determined from equations 2.5 if we assume P = Q = 0. Assuming that the separation of variables technique can be used to solve these equations of motion, let us define

$$
\begin{aligned}
u(\phi,\tau) &= \sum_{n=0}^{\infty} U_n(\phi)\, Q_n(\tau) \\
w(\phi,\tau) &= \sum_{n=0}^{\infty} W_n(\phi)\, R_n(\tau) \qquad (3.1) \\
\beta_\phi(\phi,\tau) &= \sum_{n=0}^{\infty} \beta_n(\phi)\, S_n(\tau)
\end{aligned}
$$

Substituting equations 3.1 into the homogeneous form of the equations of motion, we get

$$
\begin{aligned}
&\left[\frac{U_{n,\phi\phi} + U_{n,\phi}\operatorname{ctn}\phi - U_n(\nu + \operatorname{ctn}^2\phi)}{U_n}\right] Q_n + \left[(1+\nu) + K_s^2\right]\left(\frac{W_{n,\phi}}{U_n}\right) R_n \\
&\quad + K_s^2 \left(\frac{R}{h}\right)\left(\frac{\beta_n}{U_n}\right) S_n = Q_{n,\tau\tau} \qquad (3.2)
\end{aligned}
$$

$$-(1+\upsilon)\left(\frac{U_{n,\phi}+U_n\, ctn\,\phi}{W_n}\right)Q_n + \left[\frac{K_s^2(W_{n,\phi\phi}+W_{n,\phi}\, ctn\,\phi)-2(1+\upsilon)W_n}{W_n}\right]R_n$$
$$+ K_s^2\left(\frac{R}{h}\right)\left(\frac{\beta_{n,\phi}+\beta_n\, ctn\,\phi}{W_n}\right)S_n = R_{n,\tau\tau}$$
$$-\frac{1}{\varepsilon}K_s^2\left(\frac{W_{n,\phi}}{\beta_n}\right)R_n + \left\{\frac{\beta_{n,\phi\phi}+\beta_{n,\phi}\, ctn\,\phi-\beta_n\left[\upsilon+ctn^2\phi+\frac{1}{\varepsilon}\left(\frac{R}{h}\right)K_s^2\right]}{\beta_n}\right\}S_n = S_{n,\tau\tau}$$

If equations 3.2 are truly separable, then the functions multiplying Q_n, R_n, and S_n must be independent of ϕ (i.e., constant). Therefore, let us define

$$\begin{aligned}
\lambda_1 &= \frac{U_{n,\phi\phi}+U_{n,\phi}\, ctn\,\phi - U_n(\upsilon+ctn^2\phi)}{U_n}\\
\lambda_2 &= \left[(1+\upsilon)+K_s^2\right]\left(\frac{W_{n,\phi}}{U_n}\right)\\
\lambda_3 &= K_s^2\left(\frac{R}{h}\right)\left(\frac{\beta_n}{U_n}\right)\\
\lambda_4 &= -(1+\upsilon)\left(\frac{U_{n,\phi}+U_n\, ctn\,\phi}{W_n}\right)\\
\lambda_5 &= \frac{K_s^2(W_{n,\phi\phi}+W_{n,\phi}\, ctn\,\phi)}{W_n} - 2(1+\upsilon)\\
\lambda_6 &= K_s^2\left(\frac{R}{h}\right)\left(\frac{\beta_{n,\phi}+\beta_n\, ctn\,\phi}{W_n}\right)\\
\lambda_7 &= -\frac{1}{\varepsilon}K_s^2\left(\frac{W_{n,\phi}}{\beta_n}\right)\\
\lambda_8 &= \frac{\beta_{n,\phi\phi}+\beta_{n,\phi}\, ctn\,\phi-\beta_n\left[\upsilon+ctn^2\phi+\frac{1}{\varepsilon}\left(\frac{R}{h}\right)K_s^2\right]}{\beta_n}
\end{aligned} \tag{3.3}$$

The proper solution for U_n, W_n and β_n is one which satisfies each of equations 3.3 while at the same time keeping the coefficients λ_i constant. This solution is obtained in the following manner.

If we let $x = \cos\phi$, the first of equations 3.3 may be written [1]

$$(1-x^2)U_{n,xx} - 2x\,U_{n,x} + \left[n(n+1) - \frac{m^2}{1-x^2}\right]U_n = 0 \qquad (3.4)$$

where $m^2 = 1$ (3.5)

$\lambda_1 = 1 - \nu - n(n+1)$.

Equation 3.4 is recognized as Legendre's Associated Equation. The solution to equation 3.4 may be written

$$U_n(x) = F_1(n)\,P_n^1(x) + \bar{F}_1(n)\,Q_n^1(x)$$

where $P_n^1(x)$ = Associated Legendre polynomial of the first kind,

$Q_n^1(x)$ = Associated Legendre polynomial of the second kind.

Since $Q_n^1(x)$ has infinite singularities at $x = \pm 1$ and since the physical displacements at $x = \pm 1$ must be finite, we must assume that $\bar{F}_1(n) \equiv 0$. Therefore the final solution for $U_n(x)$ is

$$U_n(x) = P_n^1(x) \qquad (3.6)$$

if we include the arbitrary coefficient $F_1(n)$ in the function $Q_n(\tau)$.

The eighth of equations 3.3 can be put into the same form as equation 3.4. Therefore, using the same development described above, we find the solution

---

[1] See Jahnke and Emde (7) for details on the use of Legendre polynomials.

$$\beta_n(x) = P_n^1(x) \qquad (3.7)$$

and

$$\lambda_7 = 1 - \nu - \frac{1}{\varepsilon}\left(\frac{R}{h}\right)K_s^2 - n(n+1) \qquad (3.8)$$

The fifth of equations 3.3 can be put into the same form as equation 3.4 if we define

$$m^2 = 0$$

and

$$\lambda_8 = -n(n+1)K_s^2 - 2(1+\nu) \qquad (3.9)$$

The solution to this equation is

$$W_n(x) = F_3(n)\,P_n(x) + \bar{F}_3(n)\,Q_n(x)$$

where $P_n(x)$ = Legendre polynomial of the first kind

$Q_n(x)$ = Legendre polynomial of the second kind

Again considering the fact that $Q_n(x)$ has infinite singularities at the poles of the sphere, we find that

$$W_n(x) = P_n(x) \qquad (3.10)$$

if we include the arbitrary coefficient $F_3(n)$ in the function $R_n(\tau)$.

We now have solutions for U_n, W_n and β_n and the constant coefficients λ_1, λ_5 and λ_8. Using these results, the remaining coefficients λ_i are determined in the following manner.

Substituting equations 3.6 and 3.10 into the second of equations 3.3, we find that

$$\lambda_2 = -\left[(1+\nu) + K_s^2\right] \qquad (3.11)$$

Similar substitutions into the remainder of equations 3.3 result in the solutions

$$\lambda_3 = K_s^2\left(\frac{R}{h}\right) \tag{3.12}$$

$$\lambda_4 = -n(n+1)(1+\nu) \tag{3.13}$$

$$\lambda_6 = n(n+1)\,K_s^2\left(\frac{R}{h}\right) \tag{3.14}$$

$$\lambda_7 = \frac{1}{\varepsilon}\,K_s^2 \tag{3.15}$$

Using equations 3.5, 3.8, 3.9 and 3.11 to 3.15, equations 3.2 may be written in the following form which is seen to be independent of ϕ :

$$\begin{aligned} \lambda_1 Q_n + \lambda_2 R_n + \lambda_3 S_n &= Q_{n,\tau\tau} \\ \lambda_4 Q_n + \lambda_5 R_n + \lambda_6 S_n &= R_{n,\tau\tau} \\ \lambda_7 R_n + \lambda_8 S_n &= S_{n,\tau\tau} \end{aligned} \tag{3.16}$$

Equations 3.16 may now be solved, using conventional methods, for the functions Q_n , R_n , and S_n in terms of certain amplitude ratios and the natural frequencies of the system. Substituting these results and the previously determined solutions for U_n , W_n , and β_n into equations 3.1 will lead to a definition of the normal modes of the system.

Even though the natural frequencies and normal modes of the system can easily be computed, these calculations need not and will not be carried out here. The previously computed space variables U_n, W_n, and β_n are sufficient to completely determine the forced vibration solution to the problem.

The general solution developed above is now carried out for the membrane theory case. The present solution can be developed either by using the general solution developed above with the proper application of the assumptions of membrane theory or by the direct solution of the homogeneous form of the membrane theory equations of motion (equations 2.8).

In either case, we find the solution to be independent of the rotation angle β_ϕ. With this in mind, we may define the displacement variables as

$$\begin{aligned} u(\phi, \tau) &= \sum_{n=0}^{\infty} U_n(\phi)\, Q_n(\tau) \\ w(\phi, \tau) &= \sum_{n=0}^{\infty} W_n(\phi)\, R_n(\tau) \end{aligned} \qquad (3.17)$$

where the variables U_n, W_n, Q_n, and R_n have solutions similar in nature to the same parameters used previously.

Substituting equations 3.17 into the homogeneous form of the equations of motion, we get

$$\begin{aligned} &\left[\frac{U_{n,\phi\phi} + U_{n,\phi}\operatorname{ctn}\phi - U_n(\nu + \operatorname{ctn}^2\phi)}{U_n}\right]Q_n + (1+\nu)\left(\frac{W_{n,\phi}}{U_n}\right)R_n = Q_{n,\tau\tau} \\ &-(1+\nu)\left(\frac{U_{n,\phi} + U_n\operatorname{ctn}\phi}{W_n}\right)Q_n - 2(1+\nu)R_n = R_{n,\tau\tau} \end{aligned} \qquad (3.18)$$

As before, we see that if equations 3.18 are truly separable, then the functions multiplying Q_n and R_n must be constant. These functions are seen to be identical to certain of those defined by equations 3.3 if we assume that $K_5 = 0$.

Therefore, using the first of equations 3.3 and the derivation developed previously, we find that

$$U_n(x) = P_n^1(x) \tag{3.19}$$

and

$$\lambda_1 = 1 - \nu - n(n+1) \tag{3.20}$$

just as in the general case.

Using this result and the general theory developed previously, the remaining coefficients are seen to be

$$\lambda_2 = -(1+\nu) \tag{3.21}$$

$$\lambda_4 = -n(n+1)(1+\nu) \tag{3.22}$$

$$\lambda_5 = -2(1+\nu) \tag{3.23}$$

provided that

$$W_n(x) = P_n(x) \tag{3.24}$$

Using equations 3.19 to 3.24, equations 3.18 may now be written in the following form which is seen to be independent of ϕ :

$$\begin{aligned} \lambda_1 Q_n + \lambda_2 R_n &= Q_{n,\tau\tau} \\ \lambda_4 Q_n + \lambda_5 R_n &= R_{n,\tau\tau} \end{aligned} \tag{3.25}$$

As discussed before, a solution to equations 3.25 would lead to the computation of the natural frequencies and normal modes. However, these computations need not and will not be carried out here. A detailed examination of these natural frequencies and normal modes has been carried out by Baker (1).

Forced Vibration Solution

Using the solution developed in the previous article for the space dependent portion of the normal modes (i.e., U_n , W_n , and β_n), the complete solution to the equations of motion in terms of unknown applied loads is now found.

Again assuming that the separation of variables technique can be used to solve the equations of motion, let us assume that

$$\begin{aligned} u(x,\tau) &= \sum_{n=0}^{\infty} P_n^1(x)\, A_n(\tau) \\ w(x,\tau) &= \sum_{n=0}^{\infty} P_n(x)\, B_n(\tau) \\ \beta_\phi(x,\tau) &= \sum_{n=0}^{\infty} P_n^1(x)\, C_n(\tau) \end{aligned} \tag{3.26}$$

Let us also define the load distribution on the shell as the following series expansion of normal mode functions:

$$\begin{aligned} Q(x,\tau) &= \sum_{n=0}^{\infty} P_n(x)\, D_n(\tau) \\ P(x,\tau) &= \sum_{n=0}^{\infty} P_n^1(x)\, E_n(\tau) \end{aligned} \tag{3.27}$$

On substituting equations 3.26 and 3.27 into the equations of motion (equations 2.5), we find that

$$\begin{aligned} \lambda_1 A_n + \lambda_2 B_n + \lambda_3 C_n &= A_{n,\tau\tau} - E_n \\ \lambda_4 A_n + \lambda_5 B_n + \lambda_6 C_n &= B_{n,\tau\tau} - D_n \\ \lambda_7 B_n + \lambda_8 C_n &= C_{n,\tau\tau} \end{aligned} \qquad (3.28)$$

The coefficients λ_i in equations 3.28 are as determined for the free vibration solution.

Taking the Laplace transform of equations 3.28, we may write [2]

$$\begin{aligned} (s^2-\lambda_1)\bar{A}_n - \lambda_2 \bar{B}_n - \lambda_3 \bar{C}_n &= \bar{E}_n + s A_n(0) + \dot{A}_n(0) \\ -\lambda_4 \bar{A}_n + (s^2-\lambda_5)\bar{B}_n - \lambda_6 \bar{C}_n &= \bar{D}_n + s B_n(0) + \dot{B}_n(0) \\ -\lambda_7 \bar{B}_n + (s^2-\lambda_8)\bar{C}_n &= s C_n(0) + \dot{C}_n(0) \end{aligned} \qquad (3.29)$$

The solution to equations 3.29 is recognized to be of the form

$$\begin{aligned} \bar{A}_n(s) &= \bar{f}_1(\lambda_i, s)\bar{D}_n(s) + \bar{g}_1(\lambda_i, s)\bar{E}_n(s) + \bar{h}_1(\lambda_i, s) \\ \bar{B}_n(s) &= \bar{f}_2(\lambda_i, s)\bar{D}_n(s) + \bar{g}_2(\lambda_i, s)\bar{E}_n(s) + \bar{h}_2(\lambda_i, s) \\ \bar{C}_n(s) &= \bar{f}_3(\lambda_i, s)\bar{D}_n(s) + \bar{g}_3(\lambda_i, s)\bar{E}_n(s) + \bar{h}_3(\lambda_i, s) \end{aligned} \qquad (3.30)$$

The inversion of equations 3.30 will lead to the convolution integrals

---

[2] The dot in $\dot{A}_n(0)$, $\dot{B}_n(0)$, and $\dot{C}_n(0)$ indicates differentiation with respect to nondimensional time τ.

$$A_n(\tau) = \int_0^\tau \left[F_1(\lambda_i, \tau-y) D_n(y) + G_1(\lambda_i, \tau-y) E_n(y)\right] dy + H_1(\lambda_i, \tau)$$

$$B_n(\tau) = \int_0^\tau \left[F_2(\lambda_i, \tau-y) D_n(y) + G_2(\lambda_i, \tau-y) E_n(y)\right] dy + H_2(\lambda_i, \tau) \qquad (3.31)$$

$$C_n(\tau) = \int_0^\tau \left[F_3(\lambda_i, \tau-y) D_n(y) + G_3(\lambda_i, \tau-y) E_n(y)\right] dy + H_3(\lambda_i, \tau)$$

where F_j and G_j are harmonic functions and H_j are functions of the initial conditions. The detailed computation of the functions F_j , G_j , and H_j will not be carried out for the general shear theory case. Rather, the detailed solution will be carried out for the membrane theory case.

The membrane theory solution is developed in a manner similar to the above if we neglect the effect of β_ϕ . On comparison with the free vibration solution, the membrane theory form of equations 3.28 is seen to be

$$\begin{aligned} \lambda_1 A_n + \lambda_2 B_n &= A_{n,\tau\tau} - E_n \\ \lambda_4 A_n + \lambda_5 B_n &= B_{n,\tau\tau} - D_n \end{aligned} \qquad (3.32)$$

where, as previously determined,

$$\lambda_1 = 1 - \nu - n(n+1)$$

$$\lambda_2 = -(1+\nu)$$

$$\lambda_4 = -n(n+1)(1+\nu)$$

$$\lambda_5 = -2(1+\nu)$$

Taking the Laplace transform of equations 3.32, we may write

$$
\begin{aligned}
(s^2-\lambda_1)\bar{A}_n - \lambda_2 \bar{B}_n &= s\,A_n(o) + \dot{A}_n(o) + \bar{E}_n \\
-\lambda_4 \bar{A}_n + (s^2-\lambda_5)\bar{B}_n &= s\,B_n(o) + \dot{B}_n(o) + \bar{D}_n
\end{aligned}
\tag{3.33}
$$

Solving equations 3.33, and using the appropriate relations for λ_i, we find that

$$
\bar{A}_n(s) = \frac{s^3 A_n(o) + s^2\left[\dot{A}_n(o) + \bar{E}_n\right] + s(1+\nu)\left[2A_n(o) - B_n(o)\right] + (1+\nu)\left[2\left(\dot{A}_n(o) + \bar{E}_n\right) - \left(\dot{B}_n(o) + \bar{D}_n\right)\right]}{s^4 + G_4(n)\,s^2 + G_5(n)}
$$

$$
\bar{B}_n(s) = \frac{s^3 B_n(o) + s^2\left[\dot{B}_n(o) + \bar{D}_n\right] + s\left\{n(n+1)\left[B_n(o) - (1+\nu)A_n(o)\right] - (1-\nu)B_n(o)\right\} + n(n+1)\left[\dot{B}_n(o) + \bar{D}_n - (1+\nu)\left(\dot{A}_n(o) + \bar{E}_n\right)\right] - (1-\nu)\left(\dot{B}_n(o) + \bar{D}_n\right)}{s^4 + G_4(n)\,s^2 + G_5(n)}
\tag{3.34}
$$

where

$$
\begin{aligned}
G_4(n) &= n(n+1) + 1 + 3\nu \\
G_5(n) &= (1-\nu^2)\left[n(n+1) - 2\right]
\end{aligned}
$$

The inversion of equations 3.34 will give the required solutions for $A_n(\tau)$ and $B_n(\tau)$.

However, prior to carrying out this inversion, let us consider the initial conditions of the problem. If we consider the shell to have zero displacement and an initial vertical velocity V_o at $t=o$, we may write

$$
\begin{aligned}
u^*(x,o) &= w^*(x,o) = 0 \\
\frac{du^*(x,o)}{dt} &= -V_o \sin\phi \\
\frac{dw^*(x,o)}{dt} &= V_o \cos\phi
\end{aligned}
$$

Written in terms of nondimensional quantities, these conditions become

$$
\begin{aligned}
u(x,0) &= w(x,0) = 0 \\
\dot{u}(x,0) &= -\beta\left(\tfrac{R}{h}\right)\sin\phi = -\beta\left(\tfrac{R}{h}\right)P_1'(x) \\
\dot{w}(x,0) &= \beta\left(\tfrac{R}{h}\right)\cos\phi = \beta\left(\tfrac{R}{h}\right)P_1(x)
\end{aligned}
\tag{3.35}
$$

Substituting equations 3.35 into equations 3.26, we get

$$
\begin{aligned}
\sum_{n=0}^{\infty} P_n'(x)\,A_n(0) &= \sum_{n=0}^{\infty} P_n(x)\,B_n(0) = 0 \\
\sum_{n=0}^{\infty} P_n'(x)\,\dot{A}_n(0) &= -\beta\left(\frac{R}{h}\right)P_1'(x) \\
\sum_{n=0}^{\infty} P_n(x)\,\dot{B}_n(0) &= \beta\left(\frac{R}{h}\right)P_1(x)
\end{aligned}
$$

Since $P_n'(x)$ and $P_n(x)$ are not necessarily zero, these conditions imply that

$$
\begin{aligned}
A_n(0) &= B_n(0) = 0 \\
\dot{B}_n(0) &= -\dot{A}_n(0) = \begin{cases} \beta\left(\frac{R}{h}\right), & n=1 \\ 0, & n\neq 1 \end{cases}
\end{aligned}
\tag{3.36}
$$

Using relations 3.36, equations 3.34 may be written in the following simplified form:

$$
\begin{aligned}
\bar{A}_n(s) &= \frac{s^2\left[-\dot{B}_n(0)+\bar{E}_n\right]+(1+\nu)\left[-3\dot{B}_n(0)+2\bar{E}_n-\bar{D}_n\right]}{s^4+G_4(n)\,s^2+G_5(n)} \\
\bar{B}_n(s) &= \frac{s^2\left[\dot{B}_n(0)+\bar{D}_n\right]+3(1+\nu)\dot{B}_n(0)+\left[n(n+1)-1+\nu\right]\bar{D}_n-n(n+1)(1+\nu)\bar{E}_n}{s^4+G_4(n)\,s^2+G_5(n)}
\end{aligned}
\tag{3.37}
$$

The inversion of equations 3.37 is carried out in Appendix A and results in the equations

$$A_n(\tau) = -\Theta_n(\tau) + \int_0^\tau \Phi_n(\tau-y) D_n(y)\, dy + \int_0^\tau \Psi_n(\tau-y) E_n(y)\, dy$$

$$B_n(\tau) = \Theta_n(\tau) + \int_0^\tau \eta_n(\tau-y) D_n(y)\, dy + \int_0^\tau \Omega_n(\tau-y) E_n(y)\, dy \qquad (3.38)$$

where

$$\Theta_n(\tau) = \begin{cases} \beta\left(\frac{R}{h}\right)\tau , & n=1 \\ 0 , & n \neq 1 \end{cases} \qquad (3.39)$$

$$\Phi_n(\tau) = \begin{cases} \left(\frac{1+\nu}{3+\nu}\right) \frac{\sin \omega_0 \tau}{\omega_0} , & n=0 \\ \frac{1}{3}\left[\frac{\sin \omega_1 \tau}{\omega_1} - \tau \right] , & n=1 \\ \left(\frac{1+\nu}{G_6(n)}\right)\left(\frac{\sin \omega_n \tau}{\omega_n} - \frac{\sin \mu_n \tau}{\mu_n} \right) , & n>1 \end{cases} \qquad (3.40)$$

$$\Psi_n(\tau) = \begin{cases} 0 , & n=0 \\ \frac{1}{3}\left(\frac{\sin \omega_1 \tau}{\omega_1} + 2\tau \right) , & n=1 \\ \frac{1}{G_6(n)}\left\{ -\left[\frac{2(1+\nu) - \omega_n^2}{\omega_n}\right] \sin \omega_n \tau + \left[\frac{2(1+\nu) - \mu_n^2}{\mu_n}\right] \sin \mu_n \tau \right\} , & n>1 \end{cases} \qquad (3.41)$$

$$\eta_n(\tau) = \begin{cases} \frac{\sin \omega_0 \tau}{\omega_0} , & n=0 \\ \frac{1}{3}\left(\frac{2 \sin \omega_1 \tau}{\omega_1} + \tau \right) , & n=1 \\ \frac{1}{G_6(n)}\left\{ -\left[\frac{n(n+1) - 1 + \nu - \omega_n^2}{\omega_n}\right] \sin \omega_n \tau + \left[\frac{n(n+1) - 1 + \nu - \mu_n^2}{\mu_n}\right] \sin \mu_n \tau \right. , & n>1 \end{cases} \qquad (3.42)$$

$$\Omega_n(\tau) = \begin{cases} 0 , & n=0 \\ \frac{2}{3}\left(\frac{\sin \omega_1 \tau}{\omega_1} - \tau \right) , & n=1 \\ \left[\frac{n(n+1)(1+\nu)}{G_6(n)}\right]\left(\frac{\sin \omega_n \tau}{\omega_n} - \frac{\sin \mu_n \tau}{\mu_n} \right) , & n>1 \end{cases} \qquad (3.43)$$

and $$G_6(n) = \left\{ \left[G_4(n) \right]^2 - 4\, G_5(n) \right\}^{1/2}$$

$$\omega_n^2 = \frac{1}{2} \left[G_4(n) + G_6(n) \right]$$

$$\mu_n^2 = \frac{1}{2} \left[G_4(n) - G_6(n) \right]$$

It should be noted that equations 3.38 represent a rather general solution for the forced vibration of an impacting spherical shell. However, future computations will be restricted to the special case where the impact surface is as defined on pages 14-17. For this case, it is seen that $E_n(\tau) \equiv 0$.

Load-Displacement Relation

A relation between the applied radial load and the displacement of the shell will now be derived.

The shell load boundary condition has been determined in equation 2.17 to be

$$Q(x,\tau) = \begin{cases} G\left[d(x) - w(x,\tau) \right] , & x_o \leqslant x \leqslant x_o^* \\ 0 , & x_o^* \leqslant x \leqslant 1 ,\ -1 \leqslant x \leqslant x_o \end{cases} \qquad (3.44)$$

where the notation $x = \cos\phi$ has been used to define the angles ϕ, $\phi_o(\tau)$, and $\phi_o^*(\tau)$ and the relation

$$d(x) = \frac{R}{h} \left(\frac{1-x}{x} \right)$$

Since $d(x)$ is only a function of x, equation 3.44 may be written in the form

$$Q(x,\tau) = G\left[d(x,\tau) - w(x,\tau) \right] , \quad -1 \leqslant x \leqslant 1 \qquad (3.45)$$

if we redefine $d(x,\tau)$ as the time dependent function

$$d(x,\tau) = \begin{cases} \frac{R}{h}\left(\frac{1-x}{x}\right) , & x_o \leqslant x \leqslant x_o^* \\ w(x,\tau) , & x_o^* \leqslant x \leqslant 1 , -1 \leqslant x \leqslant x_o \end{cases} \tag{3.46}$$

This form of the shell load boundary condition will be used in the following discussion.

The shell displacements and applied loads have previously (see equations 3.26 and 3.27) been defined as series expansions of normal mode functions. The relation $d(x,\tau)$ will now be defined as a similar expansion with the form

$$d(x,\tau) = \sum_{n=0}^{\infty} P_n(x)\, F_n(\tau) \tag{3.47}$$

It is a well known fact (7:116) that Legendre polynomials are orthogonal over the range $-1 < x < 1$ and satisfy the relation

$$\int_{-1}^{1} P_n(x)\, P_m(x)\, dx = \begin{cases} \frac{2}{2n+1} , & n = m \\ 0 , & n \neq m \end{cases} \tag{3.48}$$

Therefore, after multiplying $P_m(x)$ through equation 3.47, integrating the result over the orthogonality range of the Legendre polynomials, and using equations 3.46 and 3.48, we find that

$$F_n(\tau) = L_n(\tau) + M_n(\tau) + N_n(\tau) \tag{3.49}$$

where

$$L_n(\tau) = \left(\frac{2n+1}{2}\right)\int_{-1}^{x_o} w(x,\tau)\, P_n(x)\, dx \tag{3.50}$$

$$M_n(\tau) = \left(\frac{2n+1}{2}\right)\left(\frac{R}{h}\right)\int_{x_o}^{x_o^*} \left(\frac{1-x}{x}\right) P_n(x)\, dx \tag{3.51}$$

$$N_n(\tau) = \left(\frac{2n+1}{2}\right)\int_{x_o^*}^{1} w(x,\tau)\, P_n(x)\, dx \tag{3.52}$$

Since $x_o(\tau)$ will have a value closer to one than to minus one, it will be more convenient to write equation 3.50 in the equivalent form

$$L_n(\tau) = \left(\frac{2n+1}{2}\right)\left[\int_{-1}^{1} w(x,\tau) P_n(x)\, dx - \int_{x_o}^{1} w(x,\tau)\, P_n(x)\, dx\right]$$

This relation may be simplified through the use of equations 3.26 and 3.48 to become

$$L_n(\tau) = B_n(\tau) - \left(\frac{2n+1}{2}\right)\int_{x_o}^{1} w(x,\tau)\, P_n(x)\, dx \tag{3.53}$$

Using equations 3.51 to 3.53, equation 3.49 may now be written

$$F_n(\tau) = B_n(\tau) + \left(\frac{2n+1}{2}\right)\int_{x_o}^{x_o^*} \left[\left(\frac{R}{h}\right)\left(\frac{1-x}{x}\right) - w(x,\tau)\right] P_n(x)\, dx \tag{3.54}$$

$M_n(\tau)$ can be determined from equation 3.51 provided that the angles $\phi_o(\tau)$ and $\phi_o^*(\tau)$ are known. The evaluation of these angles will be discussed later. On the other hand, the determination of $N_n(\tau)$ and $L_n(\tau)$ requires that the displacement $w(x,\tau)$ be known in addition to the angles $\phi_o(\tau)$ and $\phi_o^*(\tau)$. This unfortunate result reflects the inherent coupling between the load distribution and displacement of the shell. As a result of this coupling, the exact solution to the problem may only be approached through an iterative procedure.

We are now in a position to write the desired relation between the applied radial load and the displacement of the shell. Substituting equations 3.26, 3.27, and 3.47 into equation 3.45, we get

$$\sum_{n=0}^{\infty} P_n(x)\left\{ D_n(\tau) - G\left[F_n(\tau) - B_n(\tau)\right]\right\} = 0$$

Since this relation must be valid for all values of x, we see that

$$D_n(\tau) = G\left[F_n(\tau) - B_n(\tau)\right] \qquad (3.55)$$

For the special case of a rigid impact surface (i.e., $G = \infty$), equation 3.55 reduces to the form

$$F_n(\tau) = B_n(\tau) \qquad (3.56)$$

Both equations 3.55 and 3.56 are seen to reflect the desired relation between load and displacement since the load function $D_n(\tau)$ is an integral part of the displacement function $B_n(\tau)$.

Determination of $\phi_o(\tau)$ and $\phi_o^*(\tau)$

Equations 3.55 and 3.56 may be solved for the unknown load distribution provided that the angles $\phi_o(\tau)$ and $\phi_o^*(\tau)$ are known. The condition necessary to determine these angles is now presented.

As seen from Figure 3 and equation 3.46, the boundaries of the contact area between the shell and the impact surface may be defined by the relation

$$w(x,\tau) = \frac{R}{h}\left(\frac{1-x}{x}\right)$$

This relation may also be written in the equivalent but computationally more convenient form

$$x = 1 - \left(\frac{h}{R}\right) x\, w(x,\tau) \tag{3.57}$$

The root (or roots) of equation 3.57 give the cosine of the desired angle (or angles).

Certain information that will help in formulating a computational technique to solve equation 3.57 is available. First, the angle $\phi_o^*(\tau)$ will only have a nonzero value if the apex of the shell rebounds prior to other portions of the shell. Thus, this angle will initially and, perhaps, for all time be zero. On the other hand, the angle $\phi_o(\tau)$ will have a nonzero value for all time (after the initial time) until the shell completely rebounds from the impact surface. Initially, it is seen that $\phi_o(\tau)=0$.

Computational Procedure

The complete solution to the problem can be obtained from equations 3.26 and 3.27 once the values of $D_n(\tau)$, $\phi_o(\tau)$, and $\phi_o^*(\tau)$ are found. These parameters can be determined from n equations of the type given by equations 3.55 or 3.56 and equation 3.57.

A procedure is developed here to determine the unknown parameters of the problem. In this procedure the impact surface will be assumed to have a finite rigidity thus allowing the use of equation 3.55. This assumption is not considered unduly restrictive since hard impact surfaces with stiffnesses of up to 100,000 pounds/in^3 have successfully been evaluated using equation 3.55.

The problem solution is obtained through the use of various numerical techniques and a digital computer program. This program, whose flow chart is shown in Figure 4, is built up of a series of subprograms. The subprograms are listed in Table 1. A complete FORTRAN listing and a detailed description of each of the programs is given in Appendix B.

As previously stated, the inherent relation between the applied load and the displacement requires that an iterative procedure be used to solve the problem. In the present program only one such iteration is used during each time interval. This simplification is justified if sufficiently small integration intervals are used.

The solution procedure considers the following general steps. First, various initial values are assumed. Second, the displacement functions, $\mathfrak{D}_n(\tau)$, are determined. Third, the angles $\phi_o(\tau)$ and $\phi_o^*(\tau)$ are determined. Fourth, the load functions, $D_n(\tau)$, are determined. At this point the solution for a particular time is complete and the applied load and displacement relations may be evaluated

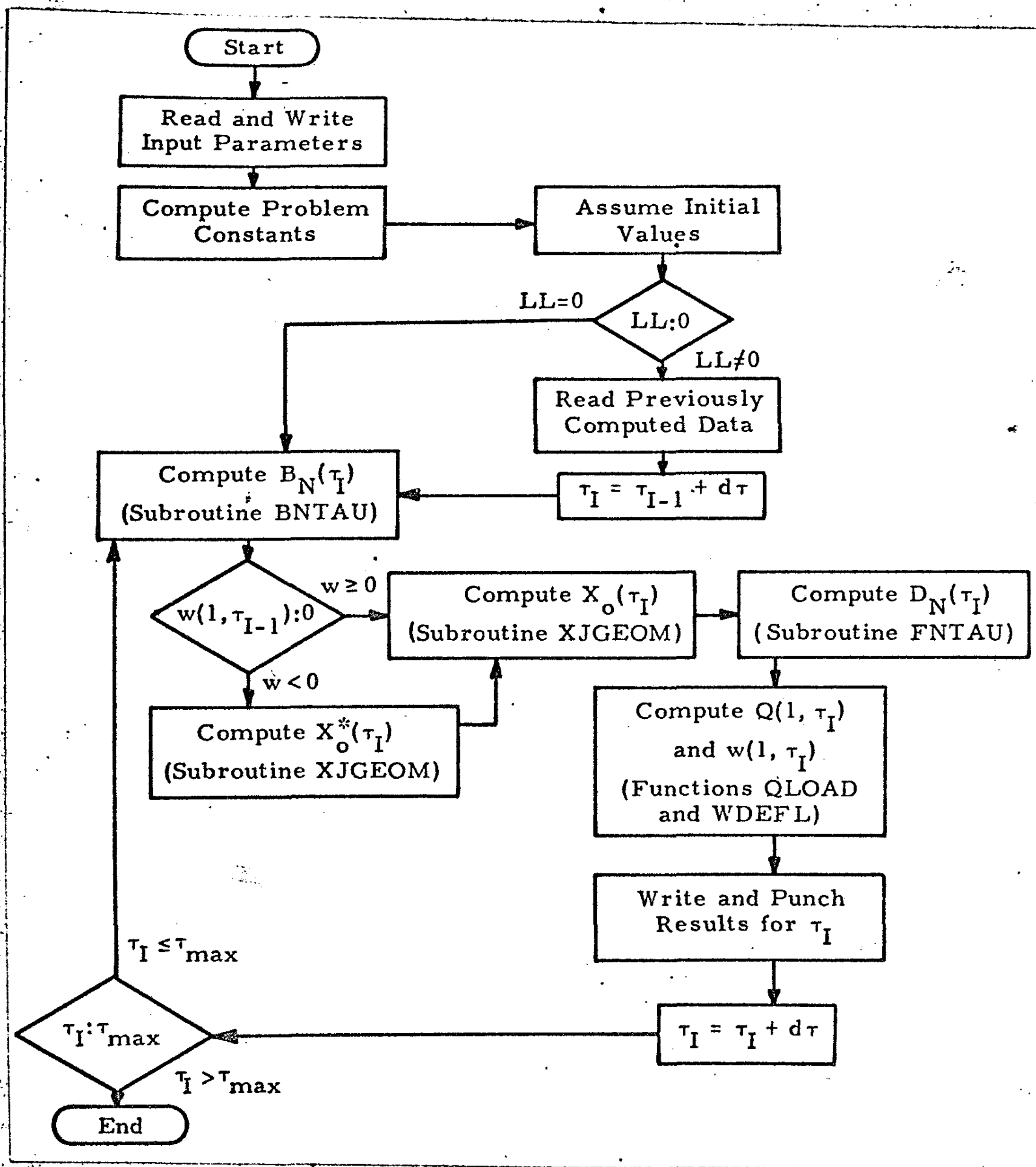

Figure 4. Flow chart--SIMPAC program

TABLE 1

SUBROUTINES USED IN SIMPAC PROGRAM

Program Name	Arguments	User Programs	Output
BNTAU	None	Main	$B_n(\tau)$
XJGEOM	None	Main	Roots of $x = 1 - \left(\frac{h}{R}\right) \times w(x,\tau)$
FNTAU	None	Main	$F_n(\tau)$
QLOAD	XK, I	Main	$Q(x, \tau)$
WDEFL	XK	Main XJGEOM FNTAU	$w(x, \tau)$
LEGFNJ	N, X, PN	BNTAU FNTAU QLOAD WDEFL	Legendre polynomial = $P_n(x)$
HYPFNR	A, B, C, z, EP, F	LEGFNJ	Hypergeometric Function = $F(A, B; C; z)$

for an arbitrary point on the shell. As a final step, a new time $\tau = \tau + d\tau$ is selected and the procedure returns to the second step.

Closing Remarks

The detailed solution carried out in this chapter is based on the membrane theory of shells. However, a similar solution considering bending, shear, and rotatory inertia effects could be directly obtained if the functions F_j and H_j in equations 3.31 were available. It is seen that the discussion presented in articles 3.4 to 3.6 is directly applicable to this latter solution.

Even though the membrane solution is presented primarily as an example illustrating the feasibility of the solution, it should be an acceptable solution in some situations. These situations would arise for cases where the shell is sufficiently thin and where the total impact time is sufficiently long so as to minimize the effect of large changes in displacement near the apex of the shell. It is to be noted that the example cases discussed in Chapter V do seem to fit this special category of solutions.

CHAPTER IV

CHARACTERISTIC SOLUTION

Introductory Remarks

There are several undesirable aspects of the normal mode expansion method as applied to this problem. In general, these aspects relate to the inherent difficulty in describing an abrupt wave front by the sum of orthogonal series relations. In order to get accurate results, it is necessary to take many terms in the appropriate series relations.

The method of characteristics is another method by which the problem solution can be obtained. With this method, the results (deflections, stresses, etc.) at or near wave fronts are readily and accurately described.

The general procedure followed in this latter method is described as follows.

The various equations of the problem are first written as first order partial differential equations and are then reduced to their normal form. The normal form of the equations (i.e., characteristic equations) are seen to be ordinary differential equations when defined in certain characteristic directions on the space-time plane.

The solution to the problem is now readily obtained by integrating the characteristic equations in the appropriate characteristic directions. While obtaining this solution, certain special conditions must be prescribed at the apex of the shell.

The solution is essentially a step-by-step integration procedure. The load-displacement boundary condition described in Chapter II, pages 14-17, is used to determine the shell-impact surface contact area at each point in time.

A solution incorporating bending, shear, and rotatory inertia effects is determined. However, numerical computations are restricted to a solution that considers only membrane theory.

Determination of Characteristic Equations

Shear Theory--The shear theory characteristic equations are determined from equations 2.2 and 2.4 using the following procedure. This procedure is developed by the method described by Courant and Hilbert (3:425).

The following new variables will be used in this derivation:

$$\begin{aligned} \dot{u} &= u_{,\tau} \\ \dot{w} &= w_{,\tau} \\ \dot{\beta}_\phi &= \beta_{\phi,\tau} \end{aligned} \qquad (4.1)$$

and
$$Y_1 = \dot{u}\ \mathrm{ctn}\,\phi$$
$$Y_2 = (n_\phi - n_\theta)\ \mathrm{ctn}\,\phi$$
$$Y_3 = \varepsilon\dot{\beta}_\phi\ \mathrm{ctn}\,\phi \qquad (4.2)$$
$$Y_4 = (m_\phi - m_\theta)\ \mathrm{ctn}\,\phi$$
$$Y_5 = q_{b\phi}\ \mathrm{ctn}\,\phi$$

The equations of motion (equations 2.2) may now be written in the form

$$-n_{\phi,\phi} + \dot{u}_{,\tau} = Y_2 + q_{b\phi} + P$$
$$-q_{b\phi,\phi} + \dot{w}_{,\tau} = Y_5 - (n_\phi + n_\theta) + Q \qquad (4.3)$$
$$-m_{\phi,\phi} + \varepsilon\dot{\beta}_{\phi,\tau} = Y_4 - q_{b\phi}$$

After differentiation with respect to non-dimensional time, the stress-displacement relations may be written

$$-\dot{u}_{,\phi} + n_{\phi,\tau} = \nu Y_1 + (1+\nu)\dot{w}$$
$$-\nu\dot{u}_{,\phi} + n_{\theta,\tau} = Y_1 + (1+\nu)\dot{w}$$
$$-\varepsilon\dot{\beta}_{\phi,\phi} + m_{\phi,\tau} = \nu Y_3 \qquad (4.4)$$
$$-\nu\varepsilon\dot{\beta}_{\phi,\phi} + m_{\theta,\tau} = Y_3$$
$$-K_s^2\dot{w}_{,\phi} + q_{b\phi,\tau} = K_s^2\left(\frac{R}{h}\right)\dot{\beta}_\phi$$

Equations 4.3 and 4.4 may also be written in the form of the matrix equation

$$A\frac{\partial v}{\partial \phi} + \frac{\partial v}{\partial \tau} = e \qquad (4.5)$$

where

$$A = \begin{bmatrix} 0 & 0 & 0 & 0 & 0 & -1 & 0 & 0 \\ 0 & 0 & 0 & 0 & 0 & -\upsilon & 0 & 0 \\ 0 & 0 & 0 & 0 & 0 & 0 & 0 & -1 \\ 0 & 0 & 0 & 0 & 0 & 0 & 0 & -\upsilon \\ 0 & 0 & 0 & 0 & 0 & 0 & -K_s^2 & 0 \\ -1 & 0 & 0 & 0 & 0 & 0 & 0 & 0 \\ 0 & 0 & 0 & 0 & -1 & 0 & 0 & 0 \\ 0 & 0 & -1 & 0 & 0 & 0 & 0 & 0 \end{bmatrix}$$

$$V = \begin{Bmatrix} n_\phi \\ n_\theta \\ m_\phi \\ m_\theta \\ q_{b\phi} \\ \dot{u} \\ \dot{w} \\ \varepsilon\dot{\beta}_\phi \end{Bmatrix}, \quad e = \begin{Bmatrix} \upsilon Y_1 + (1+\upsilon)\dot{w} \\ Y_1 + (1+\upsilon)\dot{w} \\ \upsilon Y_3 \\ Y_3 \\ K_s^2\left(\frac{R}{h}\right)\dot{\beta}_\phi \\ Y_2 + q_{b\phi} + P \\ Y_5 - (n_\phi + n_\theta) + Q \\ Y_4 - q_{b\phi} \end{Bmatrix}$$

If stress waves are to propagate through the shell, equations 4.5 must be hyperbolic. This system of equations is hyperbolic if there exist eight linearly independent eigenvectors l^s for which

$$l^s A = \lambda_s l^s \tag{4.6}$$

and λ_s are the roots of the algebraic equation

$$|A - \lambda I| = 0 \tag{4.7}$$

Equation 4.7 is evaluated in Appendix D. The values for the eigenvalues λ_s are seen to be

$$\lambda_s = 0, 0, \pm 1, \pm 1, \pm K_s \tag{4.8}$$

The eigenvectors of equation 4.6 are determined in Appendix D. These eigenvectors can be written in the form of the following transformation matrix whose rows consist of the various eigenvectors:

$$T = \begin{bmatrix} -\upsilon & 1 & 0 & 0 & 0 & 0 & 0 & 0 \\ 0 & 0 & -\upsilon & 1 & 0 & 0 & 0 & 0 \\ 1 & 0 & 0 & 0 & 0 & -1 & 0 & 0 \\ 1 & 0 & 0 & 0 & 0 & 1 & 0 & 0 \\ 0 & 0 & 1 & 0 & 0 & 0 & 0 & -1 \\ 0 & 0 & 1 & 0 & 0 & 0 & 0 & 1 \\ 0 & 0 & 0 & 0 & 1 & 0 & -K_s & 0 \\ 0 & 0 & 0 & 0 & 1 & 0 & K_s & 0 \end{bmatrix} \tag{4.9}$$

The normal form of equation 4.5 is found by multiplying T through equation 4.5. The resulting set of eight equations are written as follows:

$$\begin{aligned}
&\frac{\partial}{\partial\tau}\left(-\upsilon n_\phi + n_\theta\right) = (1-\upsilon^2)(Y_1 + \dot{w}) \\
&\frac{\partial}{\partial\tau}\left(-\upsilon m_\phi + m_\theta\right) = (1-\upsilon^2)Y_3 \\
&\left(\frac{\partial}{\partial\phi}+\frac{\partial}{\partial\tau}\right)\left(n_\phi - \dot{u}\right) = \upsilon Y_1 - Y_2 + (1+\upsilon)\dot{w} - q_{b\phi} - P \\
&\left(-\frac{\partial}{\partial\phi}+\frac{\partial}{\partial\tau}\right)\left(n_\phi + \dot{u}\right) = \upsilon Y_1 + Y_2 + (1+\upsilon)\dot{w} + q_{b\phi} + P \\
&\left(\frac{\partial}{\partial\phi}+\frac{\partial}{\partial\tau}\right)\left(m_\phi - \varepsilon\dot{\beta}_\phi\right) = \upsilon Y_3 - Y_4 + q_{b\phi} \\
&\left(-\frac{\partial}{\partial\phi}+\frac{\partial}{\partial\tau}\right)\left(m_\phi + \varepsilon\dot{\beta}_\phi\right) = \upsilon Y_3 + Y_4 - q_{b\phi} \\
&\left(K_s\frac{\partial}{\partial\phi}+\frac{\partial}{\partial\tau}\right)\left(q_{b\phi} - K_s\dot{w}\right) = K_s\left[K_s\left(\frac{R}{h}\right)\dot{\beta}_\phi - Y_5 + (n_\phi + n_\theta) - Q\right] \\
&\left(-K_s\frac{\partial}{\partial\phi}+\frac{\partial}{\partial\tau}\right)\left(q_{b\phi} + K_s\dot{w}\right) = K_s\left[K_s\left(\frac{R}{h}\right)\dot{\beta}_\phi + Y_5 - (n_\phi + n_\theta) + Q\right]
\end{aligned} \tag{4.10}$$

Equations 4.10 are the desired characteristic equations written in terms of the physical variables. These equations may be put into another form which is more appropriate for numerical integration through the introduction of a new set of dependent variables. Therefore, let

$$\begin{aligned}
V_1 &= n_\phi - \dot{u} \\
V_2 &= n_\phi + \dot{u} \\
V_3 &= q_{b\phi} - K_s \dot{w} \\
V_4 &= q_{b\phi} + K_s \dot{w} \\
V_5 &= m_\phi - \varepsilon \dot{\beta}_\phi \\
V_6 &= m_\phi + \varepsilon \dot{\beta}_\phi \\
V_7 &= -\nu n_\phi + n_\theta \\
V_8 &= -\nu m_\phi + m_\theta
\end{aligned} \tag{4.11}$$

Using equations 4.11, the following relations for the physical variables may be written:

$$\begin{aligned}
n_\phi &= \frac{1}{2}(V_1 + V_2) \\
n_\theta &= V_7 + \frac{\nu}{2}(V_1 + V_2) \\
m_\phi &= \frac{1}{2}(V_5 + V_6) \\
m_\theta &= V_8 + \frac{\nu}{2}(V_5 + V_6) \\
q_{b\phi} &= \frac{1}{2}(V_3 + V_4) \\
\dot{u} &= \frac{1}{2}(V_2 - V_1) \\
\dot{w} &= \frac{1}{2K_s}(V_4 - V_3) \\
\varepsilon \dot{\beta}_\phi &= \frac{1}{2}(V_6 - V_5)
\end{aligned} \tag{4.12}$$

Using equations 4.11 and 4.12, the characteristic equations (equations 4.10) may now be written

$$\frac{dV_7}{d\tau} = (1-\upsilon^2)\left[Y_1 + \frac{1}{2K_s}(V_4 - V_3)\right]$$

$$\frac{dV_8}{d\tau} = (1-\upsilon^2)Y_3$$

$$\frac{dV_1}{ds_1} = \upsilon Y_1 - Y_2 - \frac{1}{2}\left(\frac{1+\upsilon}{K_s}+1\right)V_3 + \frac{1}{2}\left(\frac{1+\upsilon}{K_s}-1\right)V_4 - P$$

$$\frac{dV_2}{ds_2} = \upsilon Y_1 + Y_2 - \frac{1}{2}\left(\frac{1+\upsilon}{K_s}-1\right)V_3 + \frac{1}{2}\left(\frac{1+\upsilon}{K_s}+1\right)V_4 + P$$

$$\frac{dV_5}{ds_1} = \upsilon Y_3 - Y_4 + \frac{1}{2}(V_3 + V_4) \qquad (4.13)$$

$$\frac{dV_6}{ds_2} = \upsilon Y_3 + Y_4 - \frac{1}{2}(V_3 + V_4)$$

$$\frac{dV_3}{ds_3} = K_s\left[\frac{K_s}{2}\left(\frac{R}{\varepsilon h}\right)(V_6 - V_5) + V_7 + \left(\frac{1+\upsilon}{2}\right)(V_1 + V_2) - Y_5 - Q\right]$$

$$\frac{dV_4}{ds_4} = K_s\left[\frac{K_s}{2}\left(\frac{R}{\varepsilon h}\right)(V_6 - V_5) - V_7 - \left(\frac{1+\upsilon}{2}\right)(V_1 + V_2) + Y_5 + Q\right]$$

where

$$\frac{d}{ds_1} = \frac{\partial}{\partial\phi} + \frac{\partial}{\partial\tau}$$

$$\frac{d}{ds_2} = -\frac{\partial}{\partial\phi} + \frac{\partial}{\partial\tau}$$

$$\frac{d}{ds_3} = K_s\frac{\partial}{\partial\phi} + \frac{\partial}{\partial\tau}$$

$$\frac{d}{ds_4} = -K_s\frac{\partial}{\partial\phi} + \frac{\partial}{\partial\tau}$$

The characteristic equations given above are defined for the directions shown in Figure 5. Since the slopes of the various characteristic directions in the space-time

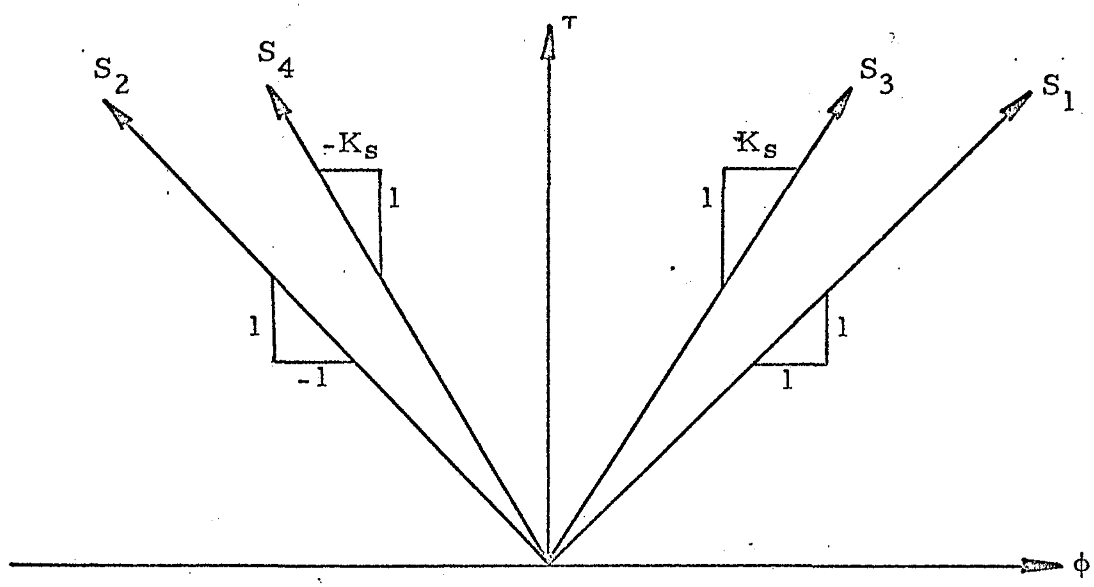

Figure 5. Characteristic directions--Shear theory

plane represent wave velocities, it is apparent from the figure that waves travel through the shell at the two non-dimensional velocities $c = 1$ and $c_s = K_s$.

The wave which travels at the velocity $c = 1$ is made up of two parts. One part is essentially an extensional wave while the other is predominantly a bending wave. The other wave, which travels at the velocity $c_s = K_s$, is essentially a shear wave.

Membrane Theory.--The shear theory characteristic equations have been developed in the first part of this section. Similar equations will now be derived for a shell which undergoes only extensional deformations (i.e., membrane theory).

The membrane theory characteristic equations can either be developed from equations 2.6 and 2.7 or from the previously developed shear theory solution. This latter method will be used here.

As discussed in Chapter II, pages 13-14, membrane theory equations can be determined from shear theory equations if it is assumed that $m_\phi = q_{b\phi} = 0$. Furthermore, this assumption infers that $\varepsilon \approx K_s \approx 0$. Using these assumptions, equations 4.10 reduce to the form

$$\begin{aligned} &\frac{\partial}{\partial \tau}\left(-\upsilon n_\phi + n_\theta\right) = \left(1-\upsilon^2\right)\left(Y_1 + \dot{w}\right) \\ &\left(\frac{\partial}{\partial \phi} + \frac{\partial}{\partial \tau}\right)\left(n_\phi - \dot{u}\right) = \upsilon Y_1 - Y_2 + (1+\upsilon)\dot{w} - P \end{aligned} \qquad (4.14)$$

$$\left(-\frac{\partial}{\partial\phi}+\frac{\partial}{\partial\tau}\right)(n_\phi+\dot{u}) = \upsilon Y_1 + Y_2 + (1+\upsilon)\dot{w} + P$$

$$\frac{\partial\dot{w}}{\partial\tau} = -(n_\phi + n_\theta) + Q$$

As with the shear theory characteristic equations, equations 4.14 may be written in terms of a new set of variables if we let

$$\begin{aligned} V_1 &= n_\phi - \dot{u} \\ V_2 &= n_\phi + \dot{u} \\ V_7 &= -\upsilon n_\phi + n_\theta \end{aligned} \tag{4.15}$$

Using equations 4.15, the following relations for the physical variables may be defined:

$$\begin{aligned} n_\phi &= \tfrac{1}{2}(V_1 + V_2) \\ n_\theta &= V_7 + \tfrac{\upsilon}{2}(V_1 + V_2) \\ \dot{u} &= \tfrac{1}{2}(V_2 - V_1) \end{aligned} \tag{4.16}$$

Using equations 4.15 and 4.16, the membrane theory characteristic equations (equations 4.14) may now be written

$$\begin{aligned} \frac{dV_1}{ds_1} &= \upsilon Y_1 - Y_2 + (1+\upsilon)\dot{w} - P \\ \frac{dV_2}{ds_2} &= \upsilon Y_1 + Y_2 + (1+\upsilon)\dot{w} + P \\ \frac{dV_7}{d\tau} &= (1-\upsilon^2)(Y_1 + \dot{w}) \\ \frac{d\dot{w}}{d\tau} &= -\left(\frac{1+\upsilon}{2}\right)(V_1 + V_2) - V_7 + Q \end{aligned} \tag{4.17}$$

where ds_1 and ds_2 are the same as in equations 4.13.

Equations 4.17 are defined for the characteristic directions shown in Figure 6. It is apparent from the figure that waves travel through the shell at only the non-dimensional velocity c = 1. This phenomena is to be expected when only extensional effects are considered.

General Solution of Characteristic Equations

When written in the form given by equations 4.13, the characteristic equations become ordinary differential equations. These equations can be easily integrated in their appropriate characteristic directions.

For example, if points R_1 and R_2 (see Figure 7) are an infinitesimal distance apart, the fifth of equations 4.13 can be integrated to get

$$V_5(R_1) = V_5(R_2) + \int_{s_1(R_2)}^{s_1(R_1)} \left[\upsilon Y_3 - Y_4 + \frac{1}{2}(V_3 + V_4) \right] ds_1 \tag{4.18}$$

This equation can be evaluated provided that the variables Y_3, Y_4, V_3, V_4, and V_5 are known at the point R_2.

Similar equations can be written by integrating the rest of equations 4.13 resulting in a set of eight equations in terms of the physical variables and the applied loads. Therefore, in theory at least, the complete solution at point R_1 can be found provided that all the variables are known in the region A.

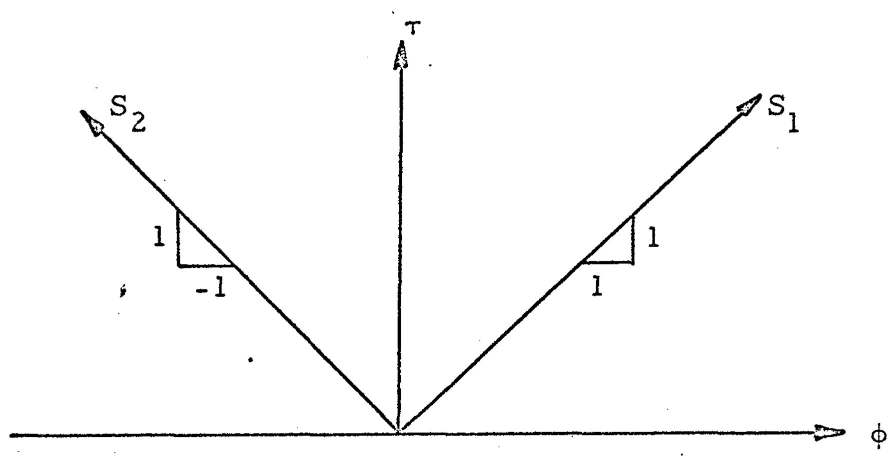

Figure 6. Characteristic Directions--
Membrane theory

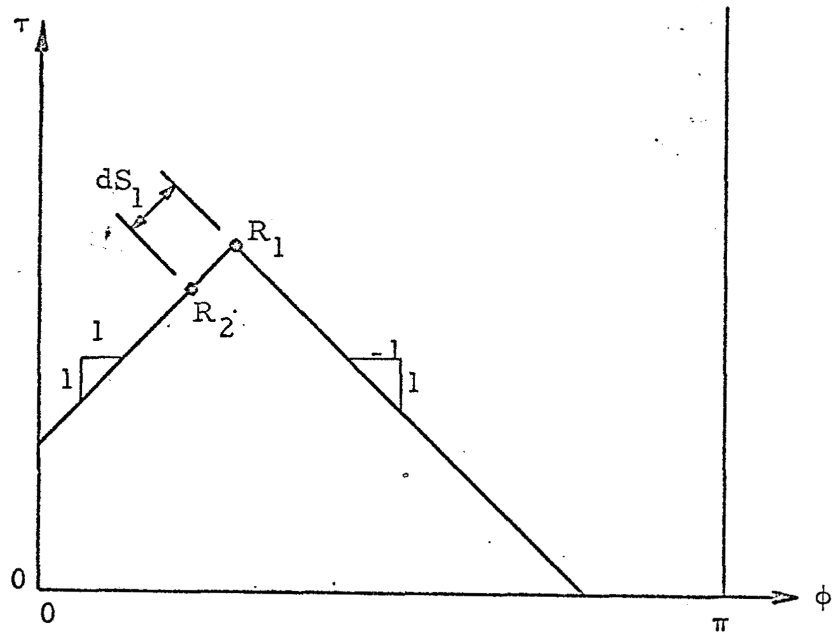

Figure 7. General solution to characteristic equations

It is noted that there are essentially ten unknown variables in equations 4.13. These include the loads P and Q and the set of eight variables represented by either V_i or the physical variables. The quantities Y_i are related to the physical variables through equations 4.2.

The unknown variables can be determined throughout region A provided that they are known along those portions of the boundaries $\phi=0$, $\phi=\pi$, and $\tau=0$ that border on the region.

Using a prescribed set of initial conditions all of the variables can be determined along the boundary $\tau=0$.

Assuming that the applied loads P and Q can be expressed as functions of the other physical variables, only the variables V_i (or the physical variables) are affected by the boundary conditions along $\phi=0$ and $\phi=\pi$.

Along the boundary $\phi=0$, the variables V_2, V_4, and V_6 can be determined by the direct integration of equations 4.13. The remaining variables can be determined through an examination of the relations Y_i as defined in equations 4.2. If the relations Y_i are to remain bounded at $\phi=0$, it is seen that

$$\begin{aligned} \dot{u} &\equiv 0 \\ n_\phi &\equiv n_\theta \\ \varepsilon\dot{\beta}_\phi &\equiv 0 \\ m_\phi &\equiv m_\theta \\ q_{\partial\phi} &\equiv 0 \end{aligned} \tag{4.19}$$

since $(\operatorname{ctn} \phi)_{\phi=0} = \infty$. Equations 4.19 are recognized as the usual boundary conditions for the apex of a spherical shell.

Equations 4.19 are sufficient to define the remaining unknown variables along the boundary $\phi=0$. However, the indeterminate quantities Y_i must be evaluated before these remaining variables can be defined. As shown in equations C.20, $(Y_i)_{\phi=0}$ are defined by the relations

$$
\begin{aligned}
Y_1 &= \frac{\partial \dot{u}}{\partial \phi} \\
Y_2 &= -\frac{\partial n_\phi}{\partial \phi} - P \\
Y_3 &= \frac{\partial \varepsilon \dot{\beta}_\phi}{\partial \phi} \\
Y_4 &= -\frac{\partial m_\phi}{\partial \phi} \\
Y_5 &= 2n_\phi - Q - \frac{\partial q_\phi}{\partial \phi} + \frac{\partial \dot{w}}{\partial \tau}
\end{aligned}
\qquad (4.20)
$$

It is further shown in equations C.20 that

$$
\begin{aligned}
\frac{\partial \dot{w}}{\partial \phi} &= 0 \\
\frac{\partial n_\phi}{\partial \tau} &= (1+\upsilon)(Y_1 + \dot{w}) \\
\frac{\partial m_\phi}{\partial \tau} &= (1+\upsilon) Y_3
\end{aligned}
\qquad (4.21)
$$

Using equations 4.19 and 4.21 and computational techniques to be discussed later, the right-hand side of equations 4.20 may always be computed.

A procedure similar to that discussed above for the boundary $\phi=0$ may be used to determine the variables V_i along the boundary $\phi = \pi$. In this latter case, the variables V_1, V_3, and V_5 may be determined by the direct integration of equations 4.13. Since $(\cot\phi)_{\phi=\pi} = -\infty$ the remaining variables are again determined through the use of equations 4.19 to 4.21.

Using the general procedures outlined above, it is seen that the complete solution for the point R_1 and, for that matter, for all points in the space-time plane can always be determined. Detailed numerical procedures and the application to the impact of a spherical shell on a deformable surface will be discussed later.

A procedure similar to that discussed above for the general shear theory can be developed for membrane theory. In this case, conditions along the boundaries $\phi=0$ and $\phi=\pi$ require that

$$\begin{aligned} \dot{u} &\equiv 0 \\ n_\phi &\equiv n_\theta \end{aligned} \qquad (4.22)$$

Furthermore, along these boundaries it is seen that

$$\begin{aligned} Y_1 &= \frac{\partial \dot{u}}{\partial \phi} \\ Y_2 &= -\frac{\partial n_\phi}{\partial \phi} - P \\ \frac{\partial n_\phi}{\partial \tau} &= (1+\nu)(Y_1 + \dot{w}) \end{aligned} \qquad (4.23)$$

Along the boundary $\phi=0$, the variable V_2 can be determined by the direct integration of the second of equations 4.19. In a similar manner, the variable V_1 can be determined along the boundary $\phi=\pi$. The remaining variables can be found by the solution of the last of equations 4.17 and equations 4.22 and 4.23.

Specific Solution of Characteristic Equations

As discussed in the previous article, a solution using the method of characteristics can be determined provided that the necessary initial conditions and load-displacement relations are prescribed.

The initial conditions for the impact of a spherical shell on a deformable surface may be defined as

$$\begin{aligned}
&u(\phi,0) = w(\phi,0) = 0 \\
&n_\phi(\phi,0) = n_\theta(\phi,0) = 0 \\
&m_\phi(\phi,0) = m_\theta(\phi,0) = 0 \\
&q_{b\phi}(\phi,0) = 0 \\
&\dot{\beta}_\phi(\phi,0) = 0
\end{aligned} \tag{4.24}$$

and, using equations 3.35,

$$\dot{u}(\phi,0) = -\beta\left(\frac{R}{h}\right)\sin\phi$$

$$\dot{w}(\phi,0) = \beta\left(\frac{R}{h}\right)\cos\phi$$

The load-displacement relation for this problem is given in Chapter II, pages 14-17 as

$$P = 0$$

$$Q = \begin{cases} G(d-w)\ , & \phi_o^* \leq \phi \leq \phi_o \\ 0\ , & 0 \leq \phi \leq \phi_o^*\ ,\ \phi_o \leq \phi \leq \pi \end{cases} \tag{4.25}$$

As will be seen in the next article, the angles ϕ_o and ϕ_o^* can be found directly through the use of equations 4.25.

Computational Procedure--Shear Theory

The numerical procedures necessary to solve the problem will now be described. Solutions are given for both shear theory and membrane theory. The complex nature of these solutions requires the use of a digital computer in the carrying out of the computations.

In the next article, a computer program based on the membrane theory solution will be described. Numerical computations will be carried out only for this solution.

Various first order ordinary differential equations must be integrated during the problem solution. In general, these equations are of the form

$$\frac{df(u_j)}{dh} = g(u_j) \tag{4.26}$$

where u_j represents the various physical variables, applied loads, and functions of h and dh represents increments in the various characteristic directions.

The integration of equation 4.26 from point 1 to point 2 results in the following solution for $f_2(u_j)$:

$$f_2(u_j) = f_1(u_j) + g_1(u_j)\,dh$$

If the function $g_1(u_j)$ is a function of ϕ rather than of h, equation 4.27 must be written in the form:

$$f_2(u_j) = f_1(u_j) + g_1(u_j)\,d\phi \tag{4.27}$$

Using the general theory described above, the shear theory solution will now be presented. In this case, solutions are found for each of the grid points defined in Figure 8. Since π is generally not an even multiple of $\Delta\tau$, the interval between points $n_{max}-1$ and n_{max} will require special consideration.

It is noted that the grid point numbering system is repeated at each time τ_i. This scheme is used to minimize the required computer storage during numerical computations.

In the derivations which follow, the i^{th} time is the one currently being evaluated. The previous time is denoted by the subscript $i-1$.

The solution of equations 4.13 for a general point n_i may be found using existing solutions at the $i-1$ time (see Figure 9) and integrals of the form given by equation 4.27. Therefore,

$$\begin{aligned}
V_1(n_i) &= V_1(n-1_{i-1}) + \Big[\upsilon Y_1(n-1_{i-1}) - Y_2(n-1_{i-1}) - \tfrac{1}{2}\Big(\tfrac{1+\upsilon}{K_s}-1\Big)V_3(n-1_{i-1}) \\
&\quad + \tfrac{1}{2}\Big(\tfrac{1+\upsilon}{K_s}-1\Big)V_4(n-1_{i-1})\Big]\Delta\tau \\
V_2(n_i) &= V_2(n+1_{i-1}) + \Big[\upsilon Y_1(n+1_{i-1}) + Y_2(n+1_{i-1}) - \tfrac{1}{2}\Big(\tfrac{1+\upsilon}{K_s}-1\Big)V_3(n+1_{i-1}) \\
&\quad + \tfrac{1}{2}\Big(\tfrac{1+\upsilon}{K_s}+1\Big)V_4(n+1_{i-1})\Big]\Delta\tau \\
V_3(n_i) &= V_3(n-\xi) + K_s^2\Big\{\tfrac{K_s}{2}\Big(\tfrac{R}{\varepsilon h}\Big)\big[V_6(n-\xi) - V_5(n-\xi)\big] + V_7(n-\xi) \\
&\quad + \Big(\tfrac{1+\upsilon}{2}\Big)\big[V_1(n-\xi) + V_2(n-\xi)\big] - Y_5(n-\xi) - Q(n-\xi)\Big\}\Delta\tau \\
V_4(n_i) &= V_4(n+\xi) + K_s^2\Big\{\tfrac{K_s}{2}\Big(\tfrac{R}{\varepsilon h}\Big)\big[V_6(n+\xi) - V_5(n+\xi)\big] - V_7(n+\xi) \\
&\quad - \Big(\tfrac{1+\upsilon}{2}\Big)\big[V_1(n+\xi) + V_2(n+\xi)\big] + Y_5(n+\xi) + Q(n+\xi)\Big\}\Delta\tau
\end{aligned} \tag{4.28}$$

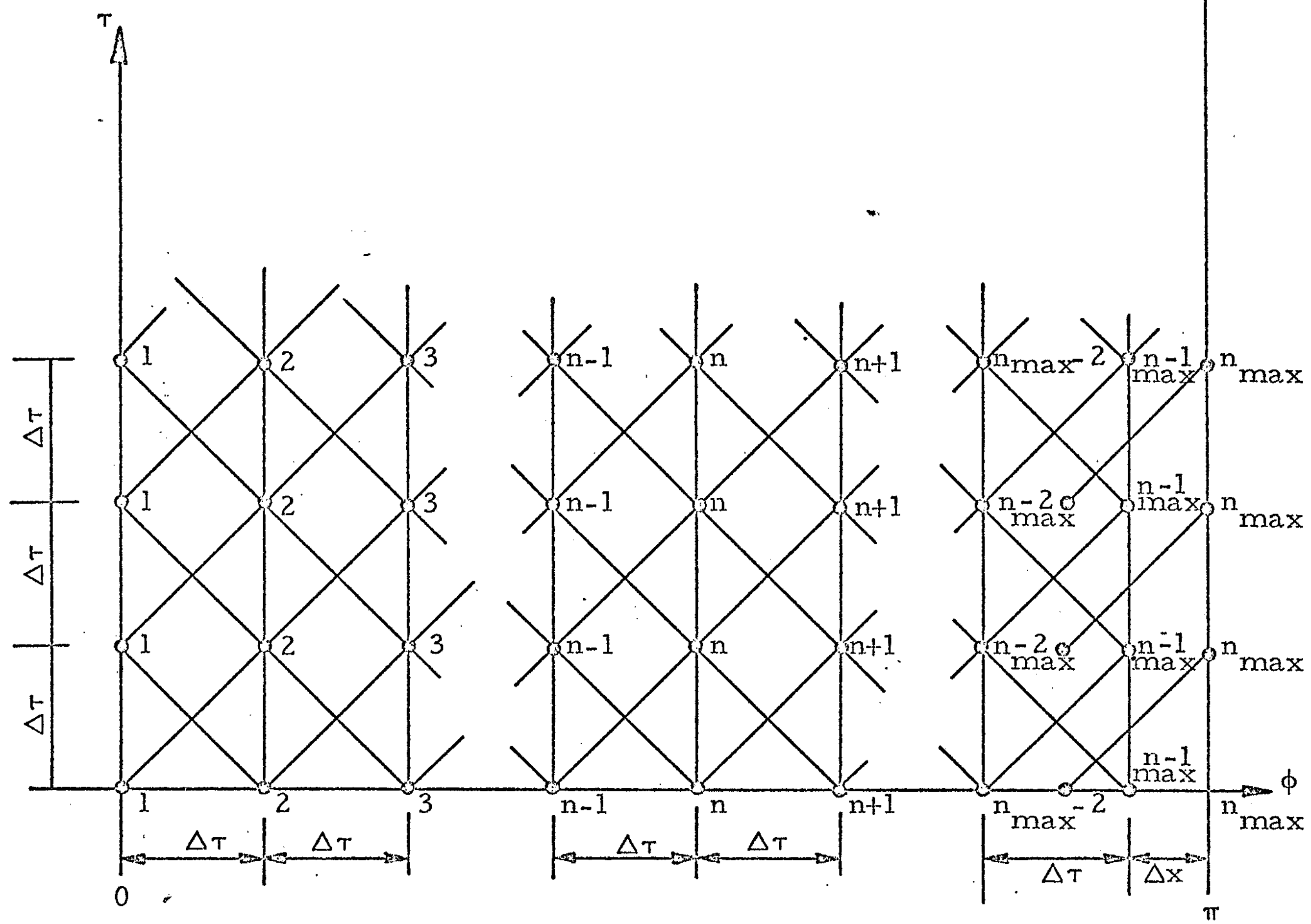

Figure 8. Characteristic solution grid point layout

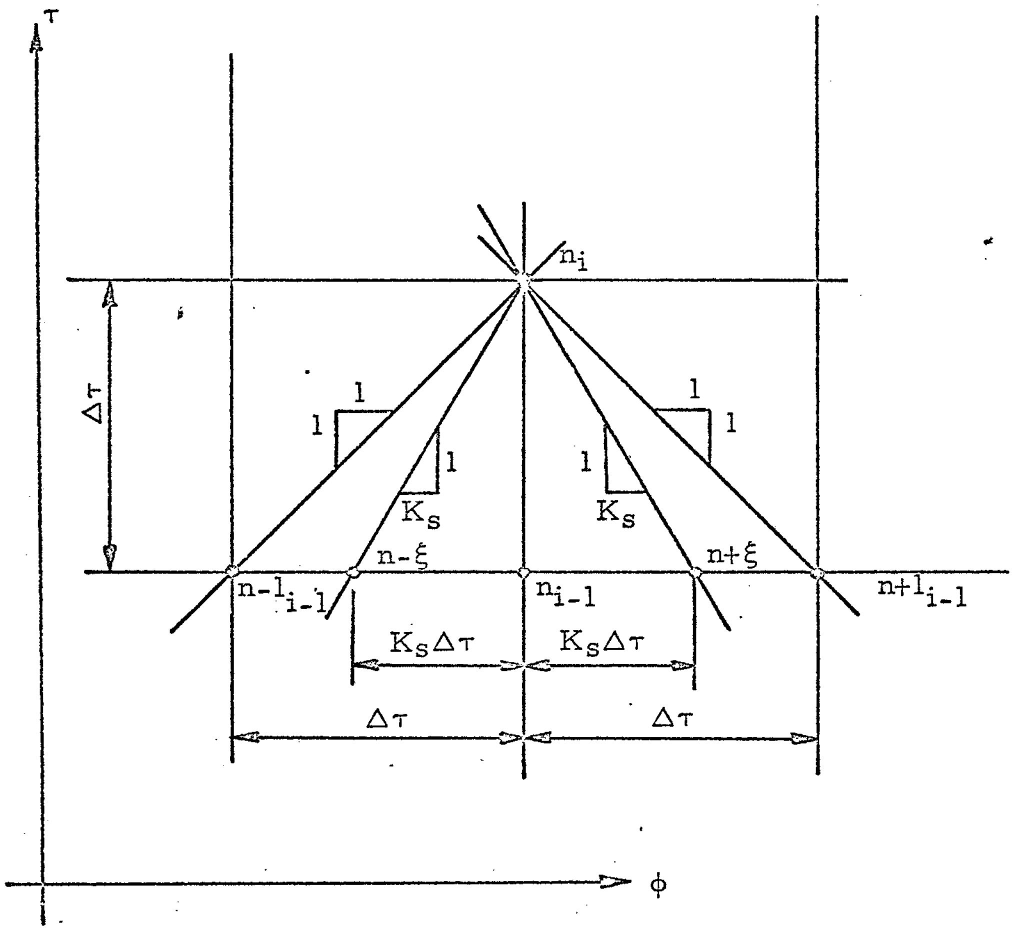

Figure 9. Layout at interior grid point

$$V_5(n_i) = V_5(n-1_{i-1}) + \left\{ \upsilon Y_3(n-1_{i-1}) - Y_4(n-1_{i-1}) + \tfrac{1}{2}\left[V_3(n-1_{i-1}) + V_4(n-1_{i-1}) \right] \right\} \Delta\tau$$

$$V_6(n_i) = V_6(n+1_{i-1}) + \left\{ \upsilon Y_3(n+1_{i-1}) + Y_4(n+1_{i-1}) - \tfrac{1}{2}\left[V_3(n+1_{i-1}) + V_4(n+1_{i-1}) \right] \right\} \Delta\tau$$

$$V_7(n_i) = V_7(n_{i-1}) + (1-\upsilon^2)\left\{ Y_1(n_{i-1}) + \frac{1}{2K_5}\left[V_4(n_{i-1}) - V_3(n_{i-1}) \right] \right\} \Delta\tau$$

$$V_8(n_i) = V_8(n_{i-1}) + (1-\upsilon^2)\, Y_3(n_{i-1})\, \Delta\tau$$

The physical variables $n_\phi(n_i)$, $n_\theta(n_i)$, $m_\phi(n_i)$, $m_\theta(n_i)$, $q_\phi(n_i)$, $\dot{u}(n_i)$, $\dot{w}(n_i)$, and $\varepsilon\dot{\beta}_\phi(n_i)$ are readily found through the use of equations 4.12 once the variables $V_j(n_i)$ are known. The displacements $u(n_i)$ and $w(n_i)$ can now be computed through the integration of $\dot{u}$ and $\dot{w}$. These relations may be written in the form

$$\begin{aligned} u(n_i) &= u(n_{i-1}) + \frac{\Delta\tau}{2}\left[\dot{u}(n_i) + \dot{u}(n_{i-1}) \right] \\ w(n_i) &= w(n_{i-1}) + \frac{\Delta\tau}{2}\left[\dot{w}(n_i) + \dot{w}(n_{i-1}) \right] \end{aligned} \qquad (4.29)$$

Using equations 4.25 and 4.29, the radial load $Q(n_i)$ can now be written in the form

$$Q(n_i) = \begin{cases} G\left[d(n) - w(n_i) \right] & , \quad w(n_i) > d(n) \\ 0 & , \quad w(n_i) \leq d(n) \end{cases} \qquad (4.30)$$

where $\quad d(n) = \frac{R}{h}\left[\frac{1-\cos\phi(n)}{\cos\phi(n)} \right]$

The angles $\phi_o^*(\tau_i)$ and $\phi_o(\tau_i)$ are defined as those values of ϕ just to the left and just to the right of the loaded area of the shell.

Except for the points where $\phi = 0$ and $\phi = \pi$, the quantities $Y_j(n_i)$ can be readily determined from equations 4.2 once the physical variables are known.

The values of the variables at the points $n-\xi$ and $n+\xi$ are found using the interpolation relations

$$f(n-\xi) = K_s f(n-1_{i-1}) + (1-K_s) f(n_{i-1})$$
$$f(n+\xi) = (1-K_s) f(n_{i-1}) + K_s f(n+1_{i-1}) \tag{4.31}$$

Solutions for the points corresponding to $\phi=0$ and $\phi=\pi$ require special consideration. In each of these cases, the general procedure outlined on pages 51-57 must be followed. Therefore, if $\phi=0$, $n=1$ and $V_2(1_i)$, $V_4(1_i)$, and $V_6(1_i)$ can be found by the direct application of equations 4.28.

The remaining variables are found through the use of equations 4.19 to 4.21. Using these relations, it is seen that

$$\dot{w}(1_i) = \dot{w}(2_i)$$
$$n_\phi(1_i) = n_\phi(1_{i-1}) + (1+\upsilon)\left[Y_1(1_{i-1}) + \dot{w}(1_{i-1})\right]\Delta\tau \tag{4.32}$$
$$m_\phi(1_i) = m_\phi(1_{i-1}) + (1+\upsilon)\, Y_3(1_{i-1})\,\Delta\tau$$

and

$$Y_1(1_i) = \frac{\dot{u}(2_i)}{\Delta\tau}$$
$$Y_2(1_i) = \frac{n_\phi(1_i) - n_\phi(2_i)}{\Delta\tau}$$
$$Y_3(1_i) = \frac{\varepsilon\dot{\beta}_\phi(2_i)}{\Delta\tau} \tag{4.33}$$
$$Y_4(1_i) = \frac{m_\phi(1_i) - m_\phi(2_i)}{\Delta\tau}$$
$$Y_5(1_i) = 2n_\phi(1_i) - Q(1_i) - \frac{q_\phi(2_i)}{\Delta\tau} + \frac{\dot{w}(1_i) - \dot{w}(1_{i-1})}{\Delta\tau}$$

Using equations 4.19 and 4.32, solutions for the remaining variables $V_j(1_i)$ can be found from equations 4.11. The displacements and applied loads are determined as in the general case. Therefore, all variables are known at the point n = 1 and the problem solution can proceed.

A similar procedure can be followed if $\phi = \pi (n = n_{max})$. However, since $\Delta x \leqslant \Delta\tau$ certain additional computations must be carried out for these points.

As described on page 55, $V_1(n_{max_i})$, $V_3(n_{max_i})$, and $V_5(n_{max_i})$ can be found by the direct application of equations 4.28. However, to do this the variables must be known at the points $n-\xi$ and $n-\eta$ (see Figure 10). The values of the variables are found at these points using the interpolation relations

$$\begin{aligned} f(n-\xi) &= \left(\frac{K_s\Delta\tau}{\Delta\tau+\Delta X}\right) f(n_{max}-2_{i-1}) + \left[\frac{(1-K_s)\Delta\tau + \Delta X}{\Delta\tau + \Delta X}\right] f(n_{max_{i-1}}) \\ f(n-\eta) &= \left(\frac{\Delta\tau - \Delta X}{\Delta\tau}\right) f(n_{max}-2_{i-1}) + \left(\frac{\Delta X}{\Delta\tau}\right) f(n_{max}-1_{i-1}) \end{aligned} \tag{4.34}$$

The remaining variables are found through the use of equations 4.19 to 4.21. Using these relations, it is seen that

$$\begin{aligned} \dot{w}(n_{max_i}) &= \dot{w}(n_{max}-2_i) \\ n_\phi(n_{max_i}) &= n_\phi(n_{max_{i-1}}) + (1+v)\left[Y_1(n_{max_{i-1}}) + \dot{w}(n_{max_{i-1}})\right]\Delta\tau \\ m_\phi(n_{max_i}) &= m_\phi(n_{max_{i-1}}) + (1+v)Y_3(n_{max_{i-1}})\,\Delta\tau \end{aligned} \tag{4.35}$$

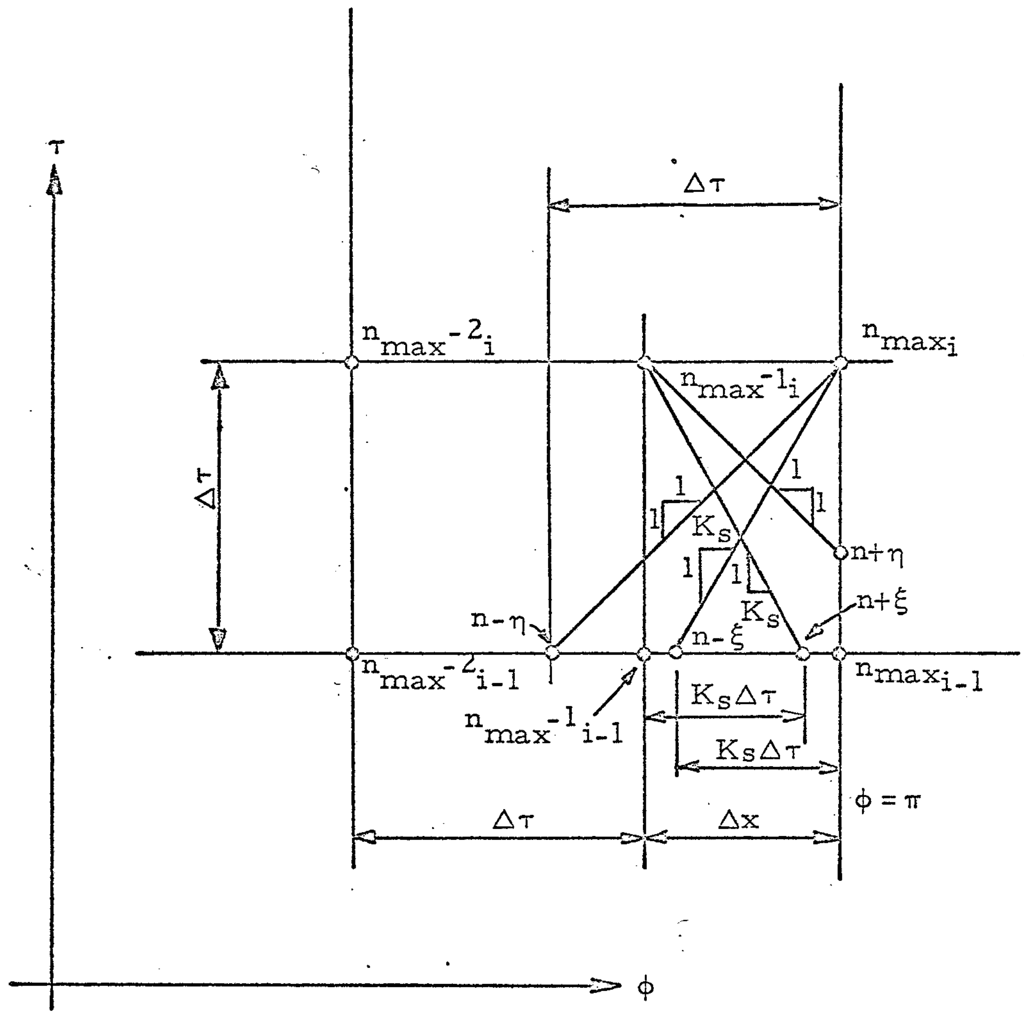

Figure 10. Layout for grid points near $\phi = \pi$

and

$$
\begin{aligned}
Y_1(n_{max_i}) &= -\frac{\dot{u}(n_{max}-2_i)}{\Delta X + \Delta\tau} \\
Y_2(n_{max_i}) &= \frac{n_\phi(n_{max}-2_i) - n_\phi(n_{max_i})}{\Delta X + \Delta\tau} \\
Y_3(n_{max_i}) &= -\frac{\varepsilon\dot{\beta}_\phi(n_{max}-2_i)}{\Delta X + \Delta\tau} \\
Y_4(n_{max_i}) &= \frac{m_\phi(n_{max}-2_i) - m_\phi(n_{max_i})}{\Delta X + \Delta\tau} \\
Y_5(n_{max_i}) &= 2n_\phi(n_{max_i}) - Q(n_{max_i}) + \frac{q_\phi(n_{max}-2_i)}{\Delta X + \Delta\tau} + \frac{\dot{w}(n_{max_i}) - \dot{w}(n_{max_{i-1}})}{\Delta\tau}
\end{aligned} \tag{4.36}
$$

Using equations 4.19 and 4.35, solutions for the remaining variables $V_j(n_{max_i})$ can be found from equations 4.11. The displacements and applied load are again determined as in the general case. Therefore, all variables are known at the point $n = n_{max}$ and the problem solution can proceed.

The solutions for the variables $V_2(n_{max}-1_i)$, $V_4(n_{max}-1_i)$ and $V_6(n_{max}-1_i)$ are also special cases since $\Delta X \leqslant \Delta\tau$ (see Figure 10). To get these results, the solution for point n_{max_i} must first be obtained. Then the required variables can be computed from the relations

$$
\begin{aligned}
V_2(n_{max}-1_i) &= V_2(n+\eta) + \Big[\upsilon Y_1(n+\eta) + Y_2(n+\eta) - \tfrac{1}{2}\Big(\tfrac{1+\upsilon}{K_s} - 1\Big) V_3(n+\eta) \\
&\quad + \tfrac{1}{2}\Big(\tfrac{1+\upsilon}{K_s} + 1\Big) V_4(n+\eta)\Big] \Delta X \\
V_4(n_{max}-1_i) &= V_4(n+\xi) + K_s\Big\{\tfrac{K_s}{2}\Big(\tfrac{R}{\varepsilon h}\Big)\big[V_6(n+\xi) - V_5(n+\xi)\big] - V_7(n+\xi) \\
&\quad - \Big(\tfrac{1+\upsilon}{2}\Big)\big[V_1(n+\xi) + V_2(n+\xi)\big] + Y_5(n+\xi) + Q(n+\xi)\Big\} \Delta R \\
V_6(n_{max}-1_i) &= V_6(n+\eta) + \Big\{\upsilon Y_3(n+\eta) + Y_4(n+\eta) - \tfrac{1}{2}\big[V_3(n+\eta) + V_4(n+\eta)\big]\Big\} \Delta X
\end{aligned} \tag{4.37}
$$

where

$$\Delta R = \begin{cases} K_s \Delta\tau & , \quad K_s \Delta\tau \leqslant \Delta x \\ \Delta x & , \quad K_s \Delta\tau \geqslant \Delta x \end{cases}$$

The values of the variables at the points $n+\xi$ and $n+\eta$ are found from the interpolation relations

$$f(n+\xi) = \begin{cases} \left(\dfrac{\Delta x - K_s \Delta\tau}{\Delta\tau + \Delta x}\right) f(n_{max} - 2_{i-1}) + \left[\dfrac{(1+K_s)\Delta\tau}{\Delta\tau + \Delta x}\right] f(n_{max_{i-1}}) \,, & K_s \Delta\tau \leqslant \Delta x \\ \left(\dfrac{K_s \Delta\tau - \Delta x}{K_s \Delta\tau}\right) f(n_{max_i}) + \left(\dfrac{\Delta x}{K_s \Delta\tau}\right) f(n_{max_{i-1}}) \,, & K_s \Delta\tau > \Delta x \end{cases} \tag{4.38}$$

$$f(n+\eta) = \left(\frac{\Delta\tau - \Delta x}{\Delta\tau}\right) f(n_{max_i}) + \left(\frac{\Delta x}{\Delta\tau}\right) f(n_{max_{i-1}})$$

The computation procedure for each time $\tau_i > 0$ will be to find the solution for each grid point defined for this time. The solution for the time $\tau_i - d\tau$ will be used in this computation. By proper manipulation of computer core storage, only the solutions for the times τ_i and $\tau_i - d\tau$ need be retained at any one time. It is noted that the values of the variables at $\tau_i = 0$ are found from the initial conditions.

The procedure is now complete. However, two additional comments are in order. First, since the shell load cannot physically occur at an angle $\phi \geqslant \frac{\pi}{2}$ and since d(n) blows up at $\phi = \frac{\pi}{2}$, it is prudent to check for these unlikely situations in the numerical procedure.

Second, for many of the examples which could be studied, the shell completely rebounds prior to the time that the fastest stress waves reach $\phi = \pi$. Therefore, to minimize computation time, some points in the space-time plane need not be computed.

For example, if the problem solution were as shown in Figure 11, only those points in the region bounded by points A, B, C, and D need be computed. It is noted that values for points along the line AD can be determined from the initial conditions.

Computation Procedure--Membrane Theory

The computation procedure for the membrane theory solution will now be presented. This procedure is essentially the same as the one developed in the last article for the shear theory solution.

A computer program has been developed to carry out this solution. The numerical results from this program are discussed in Chapter V.

The grid numbering system used for this solution will be as shown in Figures 8-10 with the exception that the points $n-\xi$ and $n+\xi$ are no longer required.

The solution of equations 4.17 for a general point n_i may be found using existing solutions at the $i-1$ time and integrals of the form given by equation 4.27. Therefore,

$$V_1(n_i) = V_1(n-1_{i-1}) + \left[\upsilon Y_1(n-1_{i-1}) - Y_2(n-1_{i-1}) + (1+\upsilon)\dot{w}(n-1_{i-1})\right]\Delta\tau \qquad (4.39)$$

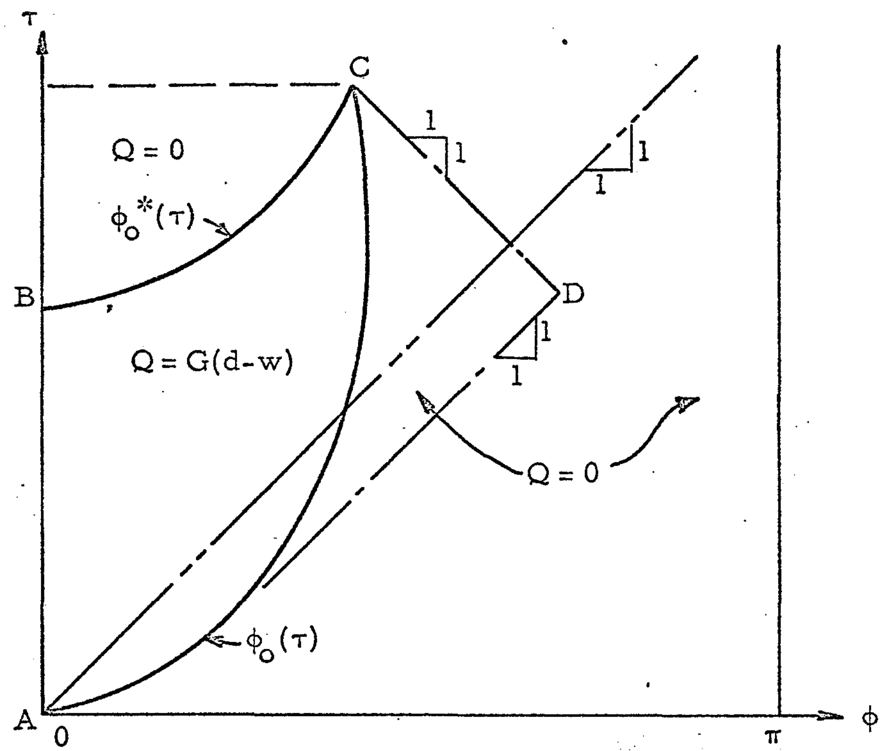

Figure 11. Illustration of shell-surface contact area

$$V_2(n_i) = V_2(n+1_{i-1}) + \left[\nu Y_1(n+1_{i-1}) + Y_2(n+1_{i-1}) + (1+\nu)\,\dot{w}(n+1_{i-1})\right]\Delta\tau$$

$$V_7(n_i) = V_7(n_{i-1}) + (1-\nu^2)\left[Y_1(n_{i-1}) + \dot{w}(n_{i-1})\right]\Delta\tau$$

$$\dot{w}(n_i) = \dot{w}(n_{i-1}) + \left\{-\left(\frac{1+\nu}{2}\right)\left[V_1(n_{i-1}) + V_2(n_{i-1})\right] - V_7(n_{i-1}) + Q(n_{i-1})\right\}\Delta\tau$$

The remaining physical variables $n_\phi(n_i)$, $n_\theta(n_i)$, and $\dot{u}(n_i)$ are readily found through the use of equations 4.16 once equations 4.39 have been evaluated. The displacements $u(n_i)$ and $w(n_i)$, the radial load $Q(n_i)$, and the angles $\phi_o^*(n_i)$ and $\phi_o^{\cdot}(n_i)$ can be computed from equations 4.29 and 4.30 just as in the shear theory solution.

Except for the points where $\phi = 0$ and $\phi = \pi$, the quantities $Y_1(n_i)$ and $Y_2(n_i)$ can be readily determined from equations 4.2 once the physical variables are known. Solutions for the points corresponding to $\phi = 0$ and $\phi = \pi$ require special consideration. In each of these cases, the general procedure outlined on pages 51-57 must be followed.

Therefore, if $\phi = 0$, $n = 1$ and $V_2(n_i)$ can be found by the direct application of the second of equations 4.39. The remaining variables can be found through the use of equations 4.22, 4.23, and the last of 4.39. Using these relations, it is seen that

$$n_\phi(1_i) = n_\phi(1_{i-1}) + (1+\nu)\left[Y_1(1_{i-1}) + \dot{w}(1_{i-1})\right]\Delta\tau$$
$$\dot{w}(1_i) = \dot{w}(1_{i-1}) + \left\{-\left(\frac{1+\nu}{2}\right)\left[V_1(1_{i-1}) + V_2(1_{i-1})\right] - V_7(1_{i-1}) + Q(1_{i-1})\right\}\Delta\tau \qquad (4.40)$$

$$Y_1(1_i) = \frac{\dot{u}(2_i)}{\Delta\tau}$$

$$Y_2(1_i) = \frac{n_\phi(1_i) - n_\phi(2_i)}{\Delta\tau}$$

Using equations 4.22 and 4.40, solutions for the remaining variables $V_1(1_i)$ and $V_7(1_i)$ can apparently be found from equations 4.15. On the other hand, a further examination of equations 4.15 shows that since $\dot{u}(1)=0$, then $V_1(1) \equiv V_2(1)$.

It is apparent that five equations are available for the computation of the four variables $V_1(1_i)$, $V_2(1_i)$, $V_7(1_i)$, and $\dot{w}(1_i)$. The accuracy of the numerical computation depends on the best selection of four equations to compute these variables. Experience has shown the best results to occur when $V_2(1_i)$ is computed using the relations $V_2(1_i) = V_1(1_i)$.

The procedure used here to compute $V_1(1_i)$, $V_2(1_i)$, $V_7(1_i)$, and $\dot{w}(1_i)$ is summarized as follows. $V_7(1_i)$ and $\dot{w}(1_i)$ are computed from the relations given in equations 4.39. $V_1(1_i)$ and $V_2(1_i)$ are then found from equations 4.15 wherein $n_\phi(1_i) \equiv n_o(1_i)$ and $\dot{u}(1_i) \equiv 0$.

The numerical computation of $Y_1(1_i)$ and $Y_2(1_i)$ may lead to erroneous results if the variation of $\dot{u}$ and n_ϕ with respect to ϕ is rapid or approximately zero near the apex of the shell. Since $\frac{\partial Q(1_i)}{\partial \phi}=0$ it seems reasonable to assume that $Y_2(1_i) \equiv 0$. This assumption has been used in all numerical computations presented herein to minimize the possibility of computational error.

Finally, the displacements and applied load are determined as in the general case. All variables are then known at the point n = 1 and the problem solution can proceed.

A similar procedure can be followed if $\phi = \pi\ (n = n_{max})$. However, since $\Delta x \leq \Delta\tau$, certain additional computations must be carried out for these points. As described on page 56, $V_1(n'_{max_i})$ can be found by the direct application of the first of equations 4.39. However, to do this the variables V_1, Y_1, Y_2, and $\dot{w}$ must be known at the point $n-\eta$. These variables are determined at this point through the use of the second of equations 4.34.

The remaining variables can then be found through the use of equations 4.22, 4.23, and the last of 4.39. Using these relations, it is seen that

$$
\begin{aligned}
n_\phi(n_{max_i}) &= n_\phi(n_{max_{i-1}}) + (1+\upsilon)\left[Y_1(n_{max_{i-1}}) + \dot{w}(n_{max_{i-1}})\right]\Delta\tau \\
\dot{w}(n_{max_i}) &= \dot{w}(n_{max_{i-1}}) + \Big\{-\left(\frac{1+\upsilon}{2}\right)\left[V_1(n_{max_{i-1}}) + V_2(n_{max_{i-1}})\right] \\
&\qquad -V_7(n_{max_{i-1}}) + Q(n_{max_{i-1}})\Big\}\Delta\tau \qquad (4.41) \\
Y_1(n_{max_i}) &= -\frac{\dot{u}(n_{max}-2_i)}{\Delta x + \Delta\tau} \\
Y_2(n_{max_i}) &= \frac{n_\phi(n_{max}-2_i) - n_\phi(n_{max_i})}{\Delta x + \Delta\tau}
\end{aligned}
$$

Using equations 4.22 and 4.41, solutions for the remaining variables $V_2(n_{max_i})$ and $V_7(n_{max_i})$ can be theoretically found from equations 4.15. Again, five equations with only four unknowns are seen to exist and the procedure outlined for n = 1 must be used to continue the computation.

The displacements and applied load are again determined as in the general case and the problem solution can proceed.

The solution for $V_2(n_{max}-l_i)$ is also a special case since $\Delta X \leq \Delta\tau$. To get this result, the solution for point $n_{max\,i}$ must first be obtained. Then the variables V_2, Y_1, Y_2, and $\dot{\omega}$ are found at the point $n+\eta$ using the second of equations 4.38. The desired variable may now be computed from the relation

$$V_2(n_{max}-l_i) = V_2(n+\eta) + \left[\upsilon Y_1(n+\eta) + Y_2(n+\eta) + (1+\upsilon)\dot{\omega}(n+\eta)\right]\Delta X \qquad (4.42)$$

As with the shear theory solution, the computation procedure for each time $\tau_i > 0$ will be to find the solution for each grid point defined for this time using the solution for the time $\tau_i - d\tau$. In this manner, only the solutions for the times τ_i and $\tau_i - d\tau$ need be stored in the computer at any one time. The values of each of the variables at $\tau_i = 0$ are found from the initial conditions.

The computer program used to carry out the above computations is shown schematically in Figure 12. The detailed development and FORTRAN listing for this program is given in Appendix D.

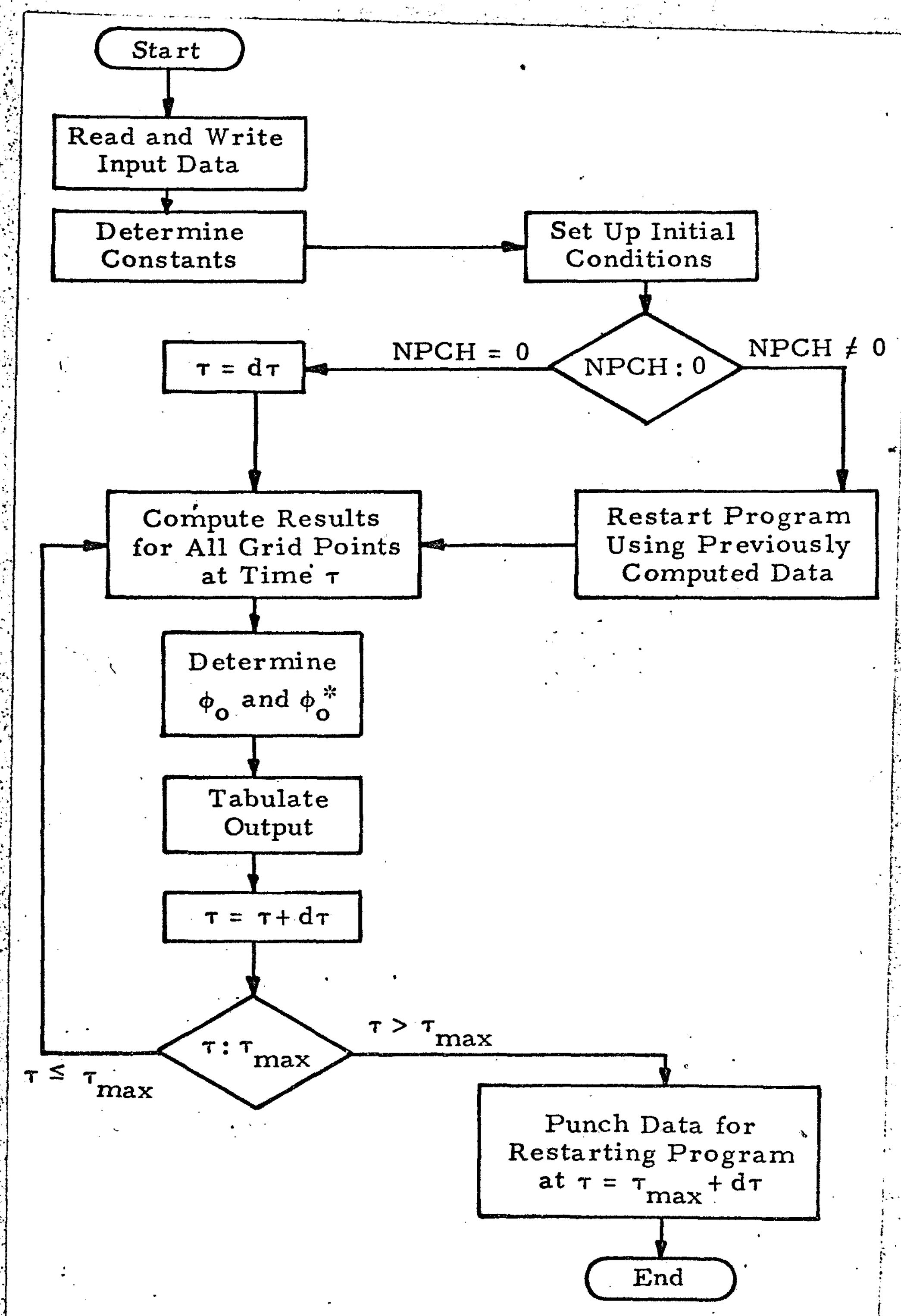

Figure 12. Flow chart--SHLWAV program

CHAPTER V

NUMERICAL COMPUTATIONS

General

The complexity of the methods derived in Chapters III and IV requires that a digital computer be used for the various problem solutions. The two methods based on the shell membrane theory equations have been programmed. The normal mode program is called SIMPAC and the characteristics program is called SHLWAV. The results obtained from these programs are described below.

As is often the case with computer solutions, many more results have been obtained than are presented. Only the results that significantly describe the behavior of an impacting shell are included.

The following types of information are presented:

(a) Radial displacement at the apex of the shell ($\phi = 0$) as a function of time.

(b) Shell-impact surface contact area as a function of time.

(c) Radial displacement and internal force as a function of ϕ for various significant times.

Three different computers have been used in carrying out the computations. An IBM 1620 computer with a 40,000 character core was used for some of the normal mode solutions. The remainder of the normal mode solutions and the characteristic solutions were carried out on either the U. S. C. - Honeywell H-800 computer or the UNIVAC 1107 computer owned and operated by the University Computing Company of El Segundo, California.

Description of Examples

The computer programs discussed above have been run for certain example cases. These examples, which are described in Table 2, represent both situations where the various theory assumptions are valid and situations where assumptions may not be valid. A critique of these assumptions and the situations wherein they apply is given in Chapter VI.

The example cases have been run for both the normal mode and the characteristic solutions. Other examples, not presented, have only been run for the normal mode solution due primarily to computer operating time limitations. Computer operating time limits the use of the characteristic solution to cases wherein the shell rebounds at a non-dimensional time of the same order of magnitude as the maximum contact angle ϕ_o.

The various solutions are based on the use of the non-dimensional variables K, β, υ, and R/h. The

TABLE 2

DESCRIPTION OF EXAMPLES

Case	K	β	υ	R/h	K* #/in^3	E #/in^2	h inches	ρ #/in^3/g
I	$(10)^{-4}$	0.1	0.3	1000	10,000	$(10)^7$	0.1	0.1
II	$(10)^{-6}$	0.01	0.3	1000	100	$(10)^7$	0.1	0.1

dimensional parameters K , E, h, and ρ are only given in Table 2 as illustrations of shell and surface parameters that will match the appropriate non-dimensional parameters.

Both cases I and II utilize a very thin shell with R/h = 1000. For case I, the initial non-dimensional impact velocity is $\beta = 0.1$ (i.e., $V_o = 0.1\,c$). This very high velocity is contrasted with the low velocity of $\beta = 0.01$ used for case II. The stiffness of the surface used for case I is two orders of magnitude harder than that used for case II.

Presentation of Results

Representative results from the examples described in Table 2 are given in Figures 13 to 32. These examples have been selected for presentation since they illustrate most of the advantages and disadvantages of the two analysis techniques used.

For case I, the shell is seen to rebound from the point $\phi = 0$ prior to complete rebound from the surface. A tendency to exhibit this same behavior is seen to exist in the case II solution although computer time limitations have prevented this latter case from being carried to complete rebound.

If the impact velocity is large, as in case I, the assumption of small changes in displacement with respect to shell angle ϕ may be violated after the time of $\phi = 0$

rebound. However, this violation should not affect the use of the resulting data in correlating the normal mode and characteristic solutions.

The case I example is described on Figures 13 to 23. The shell-surface contact area as a function of time is shown on Figure 13. Good correlation is seen to exist between the normal mode and characteristic solutions even though the normal mode solution is based on a minimum number of modes and the characteristic solution is based on a relatively large integration interval.

The radial displacement of the shell apex is given in Figure 14 for various case I solutions. It is seen that good correlation exists between the solutions when 20 modes are used in the normal mode solution and a small integration interval is used in the characteristic solution. The normal mode solution using only 10 modes is seen to be somewhat different from the characteristic solutions. This behavior tends to support the hypothesis that a large number of modes must be used to obtain an accurate normal mode solution.

Radial and tangential displacements are presented in Figure 15 for various times using characteristic solution data. Stress wave propagation effects are particularly noticeable on this figure in that the region affected by the stress waves and applied radial loads exhibit distinct

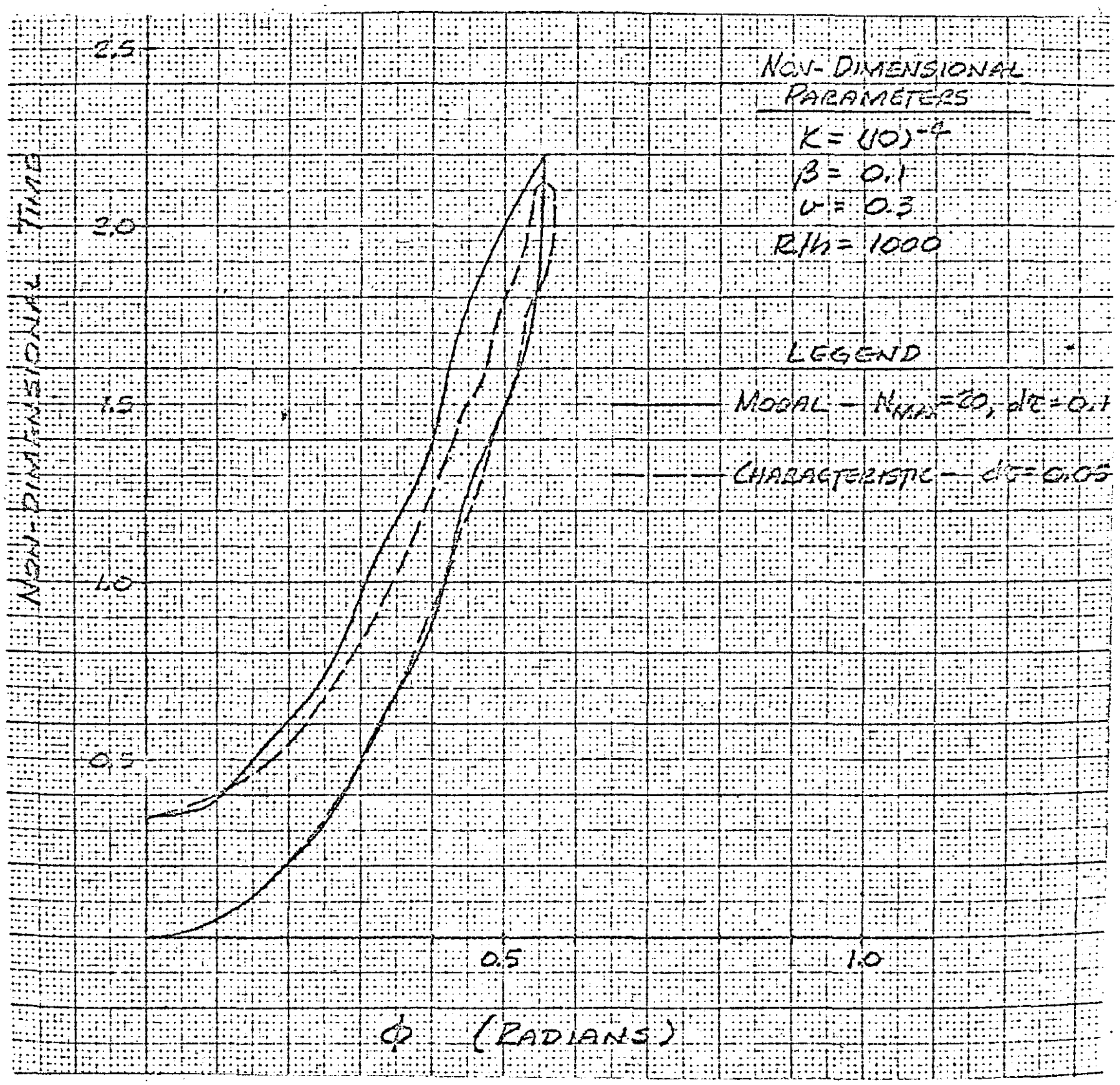

Figure 13. Case I--Description of shell-surface contact area

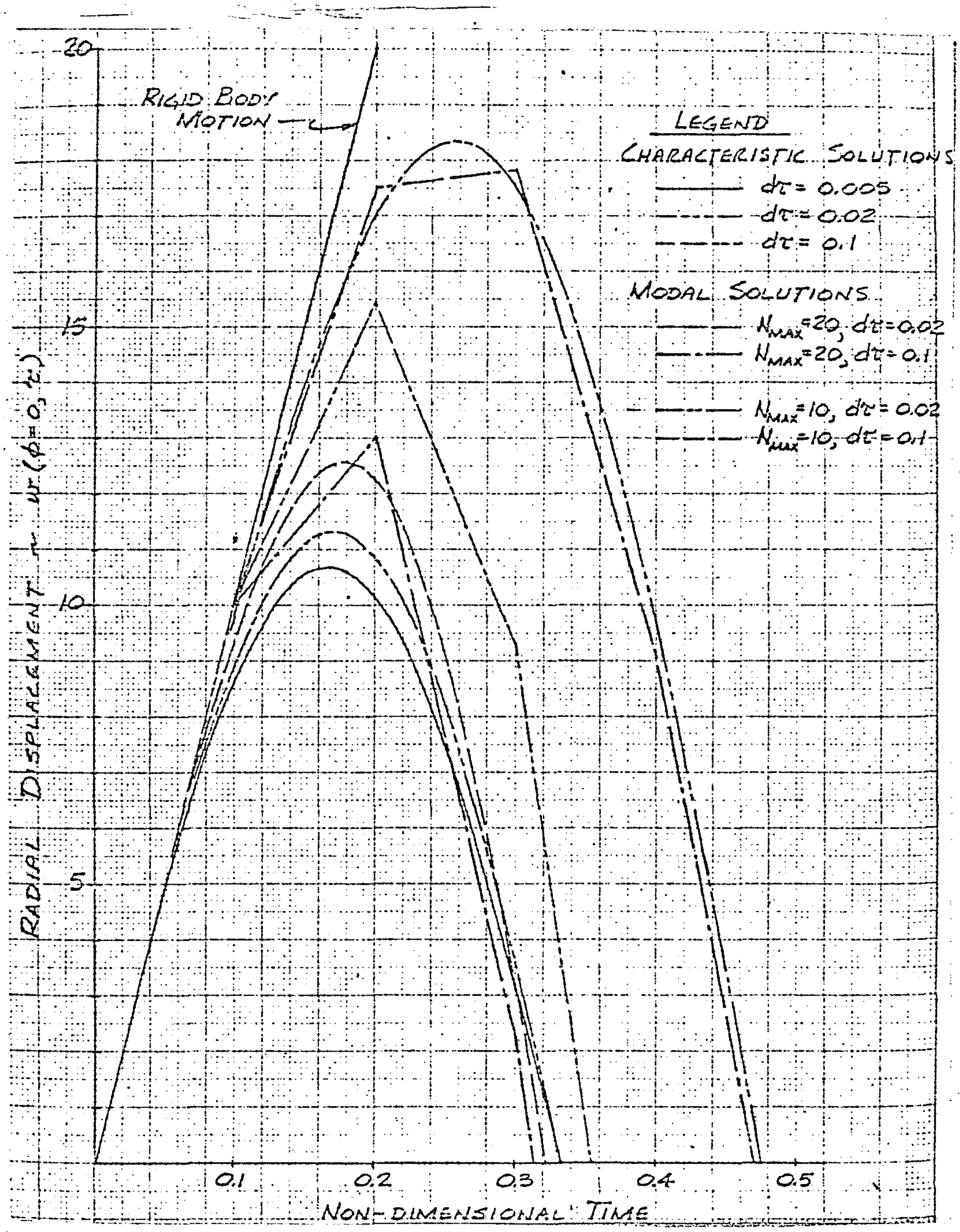

Figure 14. Case I--Radial displacement as a function of time

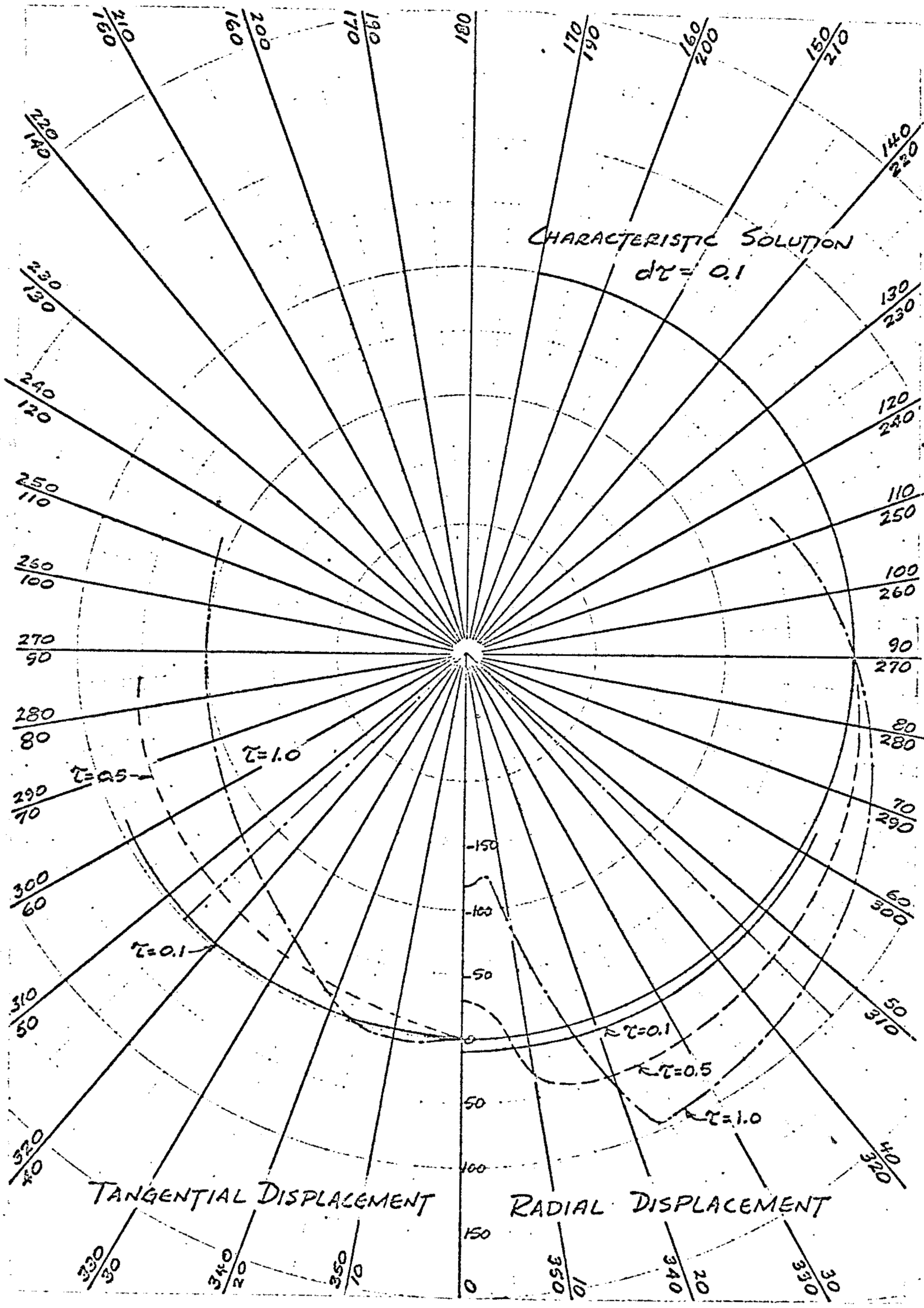

Figure 15. Case I--Radial and Tangential displacement

displacement patterns while the unaffected region exhibits pure rigid body motion.

Radial displacements at various times and for both the modal and characteristic solutions are given in Figures 16 to 19. These results indicate generally good correlation between the methods. All apparent differences between the methods are seen to be reduced by increasing the number of modes used in the modal solution or reducing the integration increment in the characteristic solution.

A comparison between the meridional and hoop stresses in the shell is given in Figures 20 to 23 for various times and characteristic solution integration increments. Good correlation between results from various integration increment solutions is seen to exist with generally smoother curves resulting from solutions using smaller increments. It is further seen that the compressive hoop stress is smaller in absolute value than the meridional stress. In some cases the hoop stress is positive.

The case II example is described on Figures 24 to 32. The results for this case are similar in most respects to those given for case I. However, certain interesting differences in behavior do appear. These differences are described below.

The differences between the case I and case II solutions can be attributed largely to the facts that for

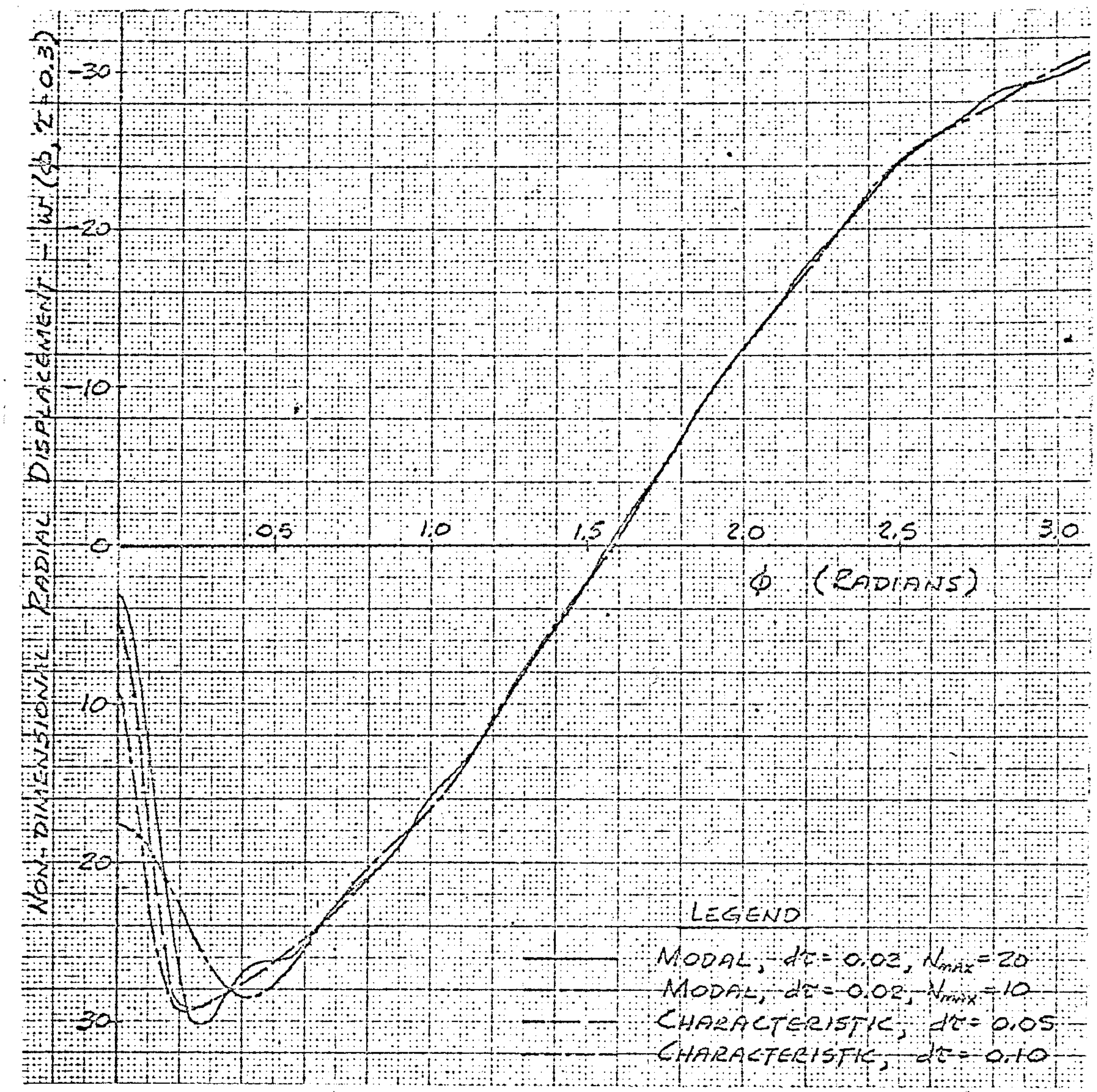

Figure 16. Case I--Radial displacement

at $\tau = 0.3$

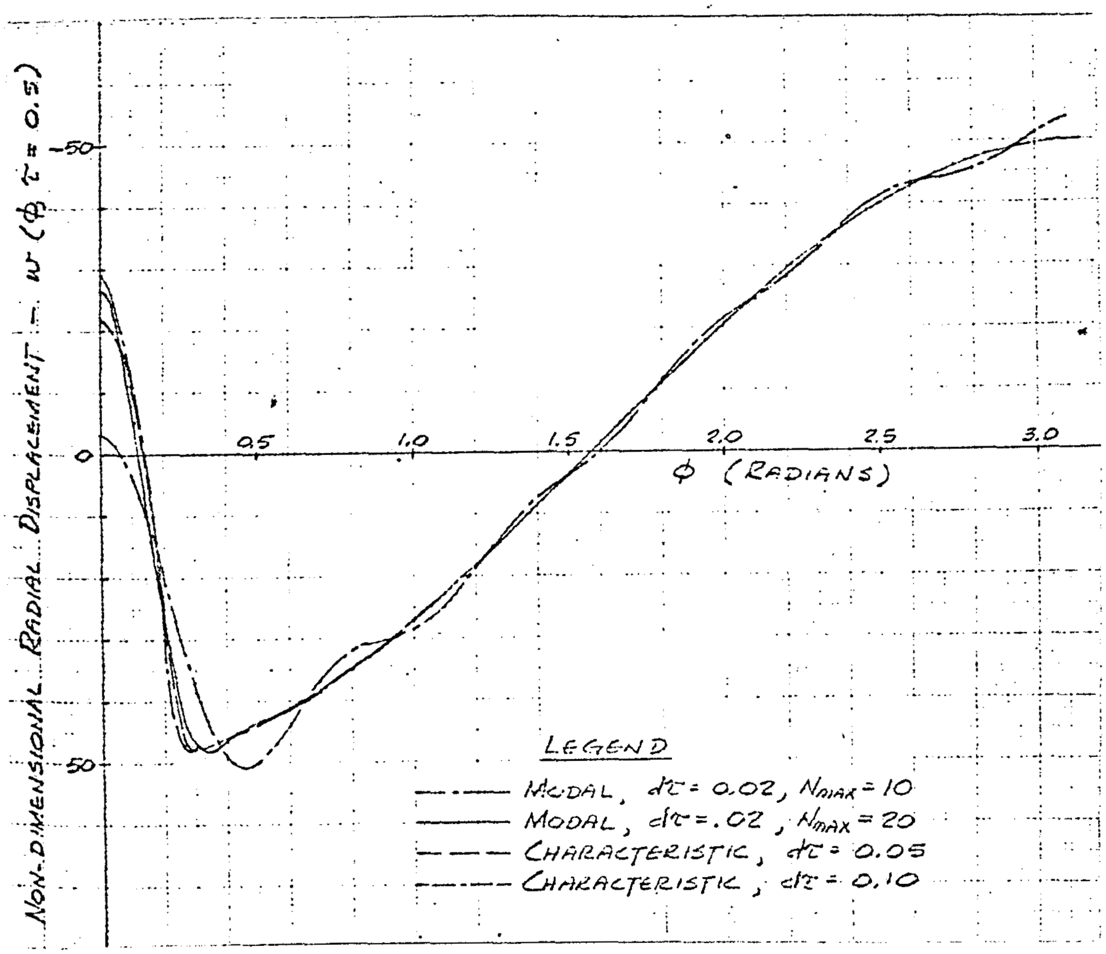

Figure 17. Case I--Radial displacement at $\tau = 0.5$

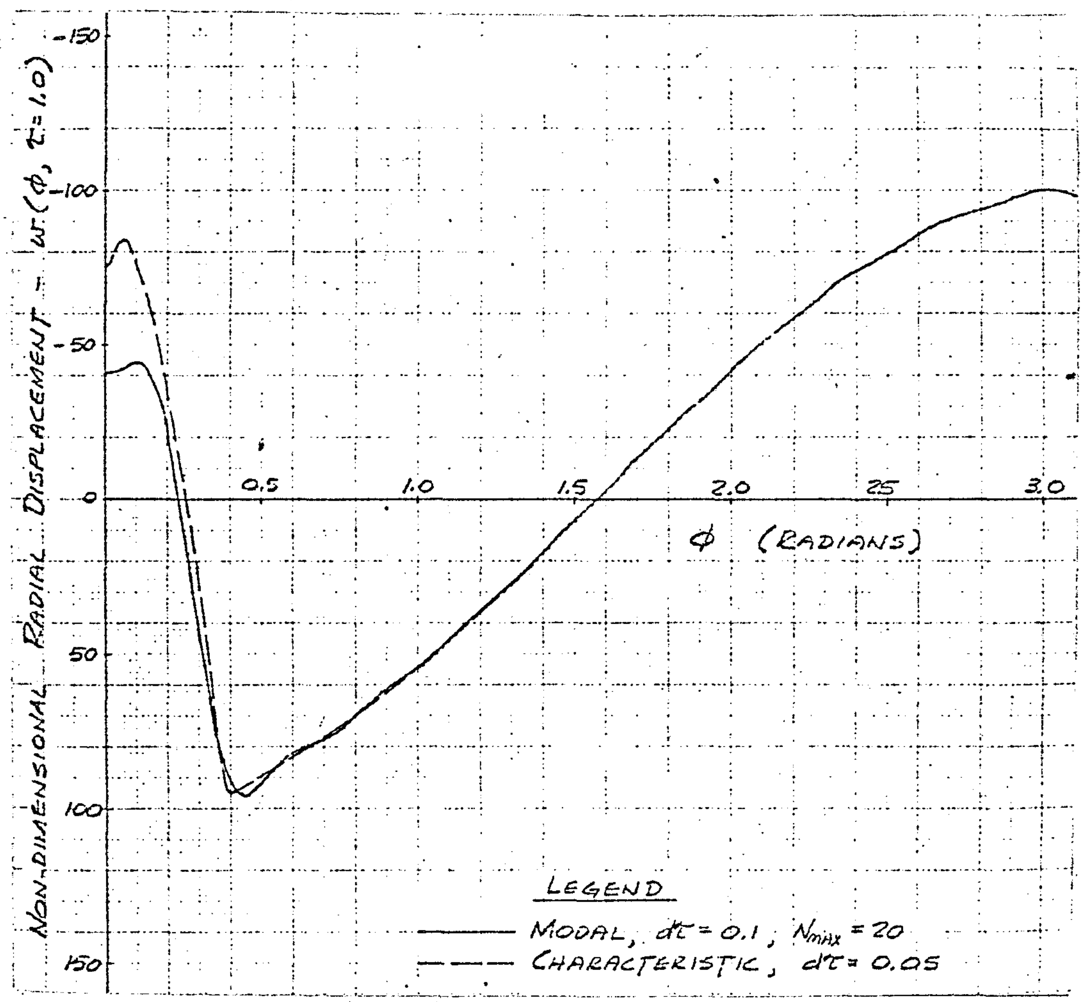

Figure 18. Case I--Radial displacement at $\tau = 1.0$

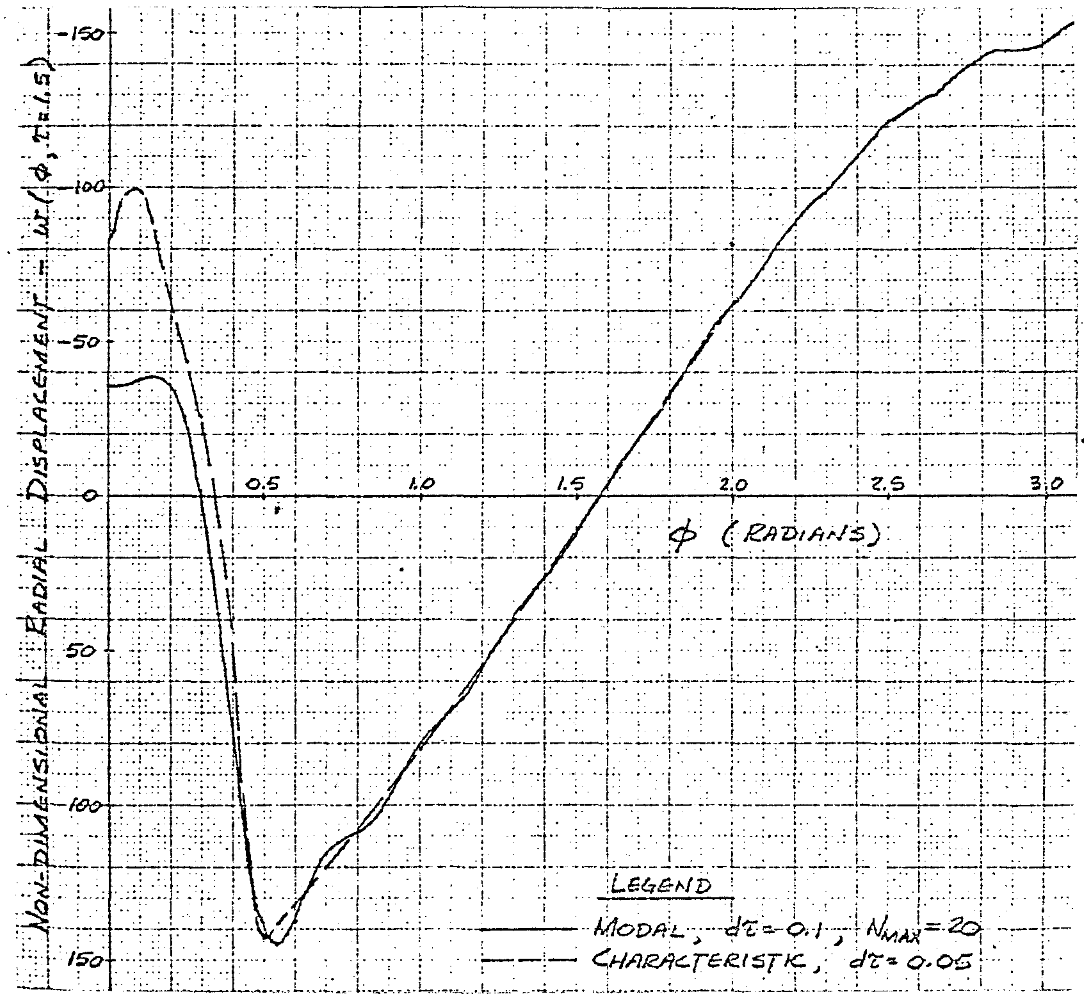

Figure 19. Case I--Radial displacement at $\tau = 1.5$

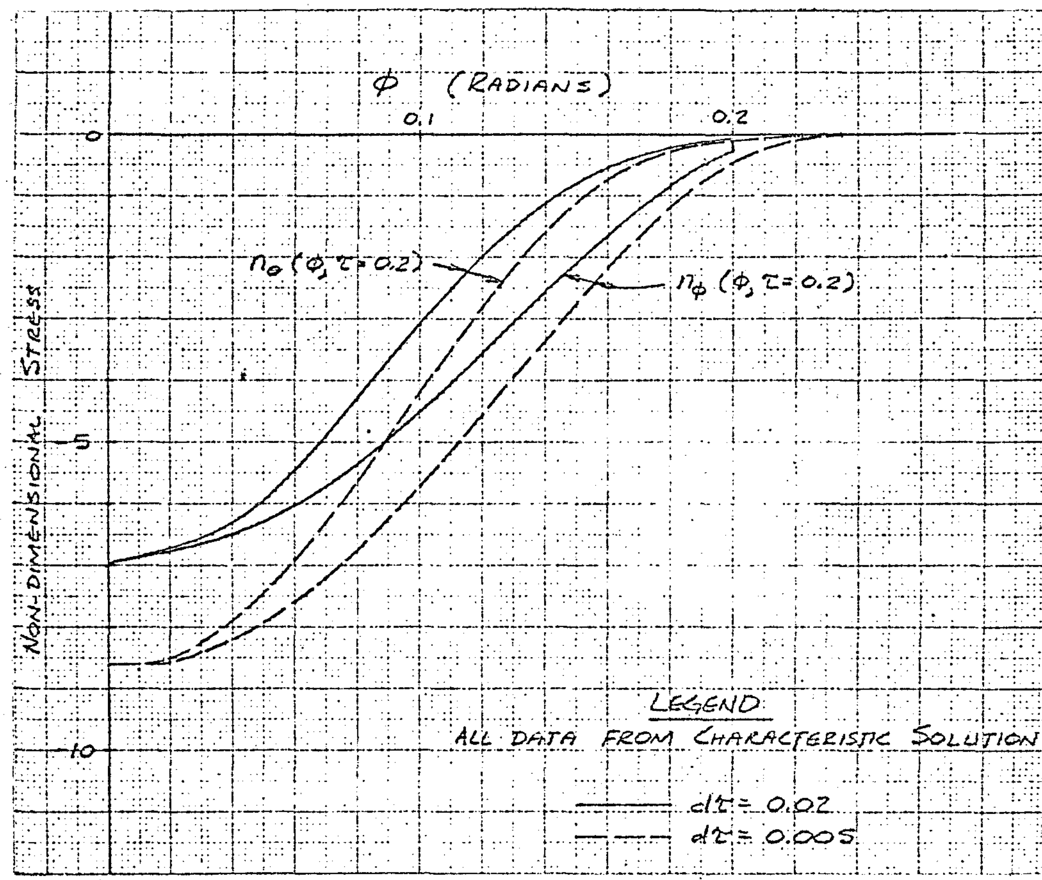

Figure 20. Case I--Stress at τ = 0.2

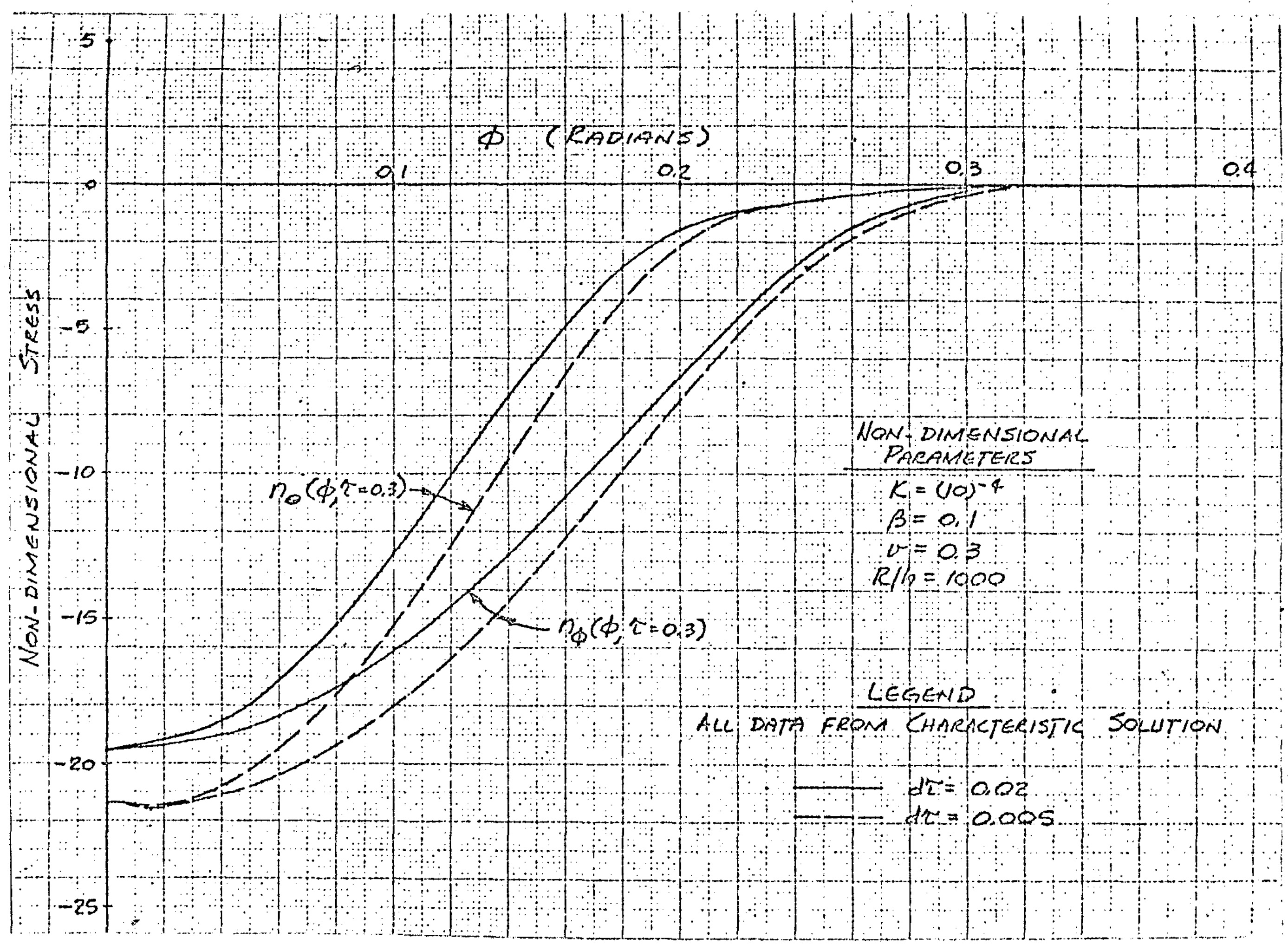

Figure 21. Case I--Stress at $\tau = 0.3$

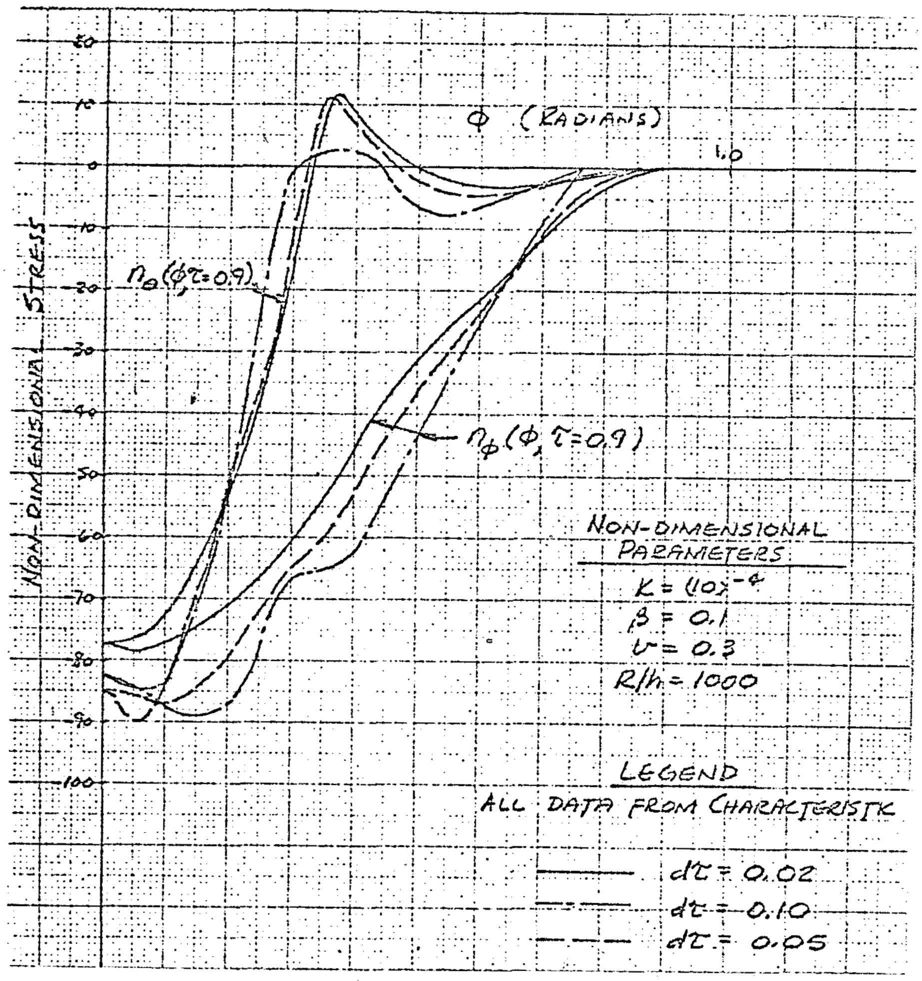

Figure 22. Case I--Stress at τ = 0.9

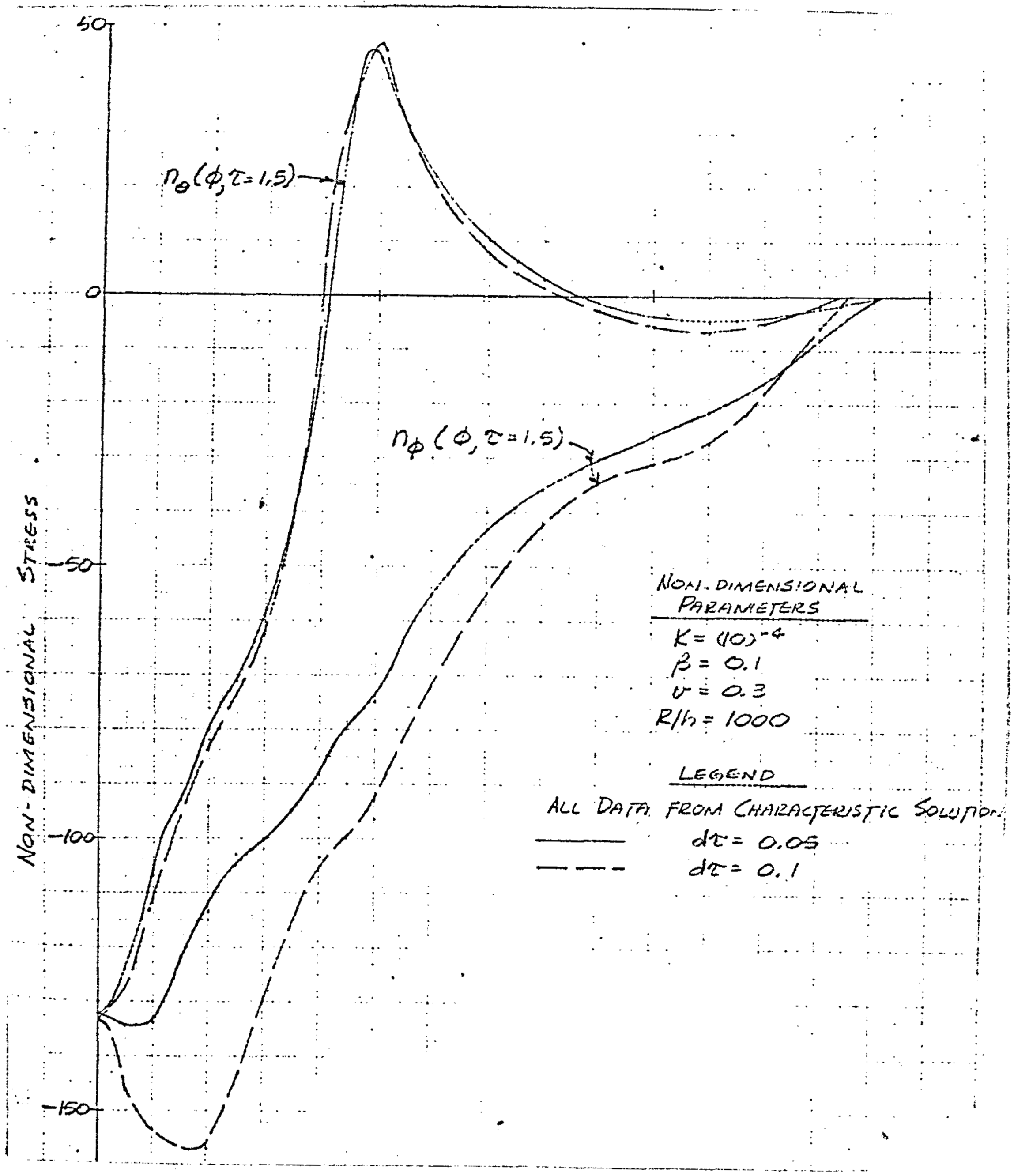

Figure 23. Case I--Stress at τ = 1.5

case II (a) complete shell rebound occurs much later and (b) the shell-surface contact area is much smaller.

The small shell-surface contact area and the large rebound time combine to limit the maximum time for which the case II solutions can be carried out. However, it is seen in Figures 24 and 25 that good correlation exists between the 20 mode normal mode and characteristic solutions for non-dimensional times of up to 3.0. As with the case I solution, results for the 10 mode normal mode solution are not nearly as accurate as those for the 20 mode solutions.

Radial and tangential displacements are presented in Figure 26 for various times. A comparison between radial displacements found using both the modal and characteristic solutions is given in Figures 27 to 29 for various times. An inspection of these results shows good correlation between the methods of analysis.

Stress distributions in the shell are illustrated in Figures 30 to 32. Good correlation is seen to exist between characteristic solutions using different integration increments for regions away from the shell apex. Differences in the stress levels at the shell apex can be attributed to the fact that the total stressed area is of the same order of magnitude as the integration increment, particularly for the case where $d\tau = 0.05$.

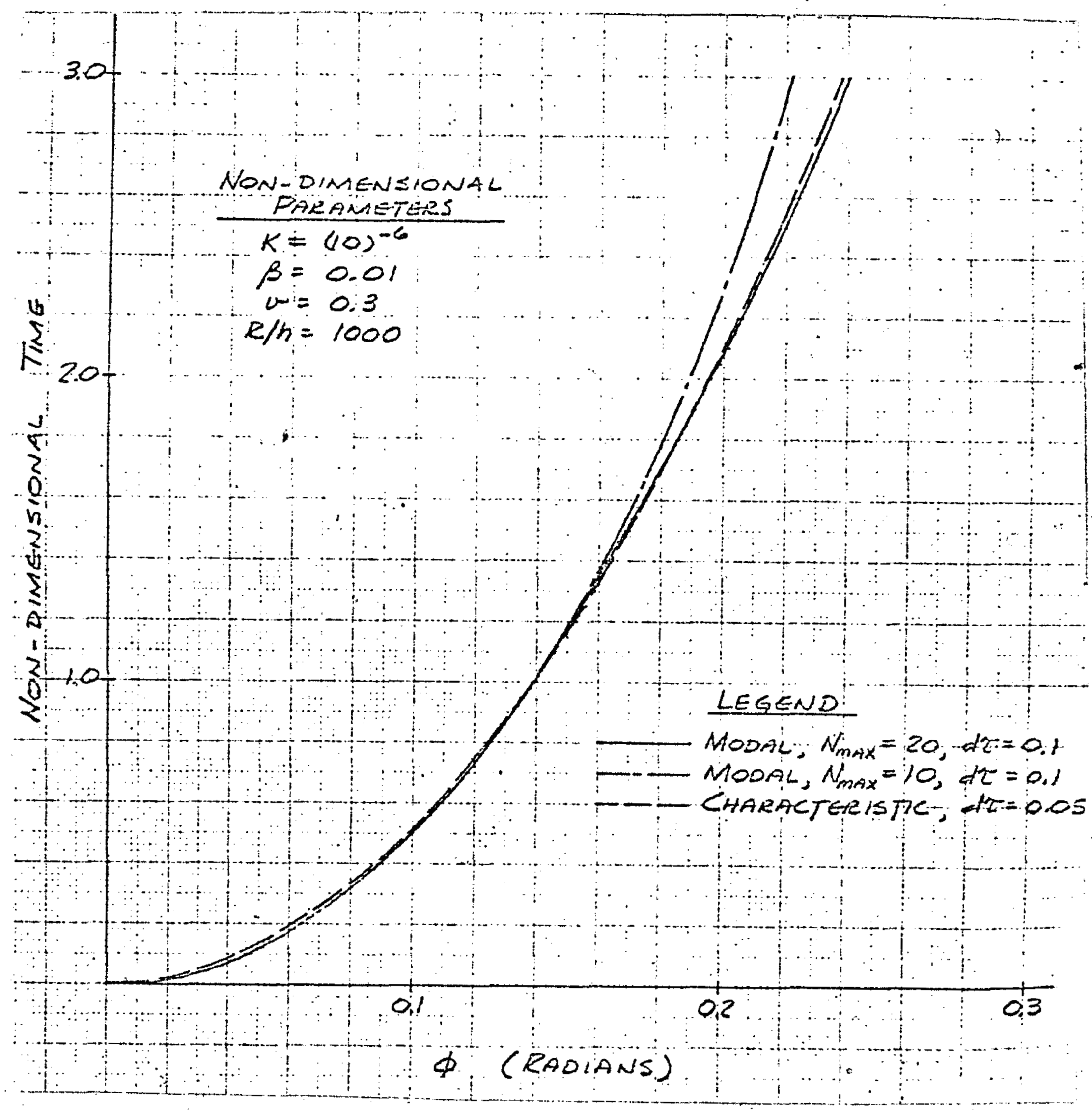

Figure 24. Case II--Description of shell-surface contact area

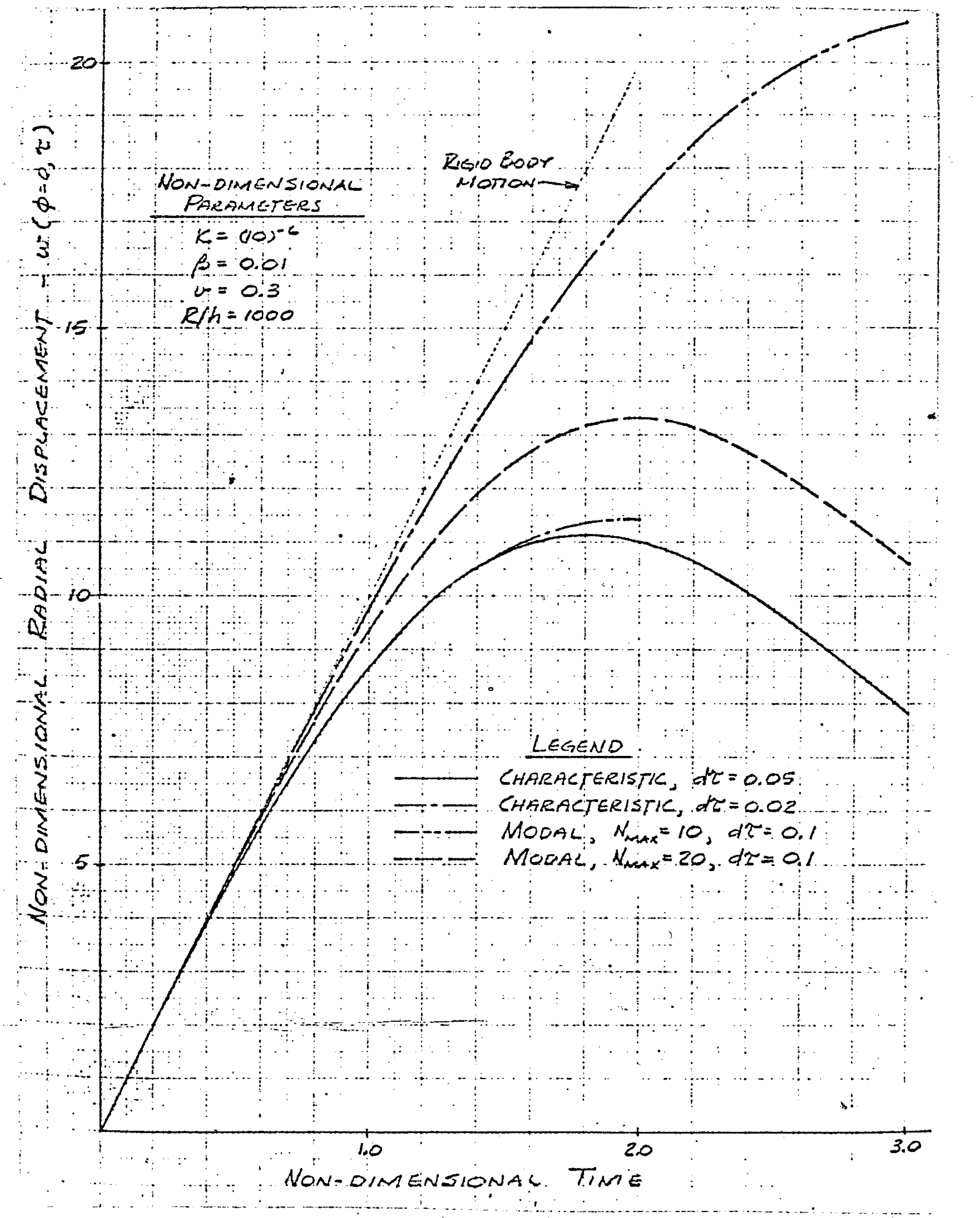

Figure 25. Case II--Radial displacement as a function of time

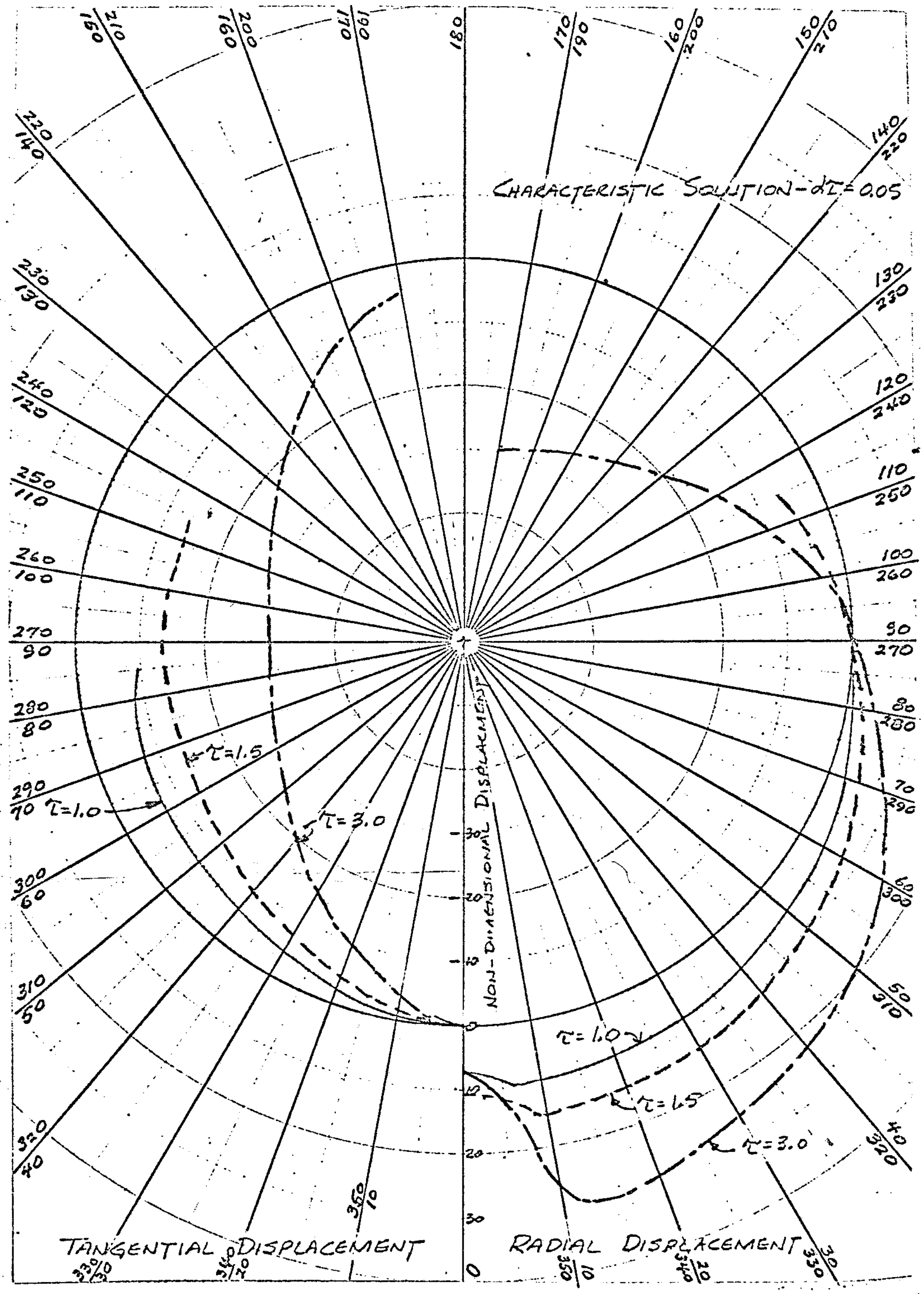

Figure 26. Case II--Radial and Tangential displacement

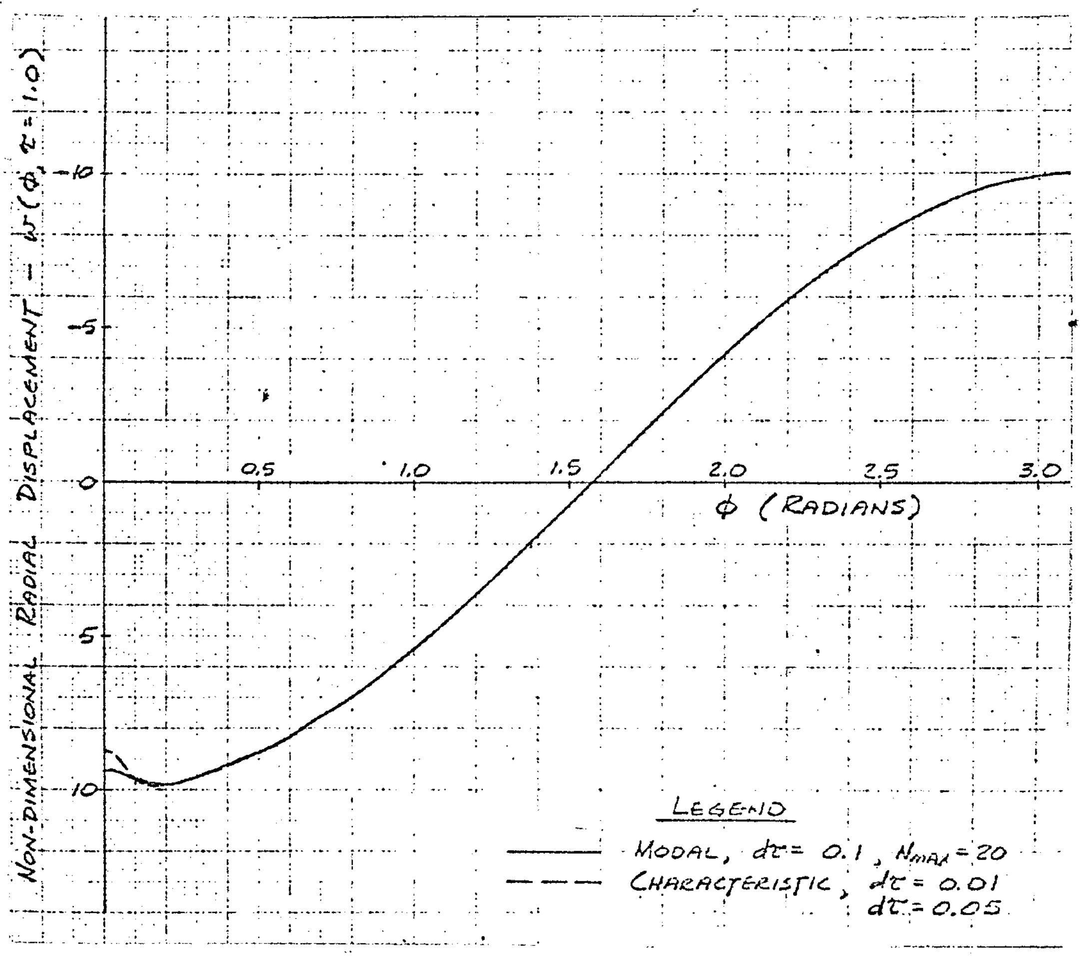

Figure 27. Case II--Radial displacement at $\tau = 1.0$

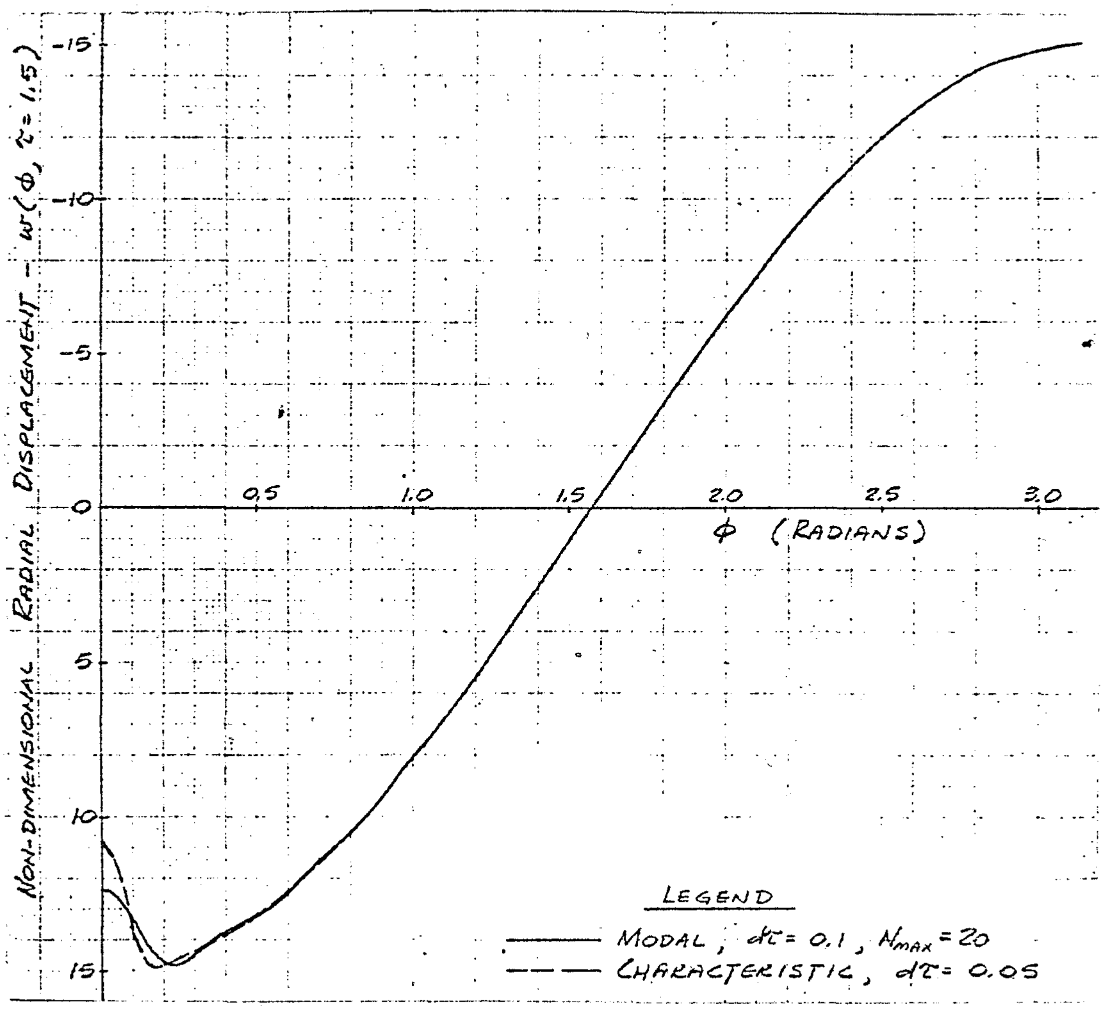

Figure 28. Case II--Radial displacement at $\tau = 1.5$

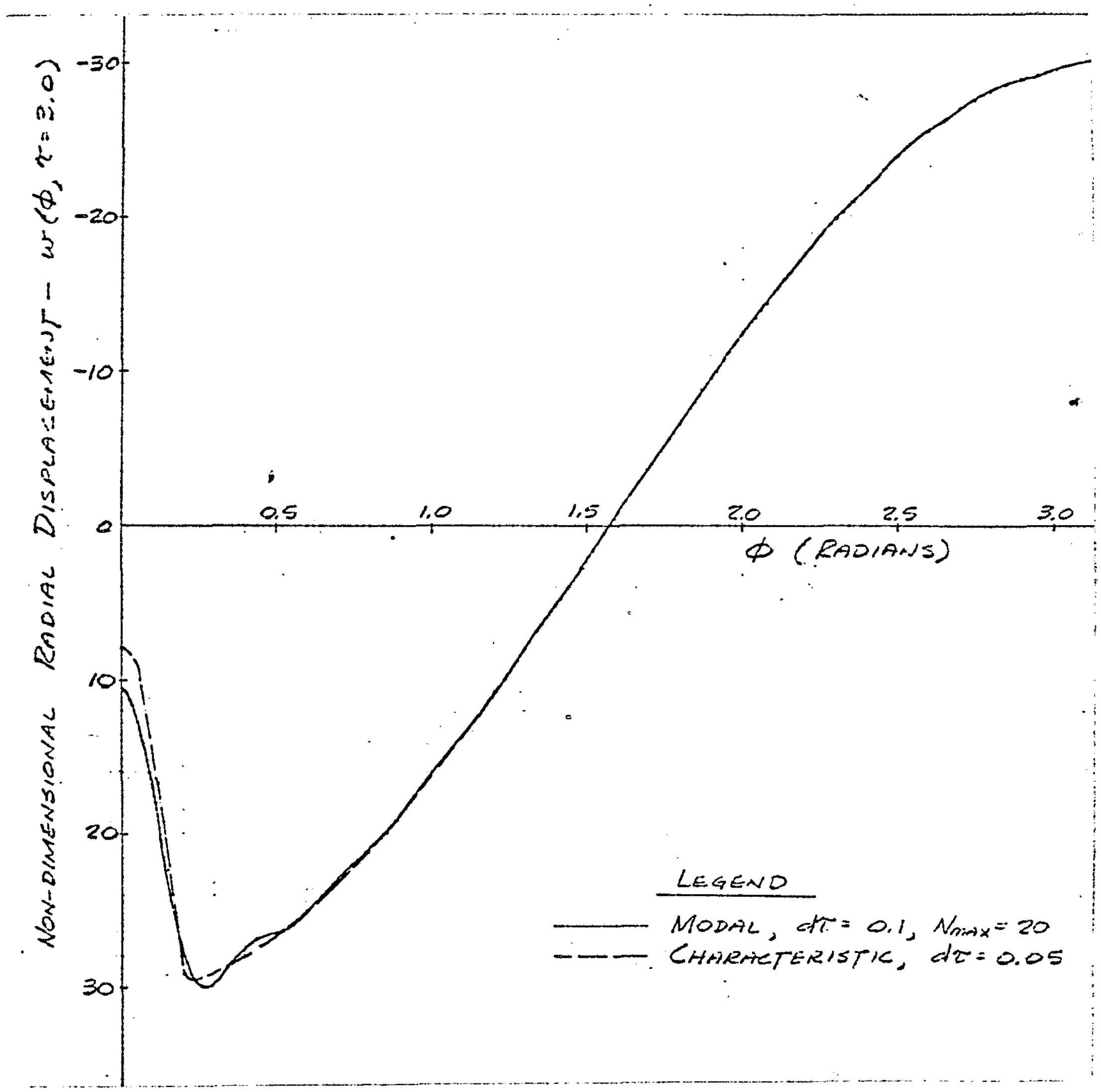

Figure 29. Case II--Radial displacement at τ = 3.0

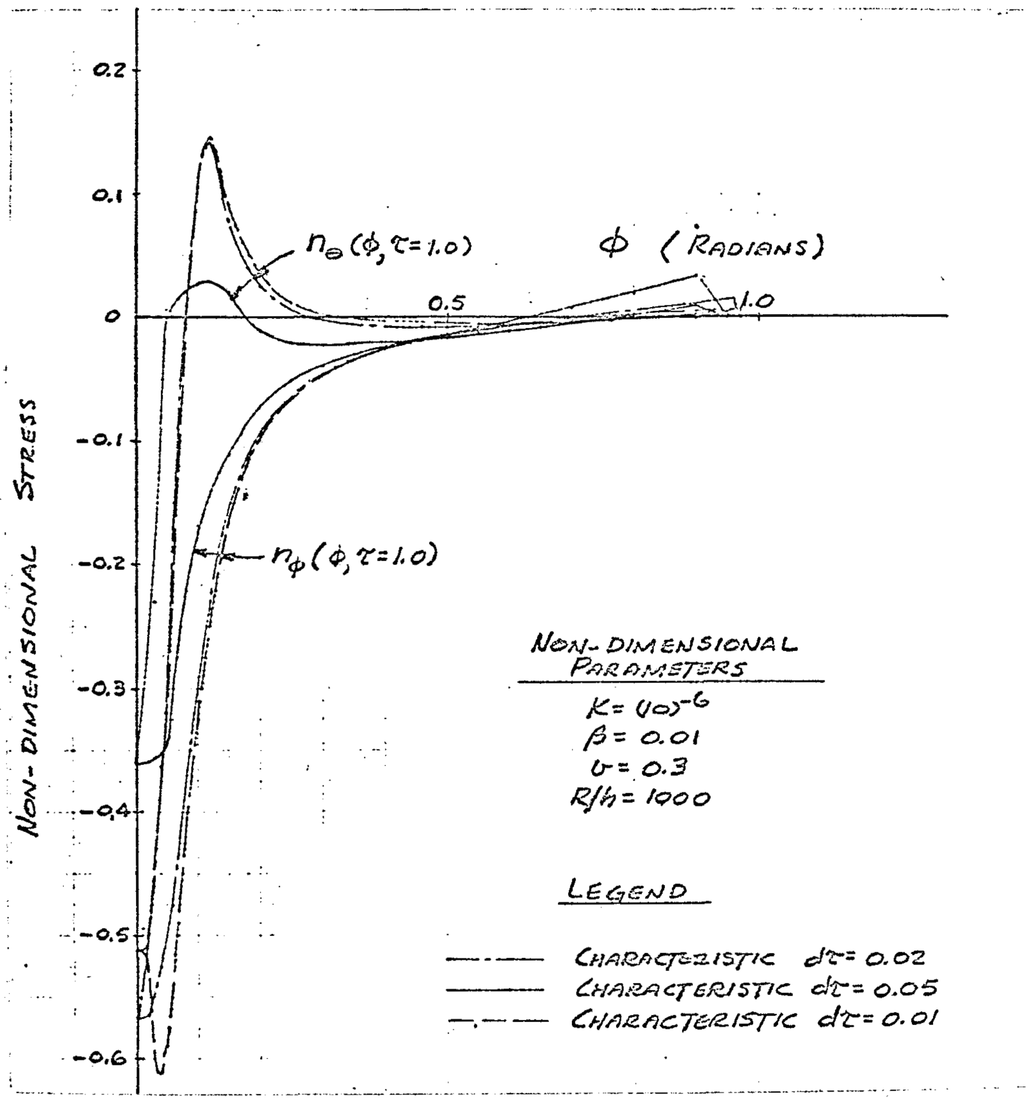

Figure 30. Case II--Stress at $\tau = 1.0$.

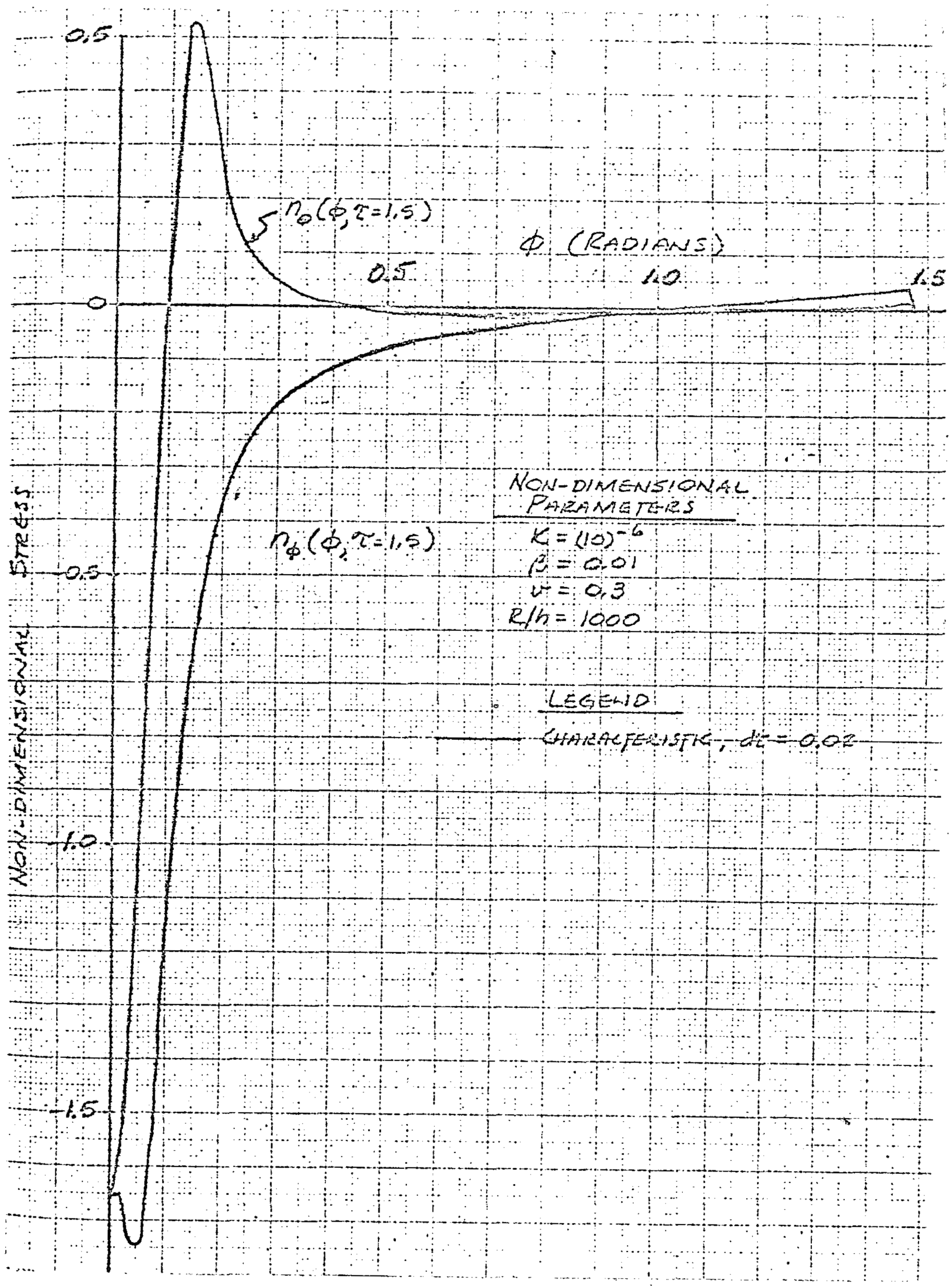

Figure 31. Case II--Stress at τ = 1.5

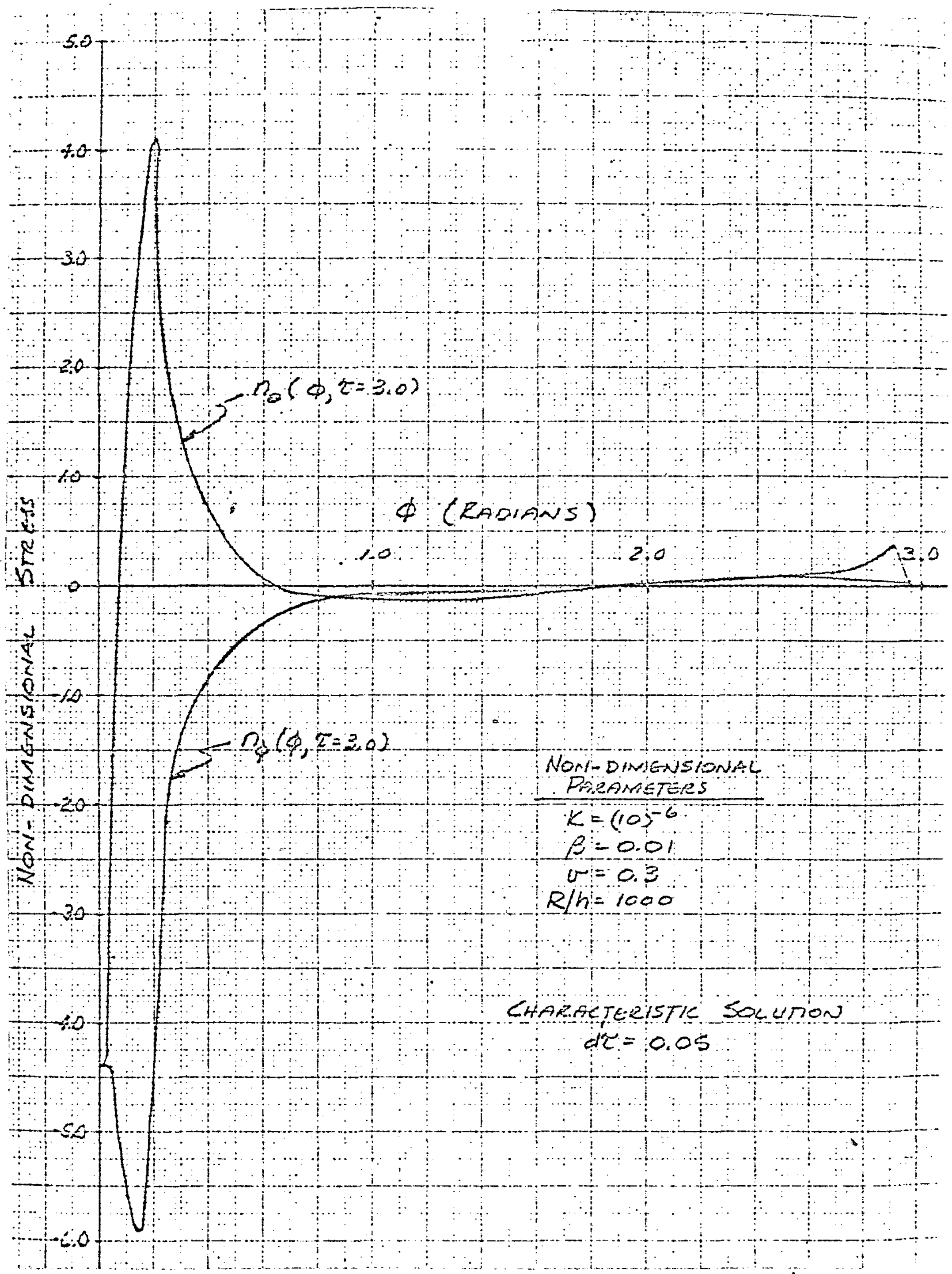

Figure 32. Case II--Stress at $\tau = 3.0$

CHAPTER VI

CONCLUSIONS

General

The most significant result of this work is the fact that a method of solution of the problem of the dynamic contact between two elastic bodies has been explored. Specifically, the problem of the dynamic contact between a spherical shell and a deformable surface has been solved using two methods--the method of characteristics and the normal mode expansion method. As discussed in Chapter I, it is felt that solutions using these methods can be extended to many other dynamic contact problems.

Since numerical computations have only been carried out for the membrane theory solutions, all conclusions concerning specific examples are based on this theory. Of most significance here is the fact that the initial shell rebound often occurs first at the apex of the shell (i.e., the initial impact point).

It is seen that the maximum stresses in the shell occur at this point well after the initial rebound time. Furthermore, for most of the cases studied, the stresses in the shell are well below the critical buckling stresses until after this initial rebound time. This result suggests that if buckling is to occur as the result of impact, it will probably not occur until after the apex of the shell has left the surface.

Comparison Between Solutions

The method of characteristics is best suited for examples where shell rebound occurs at small non-dimensional times (say $\tau < 3$). For longer times, too many time intervals and, consequently, too long a computer operating time, are required to make the method practical.

However, the method of characteristics appears to give excellent results for the appropriate short time loading problems. As seen from the case I and II results, the shell response even after the passage of 200-300 time intervals is quite smooth.

On the other hand, the normal mode expansion method gives rather poor results for problems wherein shell rebound occurs at times of the order of magnitude of the time it takes a stress wave to go entirely around the shell. This result should be anticipated as it is well known that behavior near a discontinuity such as occurs at the wave front cannot be well represented by a small number of normal modes. Furthermore, the total contact area in such cases is generally quite small. With such a small loaded area, a situation arises which is quite similar to that of a concentrated load on a beam or a plate. It is well known that many modes are required to describe the response of such systems.

Certain results do not appear sensitive to the method used. Good correlation exists between the methods, for most of the examples studied, on the description of the shell-surface contact area as a function of time. Similarly, the computation of radial displacement does not seem too sensitive to the method used.

In summary, it may be concluded that the method of characteristics is an ideal tool for describing the short time behavior of a spherical shell impacting an elastic surface. It is further concluded that the normal mode expansion technique is only practical for cases where the shell remains in contact with the surface for times long enough to minimize stress wave propagation effects.

Critique of Assumptions

The solutions derived in this paper assume a thin, elastic shell, small deformations, and a particular type of deformable surface.

As discussed in Chapter 1, the assumed surface characteristics are felt to be sufficiently representative of some practical mediums as to be useful.

The assumption of a thin shell permits one to neglect stress variations through the shell. This assumption should be valid if the shell thickness is such that $h/R < 0.1$ (14:354).

If the elastic displacements of the shell become large in comparison with the shell thickness and, moreover, if the change in displacement (i.e., slope) becomes large[1], the assumption of small deformations may become invalid. Such situations do occur when a shell is impacted at a sufficiently high velocity, especially at the apex of the shell after its initial rebound. Care must be taken to properly interpret the results for these cases.

Numerical computations have only been carried out for the membrane theory solutions. If the shell is sufficiently thin (e.g., $R/h > 100$), the effect of bending and transverse shear should be minimal.

---

[1]It is noted that the displacements used in this work are absolute displacements measured from the initial impact time and may, therefore, have large values without the corresponding slopes becoming large.

BIBLIOGRAPHY

1. Baker, W. E., "Axisymmetric Modes of Vibration of Thin Spherical Shell", Journal of the Acoustical Society of America, 33, 12 (December, 1961), pp. 1749-1758.

2. Bateman Manuscript Project, Higher Transcendental Functions, ed. A. Erdelyi (New York: McGraw-Hill Book Co., 1953), I.

3. Courant, R. and Hilbert, D., Methods of Mathematical Physics (New York: Interscience Publishers, 1962), II.

4. Flugge, W., Stresses in Shells (Berlin: Springer-Verlag, 1960).

5. Hetenyi, M., Beams on Elastic Foundation (Ann Arbor: University of Michigan Press, 1946).

6. Huth, J. H. and Cole, J. D., "Elastic Stress Waves Produced by Pressure Loads on a Spherical Shell", Journal of Applied Mechanics, 22 (1955), pp. 473-478.

7. Jahnke, E. and Emde, F., Tables of Functions with Formulae and Curves, 4th ed. (New York: Dover, 1945), pp. 107-125.

8. Kalnins, A., "Dynamic Problems of Elastic Shells", Applied Mechanics Reviews, 18, 11 (1965).

9. Levy, E. C., A New Table of Laplace Transformation Pairs (Los Angeles, 1958).

10. Medick, M. A., "On the Initial Response of a Spherical Shell to a Concentrated Force", Journal of Applied Mechanics, 29 (1962), pp. 689-695.

11. Naghdi, P. M., "On the Theory of Thin Elastic Shells", Quarterly of Applied Mathematics, XIV, 4 (1957), pp. 369-380.

12. Prasad, C., "On Vibrations of Spherical Shells", Journal of the Acoustical Society of America, 36, 3 (March, 1964), pp. 489-494.

13. Szego, G., Orthogonal Polynomials, American Mathematical Society Colloquium Publications, XXIII (New York, 1959).

14. Timoshenko, S., Theory of Plates and Shells (New York: McGraw-Hill Book Company, 1940).

15. Wilkinson, J. P., and Kalnins, A., "On Nonsymmetric Dynamic Problems of Elastic Spherical Shells", Journal of Applied Mechanics, (September, 1965), pp. 525-532.

16. Wilkinson, J. P., Capelli, A. P. and Salzman, R. N., "Hydroelastic Interaction of Shells of Revolution During Water Impact", to be published.

APPENDICES

APPENDIX A

LAPLACE TRANSFORM INVERSION

General Case

Laplace transforms of the general form

$$\bar{L}_n(s) = \frac{a_3 s^3 + a_2 s^2 + a_1 s + a_0}{s^4 + G_4(n)\, s^2 + G_5(n)} \tag{A.1}$$

occur during the development of the normal mode-membrane theory solution. The inversion of this transform is developed below using equations given by Levy (9).

From Levy (9), the following inverse is seen to exist:

$$\mathcal{L}^{-1}\left[\frac{N_3(s)}{(s^2+\omega_n^2)(s^2+\mu_n^2)}\right] = \frac{\sqrt{(C_1)^2 + (C_2)^2}}{\omega_n(\mu_n^2 - \omega_n^2)} \cos(\omega_n \tau - \psi_1)$$
$$+ \frac{\sqrt{(C_3)^2 + (C_4)^2}}{\mu_n(\omega_n^2 - \mu_n^2)} \cos(\mu_n \tau - \psi_2) \tag{A.2}$$

where $\psi_1 = \tan^{-1}\left(\frac{C_1}{C_2}\right)$

$\psi_2 = \tan^{-1}\left(\frac{C_3}{C_4}\right)$

$C_1 = R\, N_3(s)\Big|_{s=i\omega_n}$

$C_2 = I_1\, N_3(s)\Big|_{s=i\omega_n}$

$C_3 = R\, N_3(s)\Big|_{s=i\mu_n}$

$C_4 = I_1\, N_3(s)\Big|_{s=i\mu_n}$

$$N_3(s) = a_3 s^3 + a_2 s^2 + a_1 s + a_o$$

Equations A.1 and A.2 are seen to be identical provided that

$$\begin{aligned} G_4(n) &= \omega_n^2 + \mu_n^2 \\ G_5(n) &= \omega_n^2 \mu_n^2 \end{aligned} \qquad (A.3)$$

Solving equations A.3 for ω_n^2 and μ_n^2, we find that if ω_n^2 and μ_n^2 are to have independent values, then

$$\begin{aligned} \omega_n^2 &= \frac{1}{2}\left[G_4(n) + G_6(n)\right] \\ \mu_n^2 &= \frac{1}{2}\left[G_4(n) - G_6(n)\right] \end{aligned} \qquad (A.4)$$

where $G_6(n) = \left\{\left[G_4(n)\right]^2 - 4\,G_5(n)\right\}^{1/2}$ (A.5)

In Chapter III, we have defined

$$\begin{aligned} G_4(n) &= n(n+1) + 1 + 3\nu \\ G_5(n) &= (1-\nu^2)\left[n(n+1) - 2\right] \end{aligned} \qquad (A.6)$$

If we use the fact that $0 \leq \nu \leq \frac{1}{2}$, we immediately see from equations A.6 that $G_6(n)$ is a real, positive number for all values of n. Furthermore, except for the case where n = 0, it is seen that $G_4(n) > G_6(n)$. Therefore, we can say that the frequencies ω_n and μ_n are all real except for the frequency μ_o. The imaginary frequency μ_o has been shown by Baker (1) to be spurious and cause no motion.

The various coefficients in equation A.2 are now seen to be of the form

$$
\begin{aligned}
C_1 &= a_o - a_2\omega_n^2 \\
C_2 &= \omega_n(a_1 - a_3\omega_n^2) \\
C_3 &= a_o - a_2\mu_n^2 \\
C_4 &= \mu_n(a_1 - a_3\mu_n^2) \\
\psi_1 &= \tan^{-1}\left[\frac{a_o - a_2\omega_n^2}{\omega_n(a_1 - a_3\omega_n^2)}\right] \\
\psi_2 &= \tan^{-1}\left[\frac{a_o - a_2\mu_n^2}{\mu_n(a_1 - a_3\mu_n^2)}\right]
\end{aligned}
\tag{A.7}
$$

The required inverse is now completely described provided that values are available for the coefficients a_i in $N_3(s)$. The inversion corresponding to a particular set of these coefficients will be determined below.

Forced Vibration Case

a. The Laplace transformed equations given by equations 3.37 may be written in the form

$$
\begin{aligned}
\bar{A}_n(s) &= -\bar{\Theta}_n(s) + \bar{\Phi}_n(s)\bar{D}_n(s) + \bar{\Psi}_n(s)\bar{E}_n(s) \\
\bar{B}_n(s) &= \bar{\Theta}_n(s) + \bar{\eta}_n(s)\bar{D}_n(s) + \bar{\Omega}_n(s)\bar{E}_n(s)
\end{aligned}
\tag{A.8}
$$

where

$$
\begin{aligned}
\bar{\Theta}_n(s) &= \left\{\frac{s^2 + 3(1+\upsilon)}{s^4 + G_4(n)s^2 + G_5(n)}\right\}\dot{B}_n(o) \\
\bar{\Phi}_n(s) &= \frac{-(1+\upsilon)}{s^4 + G_4(n)s^2 + G_5(n)} \\
\bar{\Psi}_n(s) &= \frac{s^2 + 2(1+\upsilon)}{s^4 + G_4(n)s^2 + G_5(n)} \\
\bar{\eta}_n(s) &= \frac{s^2 + n(n+1) - 1 + \upsilon}{s^4 + G_4(n)s^2 + G_5(n)} \\
\bar{\Omega}_n(s) &= \frac{-n(n+1)(1+\upsilon)}{s^4 + G_4(n)s^2 + G_5(n)}
\end{aligned}
\tag{A.9}
$$

Each of the transforms defined by equations A.9 are seen to be of the same general form as equation A.1.

The first of equations A.9 can be put into the same form as equation A.1 if we let

$$a_1 = a_3 = 0$$
$$a_2 = \dot{B}_n(0)$$
$$a_0 = 3(1+\upsilon)\dot{B}_n(0)$$

Using these relations, equations A.7 become

$$C_2 = C_4 = 0$$
$$C_1 = \left[3(1+\upsilon) - \omega_n^2\right]\dot{B}_n(0)$$
$$C_3 = \left[3(1+\upsilon) - \mu_n^2\right]\dot{B}_n(0)$$
$$\psi_1 = \psi_2 = \tan^{-1}(\infty) = \frac{\pi}{2}$$

Therefore, the inverse is seen from equation A.2 to be

$$\theta_n(\tau) = \left\{\frac{\left[3(1+\upsilon) - \omega_n^2\right]\dot{B}_n(0)}{\omega_n(\mu_n^2 - \omega_n^2)}\right\}\cos\left(\omega_n\tau - \frac{\pi}{2}\right) + \left\{\frac{\left[3(1+\upsilon) - \mu_n^2\right]\dot{B}_n(0)}{\mu_n(\omega_n^2 - \mu_n^2)}\right\}\cos\left(\mu_n\tau - \frac{\pi}{2}\right)$$

or, since $\cos(y - \frac{\pi}{2}) = \sin y$ and $\omega_n^2 - \mu_n^2 = G_6(n)$,

$$\theta_n(\tau) = -\left\{\frac{\left[3(1+\upsilon) - \omega_n^2\right]\dot{B}_n(0)}{\omega_n G_6(n)}\right\}\sin\omega_n\tau + \left\{\frac{\left[3(1+\upsilon) - \mu_n^2\right]\dot{B}_n(0)}{\mu_n G_6(n)}\right\}\sin\mu_n\tau \qquad \text{(A.10)}$$

Using equation A.10, the remainder of equations A.9 may be inverted by inspection to give

$$\Phi_n(\tau) = \left[\frac{(1+\upsilon)}{\omega_n G_6(n)}\right]\sin\omega_n\tau - \left[\frac{(1+\upsilon)}{\mu_n G_6(n)}\right]\sin\mu_n\tau \qquad \text{(A.11)}$$

$$\Psi_n(\tau) = -\left[\frac{2(1+\upsilon)-\omega_n^2}{\omega_n G_6(n)}\right]\sin\omega_n\tau + \left[\frac{2(1+\upsilon)-\mu_n^2}{\mu_n G_6(n)}\right]\sin\mu_n\tau \qquad (A.12)$$

$$\eta_n(\tau) = -\left[\frac{n(n+1)-1+\upsilon-\omega_n^2}{\omega_n G_6(n)}\right]\sin\omega_n\tau + \left[\frac{n(n+1)-1+\upsilon-\mu_n^2}{\mu_n G_6(n)}\right]\sin\mu_n\tau \qquad (A.13)$$

$$\Omega_n(\tau) = \frac{n(n+1)(1+\upsilon)}{G_6(n)}\left[\frac{\sin\omega_n\tau}{\omega_n} - \frac{\sin\mu_n\tau}{\mu_n}\right] \qquad (A.14)$$

Recognizing that the convolution integral results from the inversion of the product of two transforms, we may now write

$$\begin{aligned} A_n(\tau) &= -\Theta_n(\tau) + \int_0^\tau \Phi_n(\tau-y)D_n(y)\,dy + \int_0^\tau \Psi_n(\tau-y)E_n(y)\,dy \\ B_n(\tau) &= \Theta_n(\tau) + \int_0^\tau \eta_n(\tau-y)D_n(y)\,dy + \int_0^\tau \Omega_n(\tau-y)E_n(y)\,dy \end{aligned} \qquad (A.15)$$

b. Some of the relations developed in part a. may be presented in a simpler form for certain values of n. These forms are developed below.

Using equations A.4 to A.6, we may determine the following relations for the special cases where n = 0 or n = 1. First, for n = 0,

$$\begin{aligned} G_4(0) &= 1+3\upsilon \\ G_5(0) &= -2(1-\upsilon^2) \\ G_6(0) &= 3+\upsilon \\ \omega_0^2 &= 2(1+\upsilon) \\ \mu_0^2 &= -(1-\upsilon) = \text{spurious frequency} \end{aligned} \qquad (A.16)$$

Second, if n = 1,

$$\begin{aligned} G_4(1) &= 3(1+\upsilon) \\ G_5(1) &= 0 \end{aligned} \qquad (A.17)$$

$$G_6(1) = 3(1+\nu)$$

$$\omega_1^2 = 3(1+\nu)$$

$$\mu_1^2 = 0$$

In the following discussion, we will also make use of the fact that

$$\underset{x \to 0}{\text{limit}} \left(\frac{\sin ax}{x} \right) = a \tag{A.18}$$

We have determined in Chapter III (equation 3.12) that

$$\dot{B}_n(0) = \begin{cases} \beta\left(\frac{R}{h}\right) & , \quad n = 1 \\ 0 & , \quad n \neq 1 \end{cases}$$

Using this relation and relations A.17 and A.18, equation A.10 may be written

$$\Theta_n(\tau) = \begin{cases} \beta\left(\frac{R}{h}\right)\tau & , \quad n = 1 \\ 0 & , \quad n \neq 1 \end{cases} \tag{A.19}$$

Using relations A.16 and ignoring the effect of the spurious frequency μ_o, equations A.11 to A.14 may be written in the following form for the case where n = 0:

$$\Phi_o(\tau) = \left(\frac{1+\nu}{3+\nu}\right) \frac{\sin \omega_o \tau}{\omega_o}$$

$$\Psi_o(\tau) = 0$$

$$\eta_o(\tau) = \frac{\sin \omega_o \tau}{\omega_o} \tag{A.20}$$

$$\Omega_o(\tau) = 0$$

Using relations A.17 and A.18, equations A.11 to A.14

may be written in the following form for the case where $n = 1$:

$$
\begin{aligned}
\Phi_1(\tau) &= \frac{1}{3}\left[\frac{\sin \omega_1 \tau}{\omega_1} - \tau\right] \\
\Psi_1(\tau) &= \frac{1}{3}\left[\frac{\sin \omega_1 \tau}{\omega_1} + 2\tau\right] \\
\eta_1(\tau) &= \frac{1}{3}\left[\frac{2\sin \omega_1 \tau}{\omega_1} + \tau\right] \\
\Omega_1(\tau) &= \frac{2}{3}\left[\frac{\sin \omega_1 \tau}{\omega_1} - \tau\right]
\end{aligned}
\qquad \text{(A.21)}
$$

APPENDIX B

MODAL MEMBRANE PROGRAM DESCRIPTION

General

The various computer programs and subprograms used in the normal mode-membrane solution are described, in detail, in the following discussion. The various numerical procedures used in the development of these programs are presented. In addition, a detailed flow chart and a complete FORTRAN listing is presented for each program.

Main Program (SIMPAC)

This program, named SIMPAC, computes the coupled variables $B_n(\tau)$, $D_n(\tau)$, $\phi_o(\tau)$, and $\phi_o^*(\tau)$ for various discrete times during the impact of the shell. In addition, the variables $w(\phi=0,\tau)$ and $Q(\phi=0,\tau)$ are also computed. The program requires the use of various subroutines which are described later in this Appendix.

An option is included in the program to insert precomputed values for $B_n(\tau)$ and $D_n(\tau)$ where $\tau \leq \tau_j$ and the next time interval to be examined is $\tau_i = \tau_j + d\tau$. Using this option, it is permissible to stop the program, use the computer for other operations, and restart the program at a later date without recomputing all previously computed data. The input data for this option is placed on punched cards during the program operation.

A detailed flow chart for this program is shown in Figure 33. As seen from this flow chart, the solution procedure considers the following general steps. First, various initial values are assumed. Second, the displacement functions $(B_n(\tau), n=0, N_{max})$ are determined. Third, the angles $\phi_o(\tau)$ and $\phi_o^*(\tau)$ are determined. Fourth, the load functions $(D_n(\tau), n=0, N_{max})$ are determined. Fifth, the quantities $w(\phi=0,\tau)$ and $Q(\phi=0,\tau)$ are determined. Finally, a new time $\tau=\tau+d\tau$ is selected and the procedure returns to the second step.

Subroutine BNTAU

This subprogram computes $B_n(\tau)$ from the relation (see equation 3.38)

$$B_n(\tau) = \Theta_n(\tau) + \int_0^\tau \eta_n(\tau-y)\, D_n(y)\, dy \tag{B.1}$$

where

$$\Theta_n(\tau) = \begin{cases} \beta\left(\frac{R}{h}\right)\tau & , n=1 \\ 0 & , n\neq 1 \end{cases}$$

$$\eta_n(\tau) = \begin{cases} \frac{\sin\omega_o\tau}{\omega_o} & , n=0 \\ B_1^{(n)}\sin\mu_n\tau + B_2^{(n)}\sin\omega_n\tau & , n\geqslant 1 \end{cases}$$

and $\omega_o = \sqrt{2(1+\nu)}$

The resulting value for $B_n(\tau)$ is returned to the

Figure 33. Detailed Flow Chart--SIMPAC Program

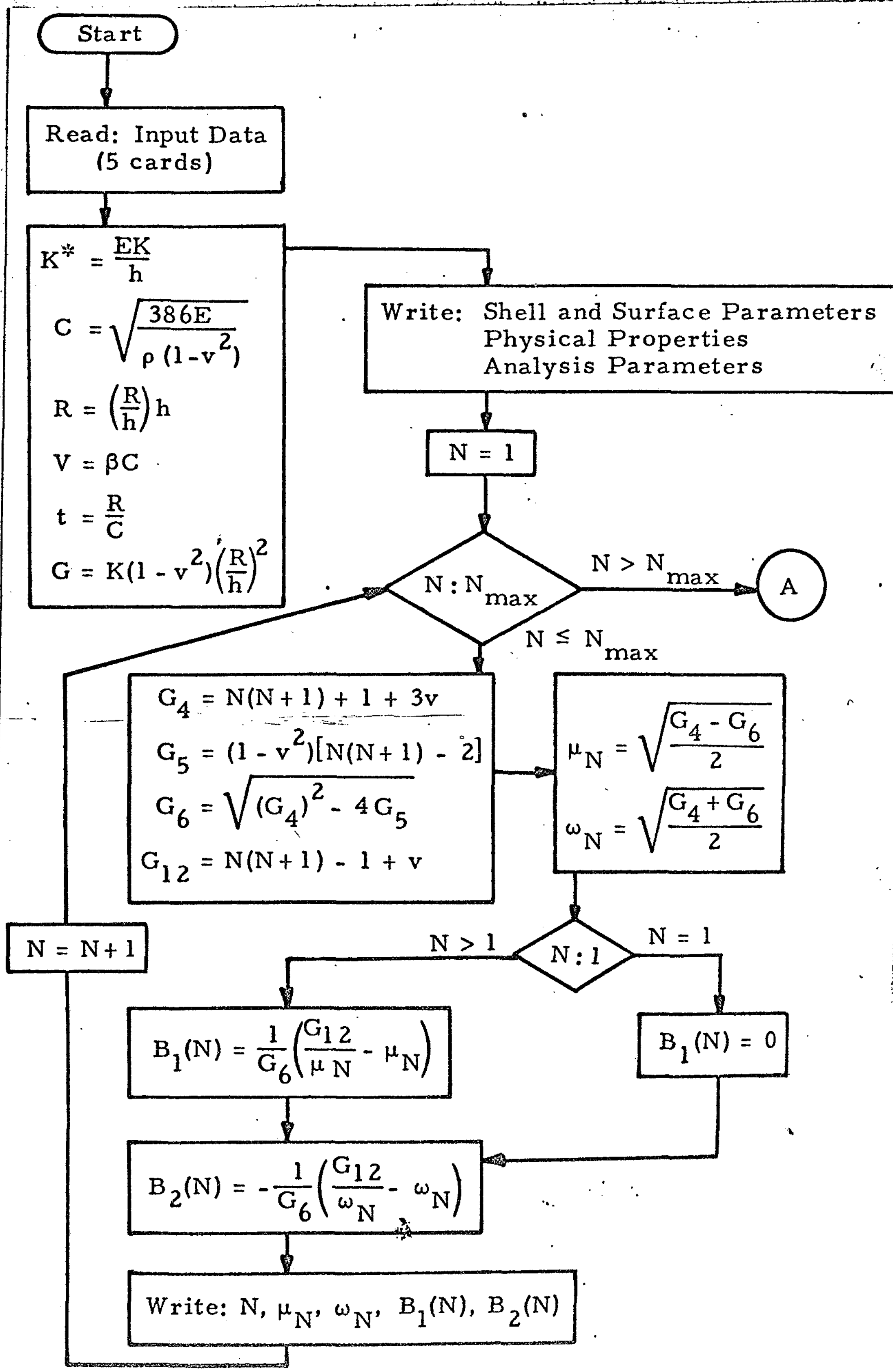
Start
Read: Input Data (5 cards)
$K^* = \frac{EK}{h}$
$C = \sqrt{\frac{386E}{\rho(1-v^2)}}$
$R = \left(\frac{R}{h}\right)h$
$V = \beta C$
$t = \frac{R}{C}$
$G = K(1 - v^2)\left(\frac{R}{h}\right)^2$
Write: Shell and Surface Parameters
Physical Properties
Analysis Parameters
N = 1
$N : N_{max}$
$N > N_{max}$
A
$N \leq N_{max}$
$G_4 = N(N+1) + 1 + 3v$
$G_5 = (1 - v^2)[N(N+1) - 2]$
$G_6 = \sqrt{(G_4)^2 - 4G_5}$
$G_{12} = N(N+1) - 1 + v$
$\mu_N = \sqrt{\frac{G_4 - G_6}{2}}$
$\omega_N = \sqrt{\frac{G_4 + G_6}{2}}$
N = N + 1
N : 1
N > 1
N = 1
$B_1(N) = \frac{1}{G_6}\left(\frac{G_{12}}{\mu_N} - \mu_N\right)$
$B_1(N) = 0$
$B_2(N) = -\frac{1}{G_6}\left(\frac{G_{12}}{\omega_N} - \omega_N\right)$
Write: N, μ_N, ω_N, $B_1(N)$, $B_2(N)$

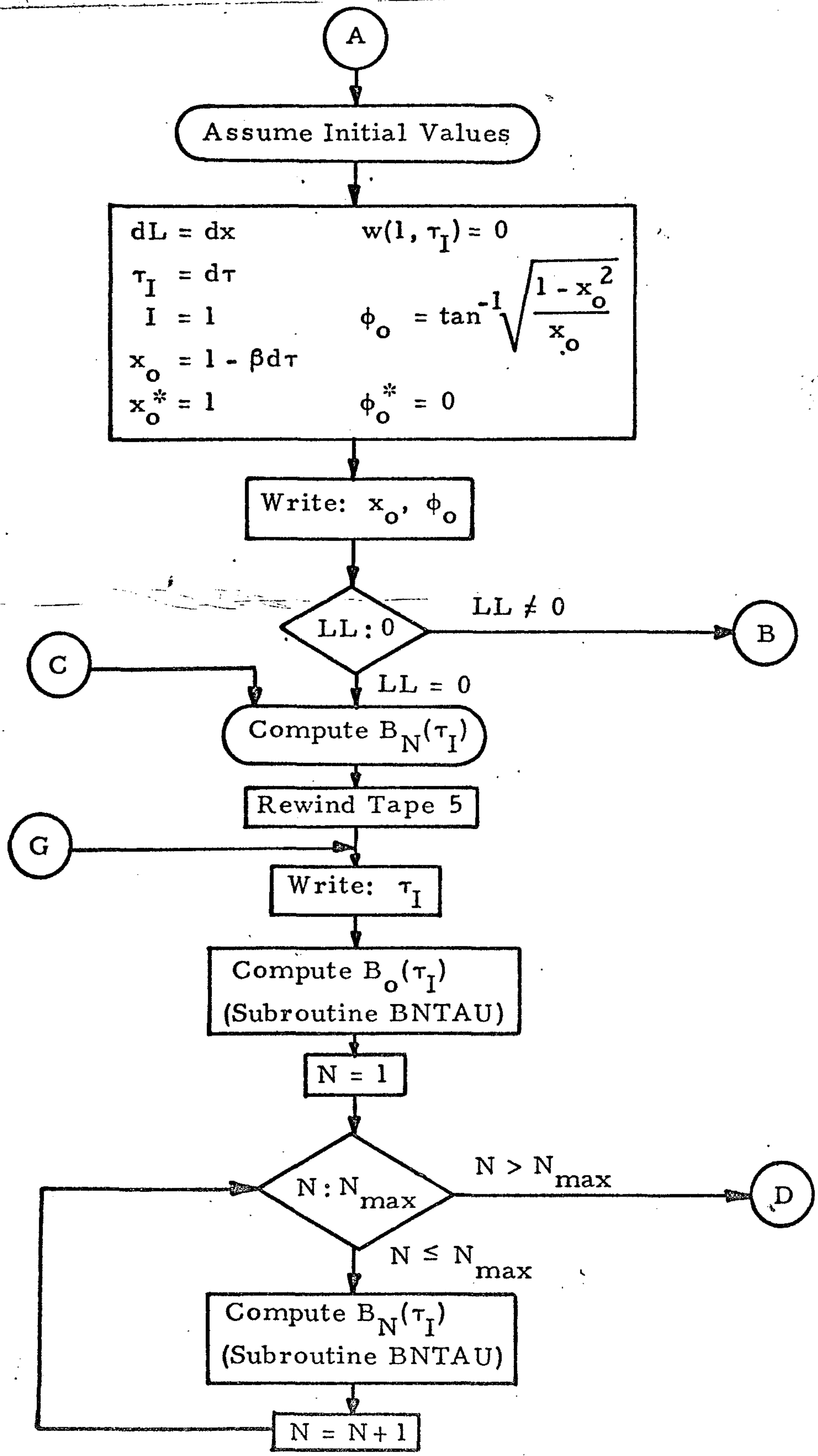
A
Assume Initial Values
dL = dx
$\tau_I = d\tau$
I = 1
$x_o = 1 - \beta d\tau$
$x_o^* = 1$
$w(1, \tau_I) = 0$
$\phi_o = \tan^{-1}\sqrt{\frac{1 - x_o^2}{x_o}}$
$\phi_o^* = 0$
Write: x_o, ϕ_o
LL : 0
LL ≠ 0
B
LL = 0
C
Compute $B_N(\tau_I)$
Rewind Tape 5
G
Write: τ_I
Compute $B_o(\tau_I)$
(Subroutine BNTAU)
N = 1
$N : N_{max}$
$N > N_{max}$
D
$N \leq N_{max}$
Compute $B_N(\tau_I)$
(Subroutine BNTAU)
N = N+1

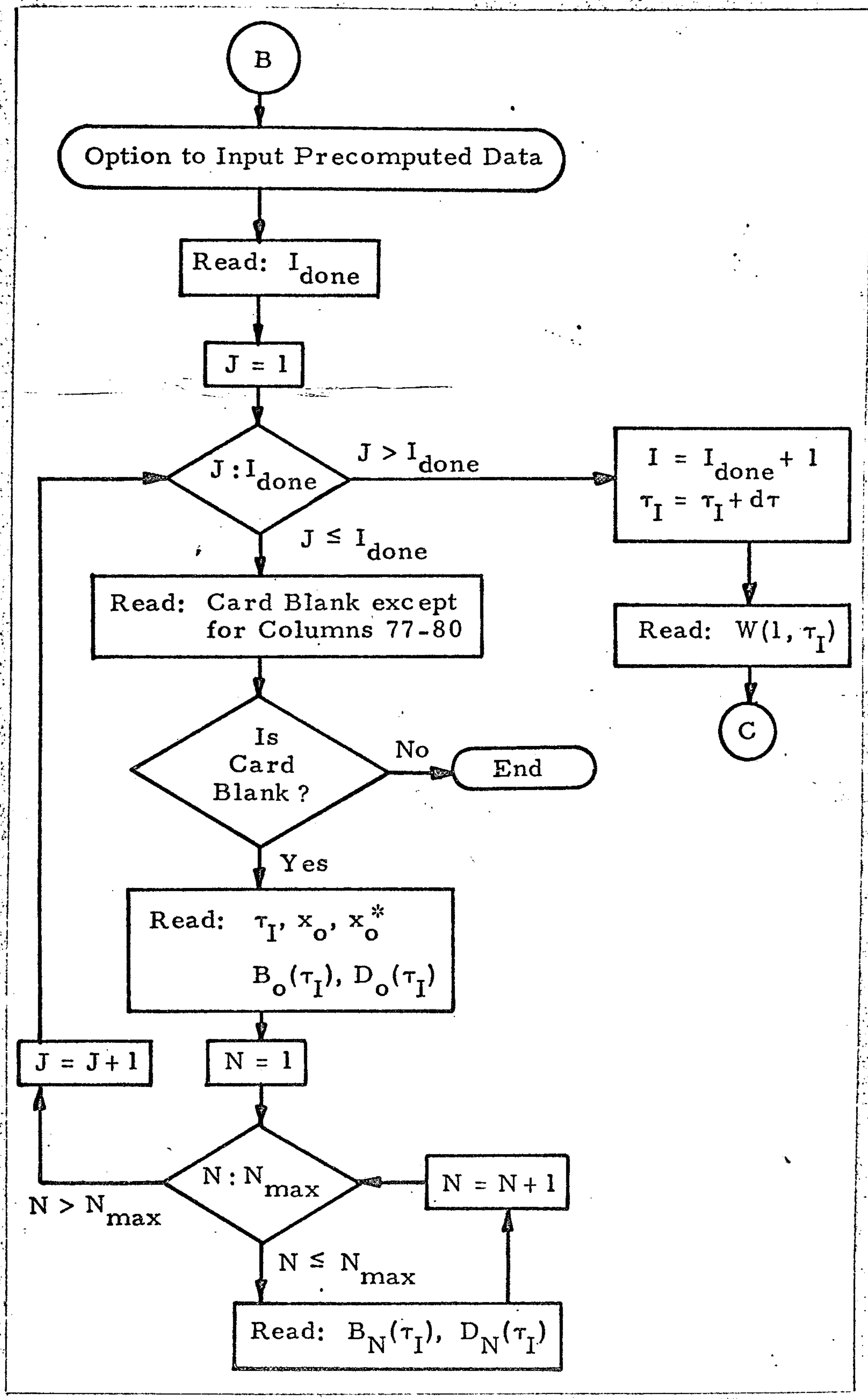
B
Option to Input Precomputed Data
Read: I_{done}
J = 1
$J : I_{done}$
$J > I_{done}$
$I = I_{done} + 1$
$\tau_I = \tau_I + d\tau$
Read: $W(1, \tau_I)$
C
$J \le I_{done}$
Read: Card Blank except for Columns 77-80
Is Card Blank ?
No
End
Yes
Read: τ_I, x_o, x_o^*
$B_o(\tau_I), D_o(\tau_I)$
J = J + 1
N = 1
$N : N_{max}$
$N > N_{max}$
N = N + 1
$N \le N_{max}$
Read: $B_N(\tau_I), D_N(\tau_I)$

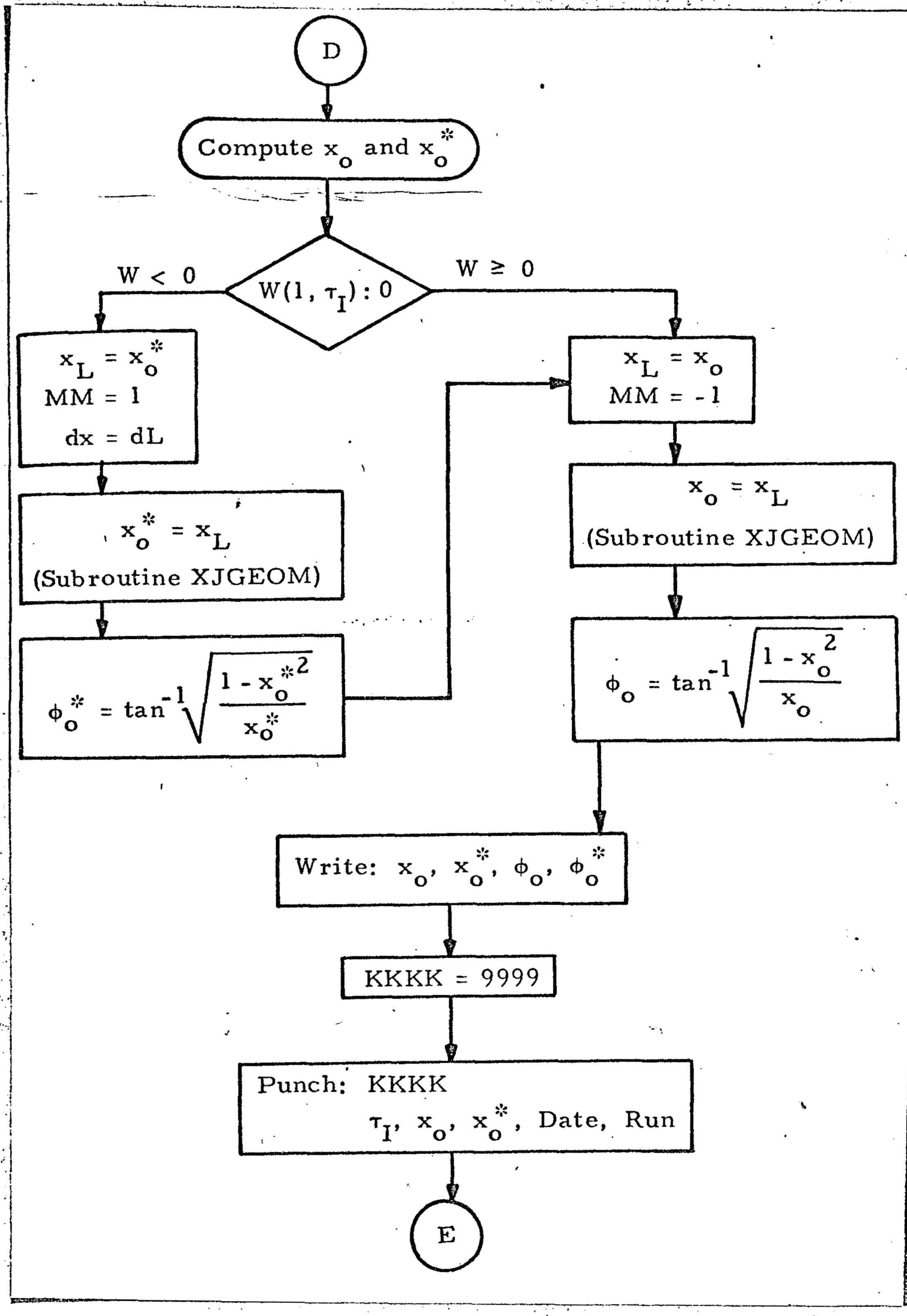
D
Compute x_o and x_o^*
$W(1, \tau_I) : 0$
W < 0
W ≥ 0
$x_L = x_o^*$
MM = 1
dx = dL
$x_o^* = x_L$
(Subroutine XJGEOM)
$\phi_o^* = \tan^{-1}\sqrt{\frac{1 - x_o^{*2}}{x_o^*}}$
$x_L = x_o$
MM = - 1
$x_o = x_L$
(Subroutine XJGEOM)
$\phi_o = \tan^{-1}\sqrt{\frac{1 - x_o^2}{x_o}}$
Write: x_o, x_o^*, ϕ_o, ϕ_o^*
KKKK = 9999
Punch: KKKK
τ_I, x_o, x_o^*, Date, Run
E

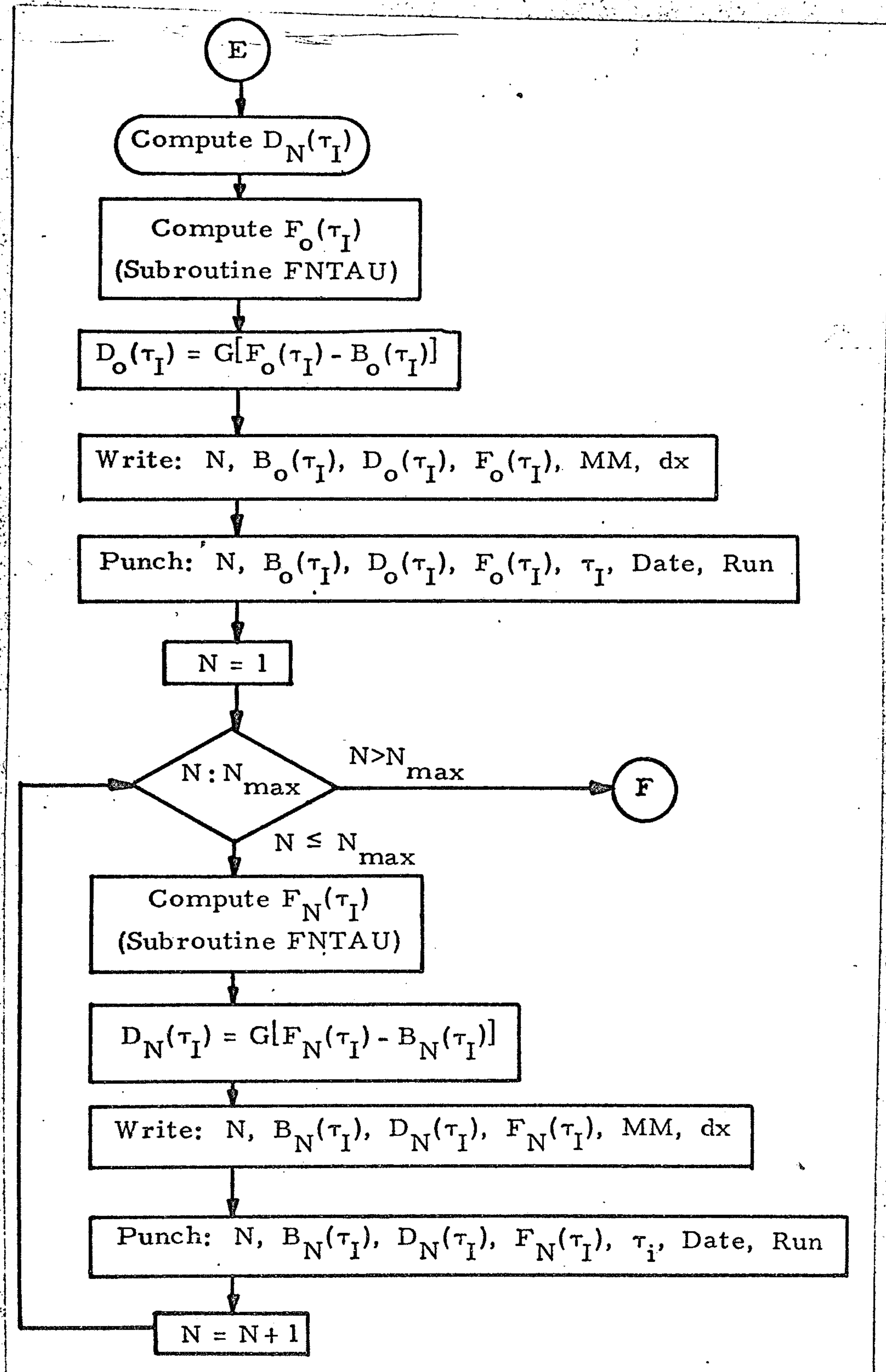
E
Compute $D_N(\tau_I)$
Compute $F_o(\tau_I)$ (Subroutine FNTAU)
$D_o(\tau_I) = G[F_o(\tau_I) - B_o(\tau_I)]$
Write: N, $B_o(\tau_I)$, $D_o(\tau_I)$, $F_o(\tau_I)$, MM, dx
Punch: N, $B_o(\tau_I)$, $D_o(\tau_I)$, $F_o(\tau_I)$, τ_I, Date, Run
N = 1
$N : N_{max}$
$N > N_{max}$
F
$N \leq N_{max}$
Compute $F_N(\tau_I)$ (Subroutine FNTAU)
$D_N(\tau_I) = G[F_N(\tau_I) - B_N(\tau_I)]$
Write: N, $B_N(\tau_I)$, $D_N(\tau_I)$, $F_N(\tau_I)$, MM, dx
Punch: N, $B_N(\tau_I)$, $D_N(\tau_I)$, $F_N(\tau_I)$, τ_i, Date, Run
N = N + 1

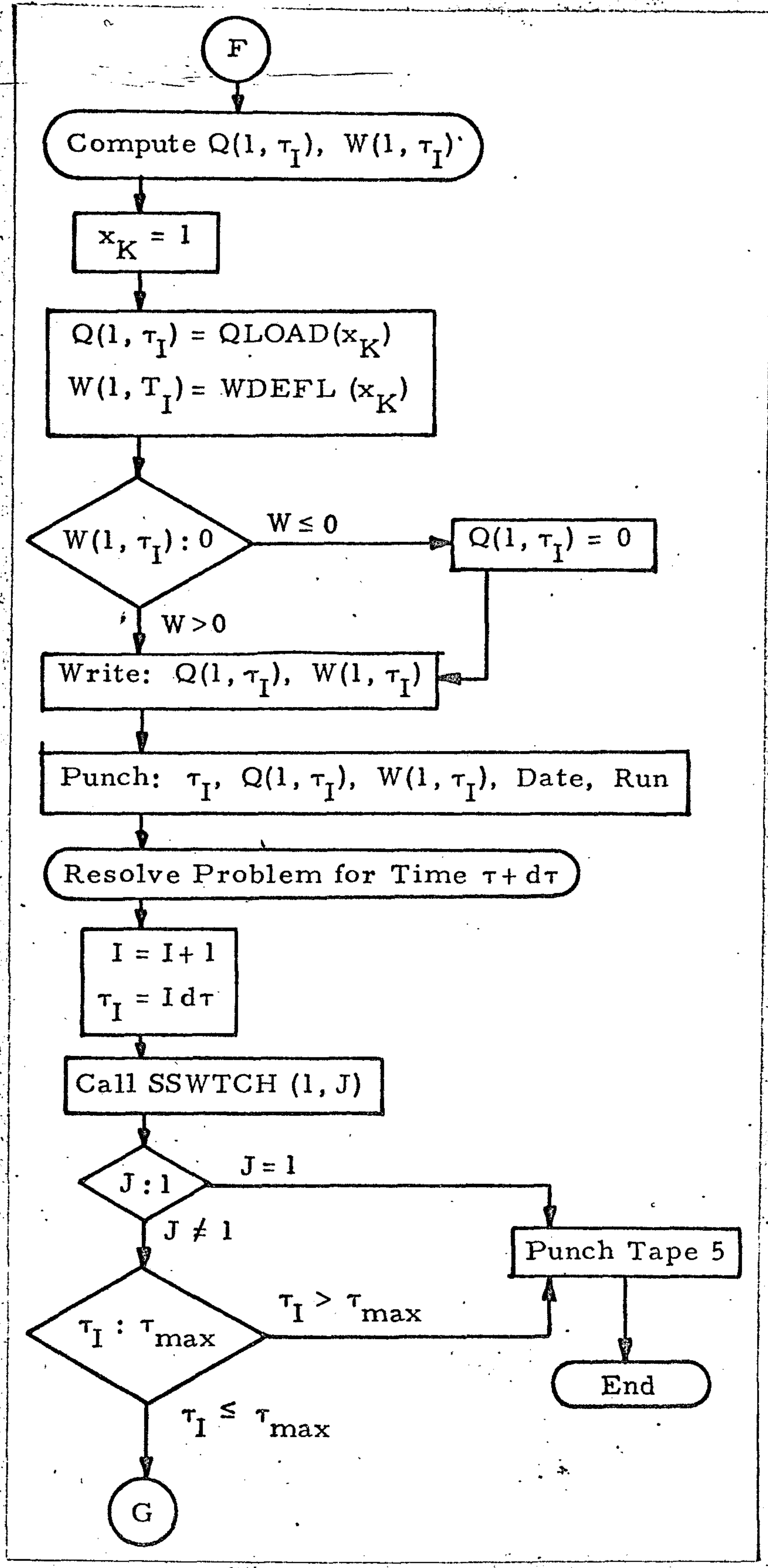
F
Compute Q(1, τI), W(1, τI)
xK = 1
Q(1, τI) = QLOAD(xK)
W(1, TI) = WDEFL (xK)
W(1, τI) : 0
W ≤ 0
Q(1, τI) = 0
W > 0
Write: Q(1, τI), W(1, τI)
Punch: τI, Q(1, τI), W(1, τI), Date, Run
Resolve Problem for Time τ + dτ
I = I + 1
τI = I dτ
Call SSWTCH (1, J)
J : 1
J = 1
J ≠ 1
Punch Tape 5
τI : τmax
τI > τmax
End
τI ≤ τmax
G

main program by way of COMMON storage. The quantities μ_n, ω_n, $B_1^{(n)}$, and $B_2^{(n)}$ for $n \geq 1$ have previously been stored in COMMON by the SIMPAC program.

Equation B.1 is integrated numerically using the trapezoidal rule and the constant integration interval $d\tau$. In computational form, equation B.1 may be written

$$B_n(\tau_i) = \begin{cases} 0, & i = 1, \; n \neq 1 \\ \beta\left(\frac{R}{h}\right) d\tau, & i = 1, \; n = 1 \\ \sum_{j=1}^{i-1} \eta_n(\tau_i - \tau_j)\, D_n(\tau_j)\, d\tau, & i > 1, \; n \neq 1 \\ \beta\left(\frac{R}{h}\right)\tau_i + \sum_{j=1}^{i-1} \eta_1(\tau_i - \tau_j)\, D_1(\tau_j)\, d\tau, & i > 1, \; n = 1 \end{cases} \tag{B.2}$$

The flow chart for this subprogram is shown in Figure 34.

Subroutine XJGEOM

This subprogram finds the cosines $x_0(\tau_i)$ or $x_0^*(\tau_i)$ as roots of the equation (see equation 3.57)

$$x = 1 - \left(\frac{h}{R}\right) x \; \omega(x, \tau_i) \tag{B.3}$$

The required cosine x_0 is found from equation B.3 using the method of successive approximations. In this procedure, a trial cosine x_K is first assumed. An improved value, x_{K+1}, is then found from equation B.3 when written in the form

$$x_{K+1} = 1 - \left(\frac{h}{R}\right) x_K \; \omega(x_K, \tau_i) \tag{B.4}$$

Figure 34. Flow Chart--Subroutine BNTAU

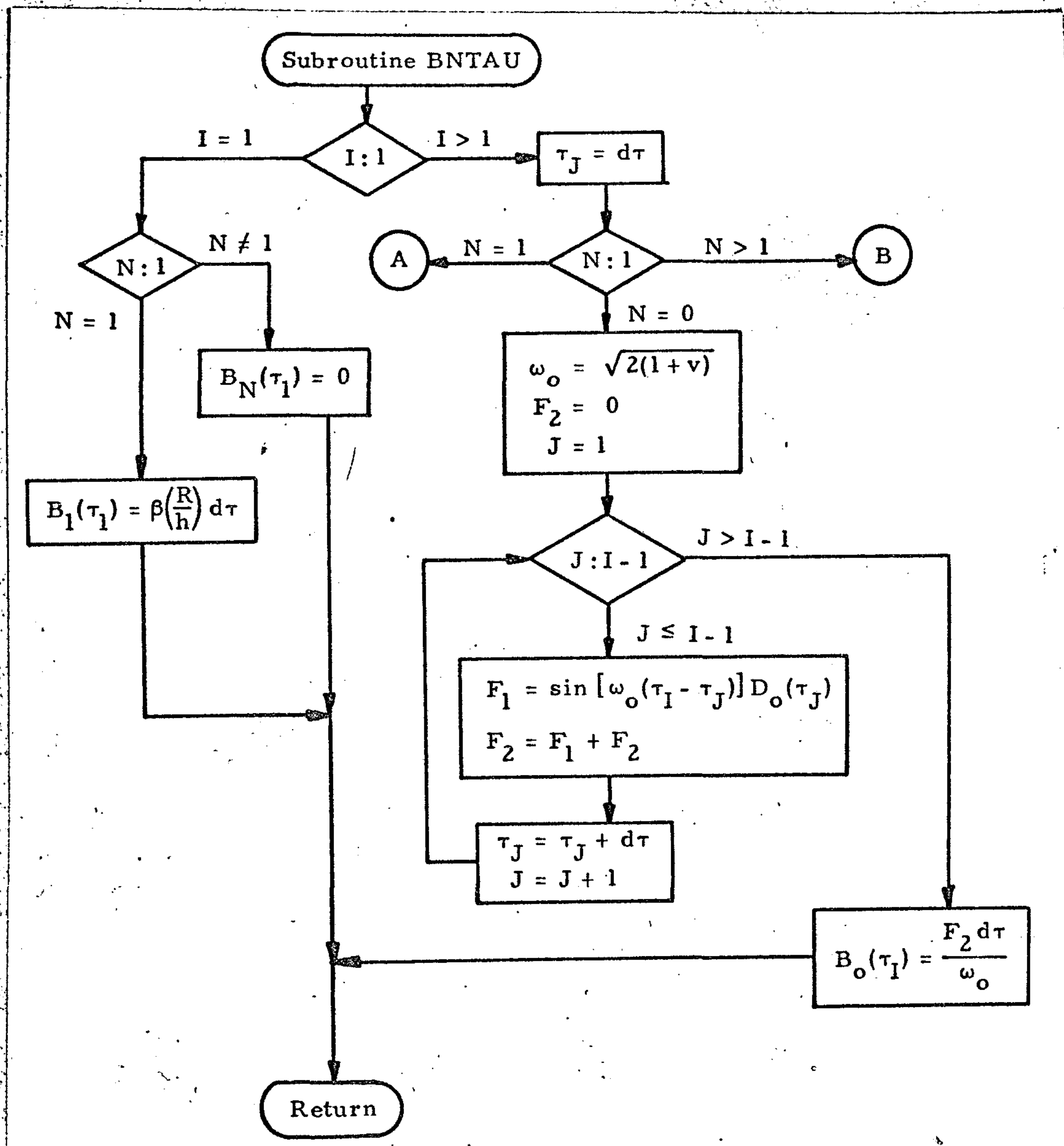
Subroutine BNTAU
I : 1
I = 1
I > 1
τ_J = dτ
N : 1
N ≠ 1
N = 1
B_N(τ_1) = 0
B_1(τ_1) = β(R/h) dτ
A
N = 1
N : 1
N > 1
B
N = 0
ω_o = √(2(1 + ν))
F_2 = 0
J = 1
J : I - 1
J > I - 1
J ≤ I - 1
F_1 = sin [ω_o(τ_I - τ_J)] D_o(τ_J)
F_2 = F_1 + F_2
τ_J = τ_J + dτ
J = J + 1
B_o(τ_I) = F_2 dτ / ω_o
Return

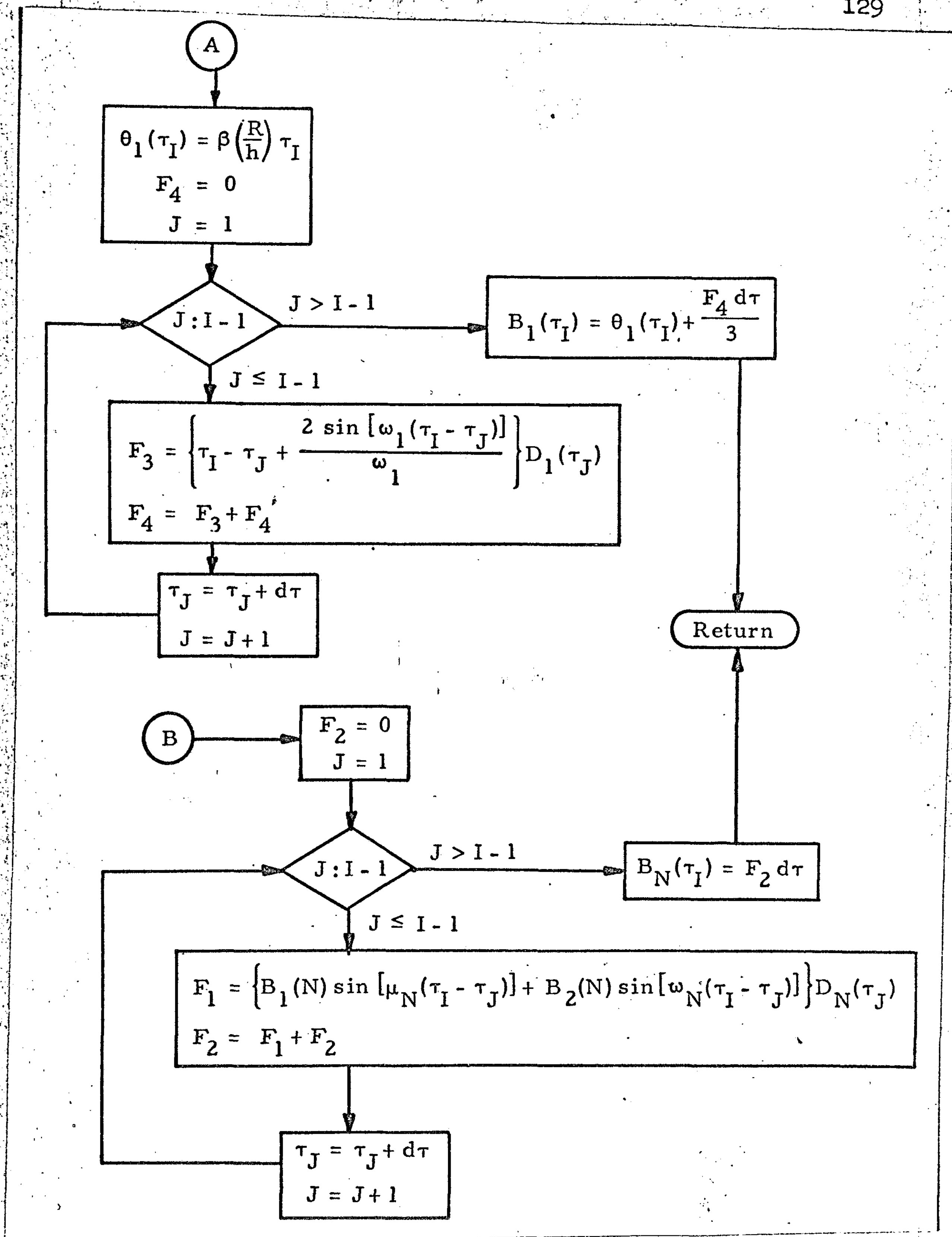
A
$\theta_1(\tau_I) = \beta\left(\frac{R}{h}\right)\tau_I$
$F_4 = 0$
$J = 1$
$J : I - 1$
$J > I - 1$
$B_1(\tau_I) = \theta_1(\tau_I) + \frac{F_4\,d\tau}{3}$
$J \leq I - 1$
$F_3 = \left\{\tau_I - \tau_J + \frac{2\sin[\omega_1(\tau_I - \tau_J)]}{\omega_1}\right\}D_1(\tau_J)$
$F_4 = F_3 + F_4$
$\tau_J = \tau_J + d\tau$
$J = J + 1$
Return
B
$F_2 = 0$
$J = 1$
$J : I - 1$
$J > I - 1$
$B_N(\tau_I) = F_2\,d\tau$
$J \leq I - 1$
$F_1 = \left\{B_1(N)\sin[\mu_N(\tau_I - \tau_J)] + B_2(N)\sin[\omega_N(\tau_I - \tau_J)]\right\}D_N(\tau_J)$
$F_2 = F_1 + F_2$
$\tau_J = \tau_J + d\tau$
$J = J + 1$

This procedure is repeated using a new trial value $x_K = x_{K+1}$. The iteration is repeated until either $\left|\frac{x_{K+1} - x_K}{x_{K+1}}\right| \leq$ Error or 30 iterations have been completed. The final value of x_{K+1} is the desired cosine. This value is returned to the main program through COMMON storage.

An error statement is given for any case where 30 iterations are required for the solution. However, experience has indicated that equation B.4 converges rapidly to the desired result with the possible exception of some cases where the change in x_o from one time to the next is very large.

In the computation of x_o (or x_o^*), we must insure that $0 \leq x_o \leq 1$. x_o cannot be greater than one since the cosine of an angle cannot be greater than one. x_o cannot be less than zero since this would infer that the shell was loaded to an angle $\phi > \frac{\pi}{2}$ which is an unattainable condition.

It is noted that the two cosines $x_o(\tau_i)$ and $x_o^*(\tau_i)$ are both found by using this subprogram. The procedure by which the two cosines are distinguished during the computation is predicated on the proper selection of the trial cosine x_K .

It is further noted that the cosine $x_o^*(\tau_i)$ will not appear as a root of equation B.4 until such time as the apex of the shell rebounds prior to the complete rebound of the shell.

The flow chart for this subprogram is shown in Figure 35.

Subroutine FNTAU

This subprogram computes $F_n(\tau)$ from the relation (see equation 3.54)

$$F_n(\tau) = B_n(\tau) + \left(\frac{2n+1}{2}\right)\int_{x_o}^{x_o^*}\left[\left(\frac{R}{h}\right)\left(\frac{1-x}{x}\right) - w(x,\tau)\right]P_n(x)\,dx \qquad \text{(B.5)}$$

where $B_n(\tau)$ is taken from COMMON storage, $w(x,\tau)$ is computed using the function subprogram WDEFL, and $P_n(x)$ is computed using the subprogram LEGFNJ. The resulting value for $F_n(\tau)$ is returned to the main program through COMMON storage.

The integral in equation B.5 is integrated numerically using the trapezoidal rule. The integration interval dx is selected in such a manner that it is smaller than the distance between two adjacent zeros of $P_n(x)$.

Since the distance between x = 1 and the largest zero of $P_n(x)$ is smaller than the distance between any two adjacent zeros of $P_n(x)$ [1], a conservative value for dx may be found in the manner of Szego (13:119, equation 6.2.17) to be

$$dx = \frac{5}{4n^2} \qquad \text{(B.6)}$$

[1]Compare with (7:118, Figure 64)

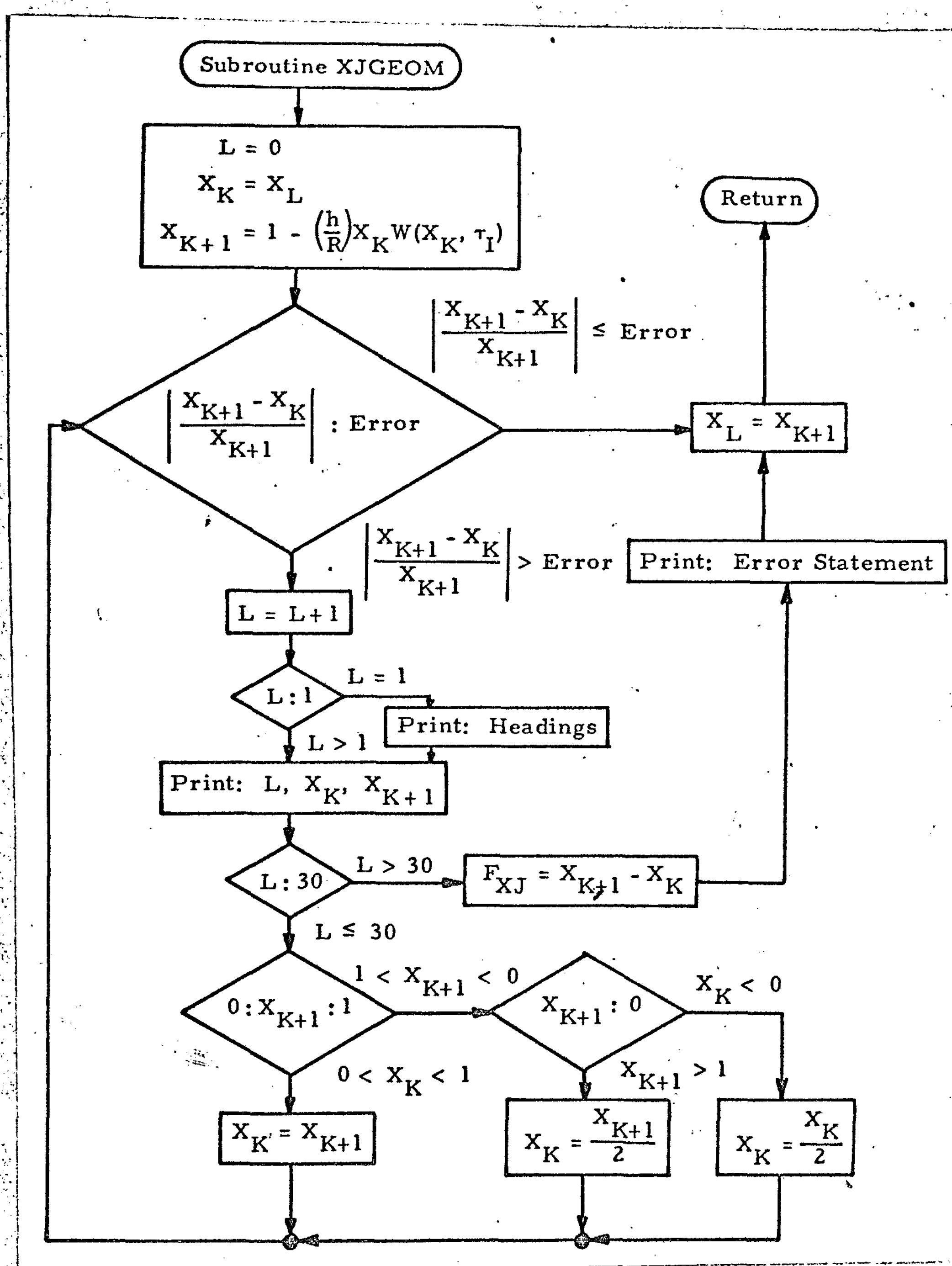

Figure 35. Flow chart--Subroutine XJGEOM

As further restrictions on dx, a minimum of 5 integration intervals are used in the integral, the maximum value of dx is taken to be dx = 0.05, and $m = \frac{x_o^* - x_o}{dx}$ is defined to be an integer value.

Using the above information, equation B.5 can be written in the following computational form:

$$F_n(\tau_i) = B_n(\tau_i) + \left[\frac{f(x_o^*)}{2} + \sum_{k=1}^{m-1} f(x_k) + \frac{f(x_o)}{2} \right] dx \qquad \text{(B.7)}$$

where

$$f(x_k) = \left(\frac{2n+1}{2}\right)\left[\left(\frac{R}{h}\right)\left(\frac{1-x_k}{x_k}\right) - w(x_k, \tau_i)\right] P_n(x_k)$$

The flow chart for this subprogram is shown in Figure 36.

Function QLOAD (XK, I)

This subprogram computes $Q(x,\tau)$ from the relation (see equation 3.27)

$$Q(x,\tau) = \sum_{n=0}^{N_{max}} P_n(x)\ D_n(\tau) \qquad \text{(B.8)}$$

where $P_n(x)$ is computed using the subprogram LEGFNJ and $D_n(\tau)$ is taken from COMMON storage.

The program is written as a FUNCTION subprogram with the arguments XK and I representing the space variable and time interval, respectively. The flow chart for this subprogram is shown in Figure 37.

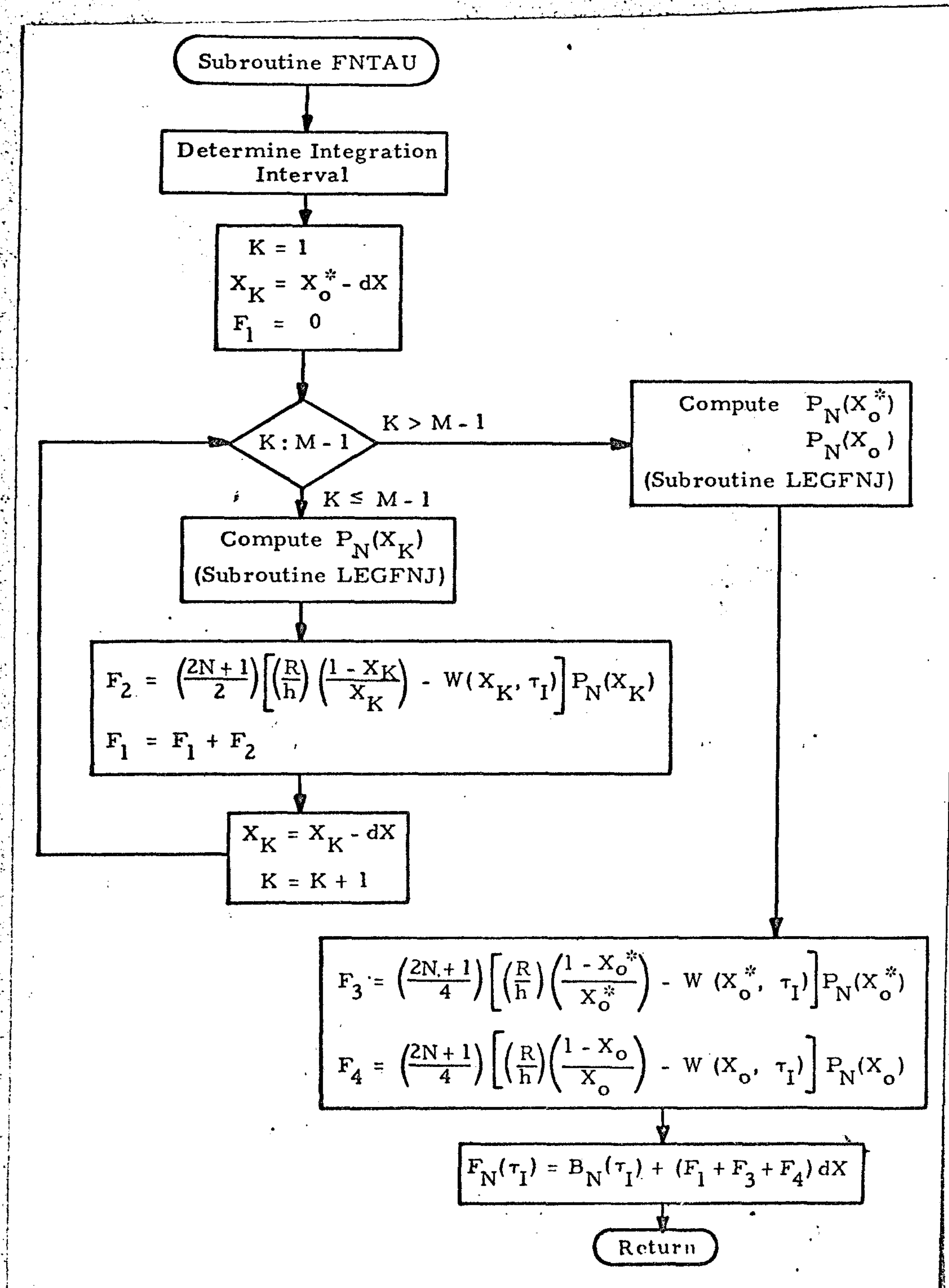

Figure 36. Flow chart--Subroutine FNTAU

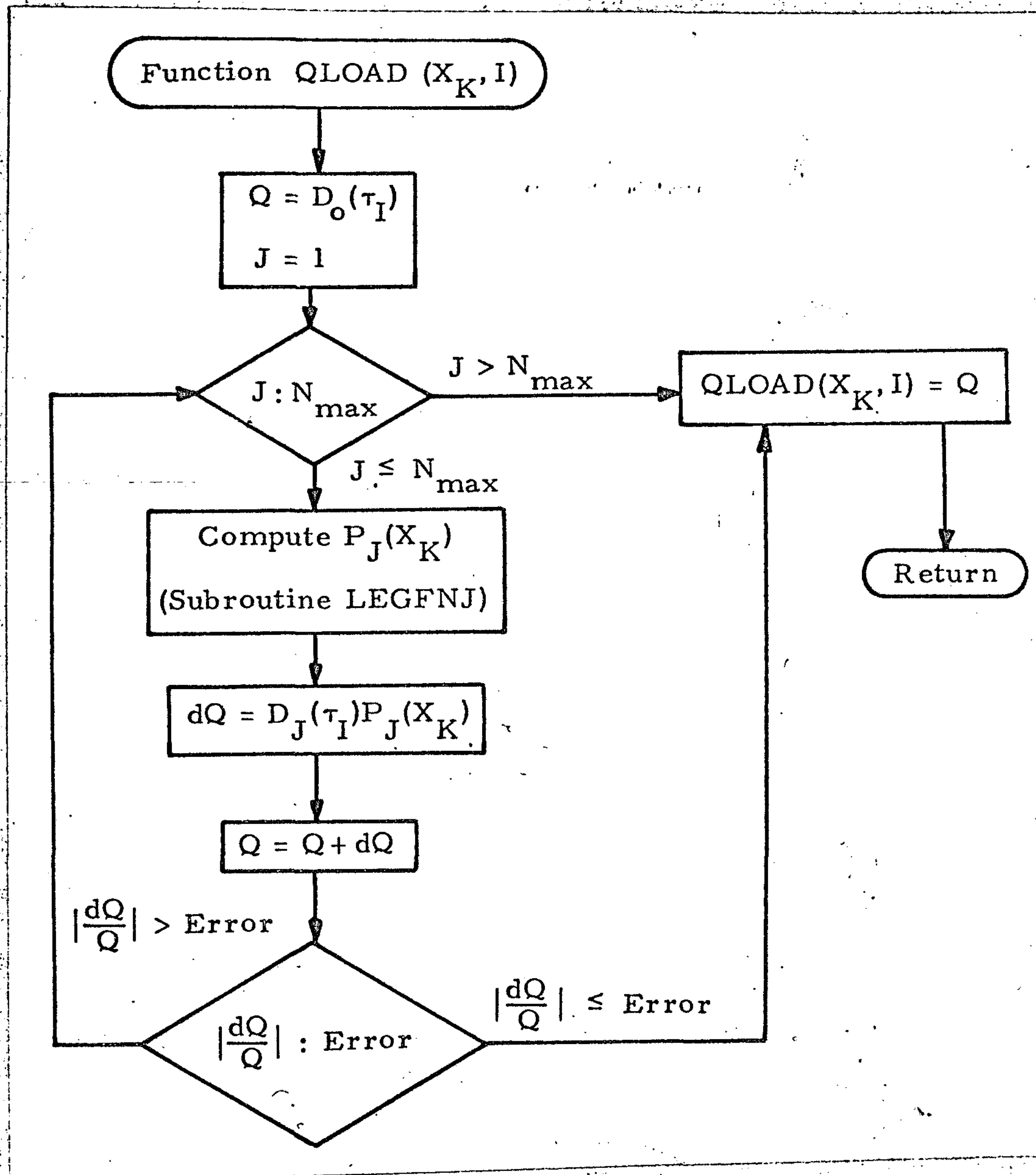

Figure 37. Flow chart--Function QLOAD

Function WDEFL (XK)

This subprogram computes $w(x,\tau)$ from the relation (see equation 3.26)

$$w(x,\tau) = \sum_{n=0}^{N_{max}} P_n(x)\, B_n(\tau) \qquad \text{(B.9)}$$

where $P_n(x)$ is computed using the subprogram LEGFNJ and $B_n(\tau)$ is taken from COMMON storage.

The program is written as a FUNCTION subprogram with the argument XK representing the space variable. The flow chart for this subprogram is shown in Figure 38.

Subroutine LEGFNJ (N, X, PN)

This subroutine computes the Legendre polynomials, $P_n(x)$, of real argument using the hypergeometric series. The arguments N, X, and PN represent the degree, argument, and value of the polynomial, respectively.

The accuracy of these computations depends on the accuracy of the computation for the hypergeometric series. Using the hypergeometric series computed from the subroutine HYPFNR, we are restricted to Legendre polynomials of degree less than 30. For $n > 30$, either the subprogram HYPFNR must be modified or the Legendre polynomials must be derived from some other method such as through the use of asymptotic formulae.

The particular equation used to determine $P_n(x)$

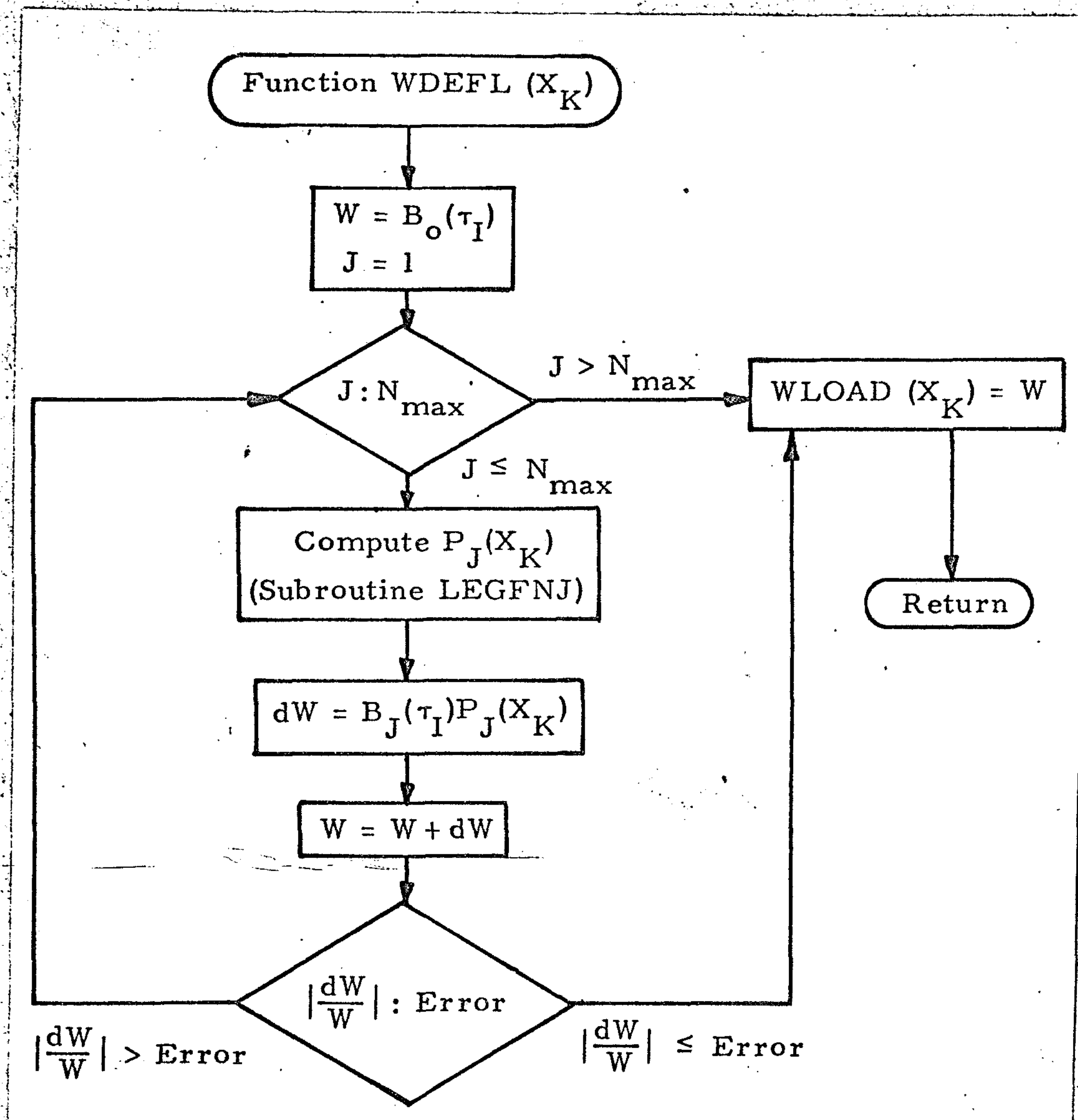

Figure 38. Flow chart--Function WDEFL

depends on the values of n and x. For the special cases of n = 0 and n = 1, we have that

$$P_0(x) = 1 \quad , \quad -1 \leq x \leq 1$$
$$P_1(x) = x \quad , \quad -1 \leq x \leq 1 \qquad \text{(B.10)}$$

For the special cases of x = 1 and x = -1, we have that

$$P_n(1) = 1$$
$$P_n(-1) = (-1)^n \qquad \text{(B.11)}$$

If $0.8 \leq x < 1$, we use the Bateman solution (2:124, equation 3.2 (14))

$$P_n(x) = F(-n, n+1 ; 1 ; \frac{1-x}{2}) \qquad \text{(B.12)}$$

If $0 \leq x < 0.8$, we use the relations (2:150, equations 3.6.2 (15 and 16)

$$P_{2n}(x) = \frac{(-1)^n (2n)! \, F(-n, n+\frac{1}{2} ; \frac{1}{2} ; x^2)}{(2)^{2n} \, (n!)^2}$$
$$P_{2n+1}(x) = \frac{(-1)^n (2n+1)! \, x \, F(-n, n+\frac{3}{2} ; \frac{3}{2} ; x^2)}{(2)^{2n} \, (n!)^2} \qquad \text{(B.13)}$$

If $-1 < x < 0$, we use the appropriate one of equations B.12 to B.13 and the relation (2:151)

$$P_n(-x) = (-1)^n P_n(x) \qquad \text{(B.14)}$$

Using equations B.10 to B.14, the program computes the Legendre polynomials according to the procedure outlined in Figure 39.

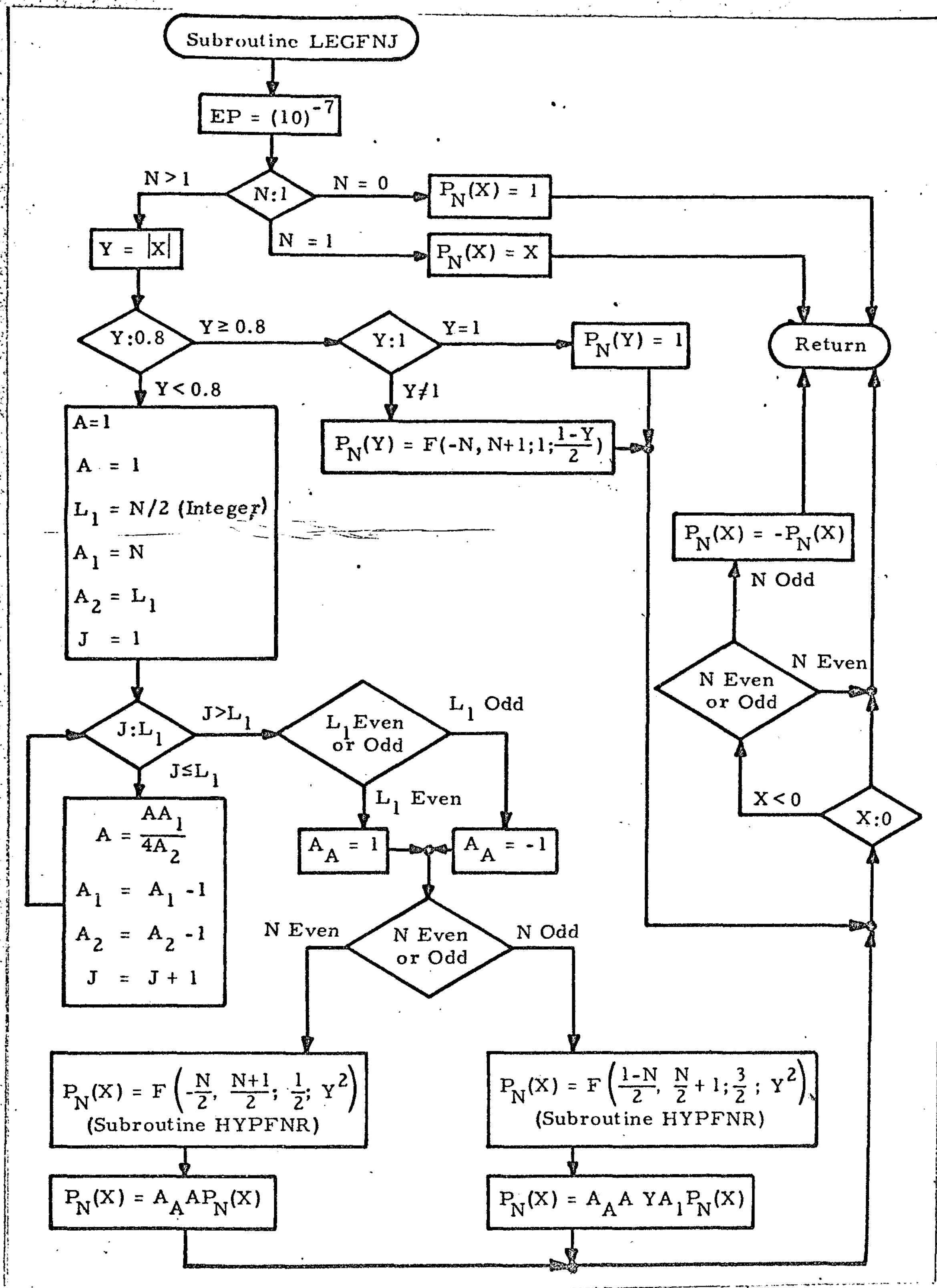

Figure 39. Flow chart--Subroutine LEGFNJ

Subroutine HYPFNR (A, B, C, Z, EP, F)

This subroutine computes the hypergeometric function of real argument and returns the result to the calling program. The hypergeometric function may be computed from the equation

$$F(A, B; C; z) = \sum_{r=0}^{\infty} \frac{(A)_r \; (B)_r}{(C)_r \; r!} z^r \tag{B.15}$$

where

$$(A)_r = \begin{cases} A(A+1)(A+2)\ldots\ldots(A+r-1) & , r \geq 1 \\ 0 & , r = 0 \end{cases}$$

The series given by equation B.15 is evaluated in the manner shown on the flow chart given in Figure 40. The various arguments of this subroutine are A, B, C, and Z as defined in equation B.15, an allowable error EP, and the output function F.

FORTRAN Listing

The complete FORTRAN listing for the SIMPAC program and its subroutines is given in Figures 41 to 48. The program is written in the FORTRAN IV language and as listed has been run on the Honeywell H-800 computer.

The main program is named SIMPAC. The subroutines BNTAU, XJGEOM, FNTAU, LEGFNJ, and HYPFNR and the function subprograms QLOAD and WDEFL are used during the computation.

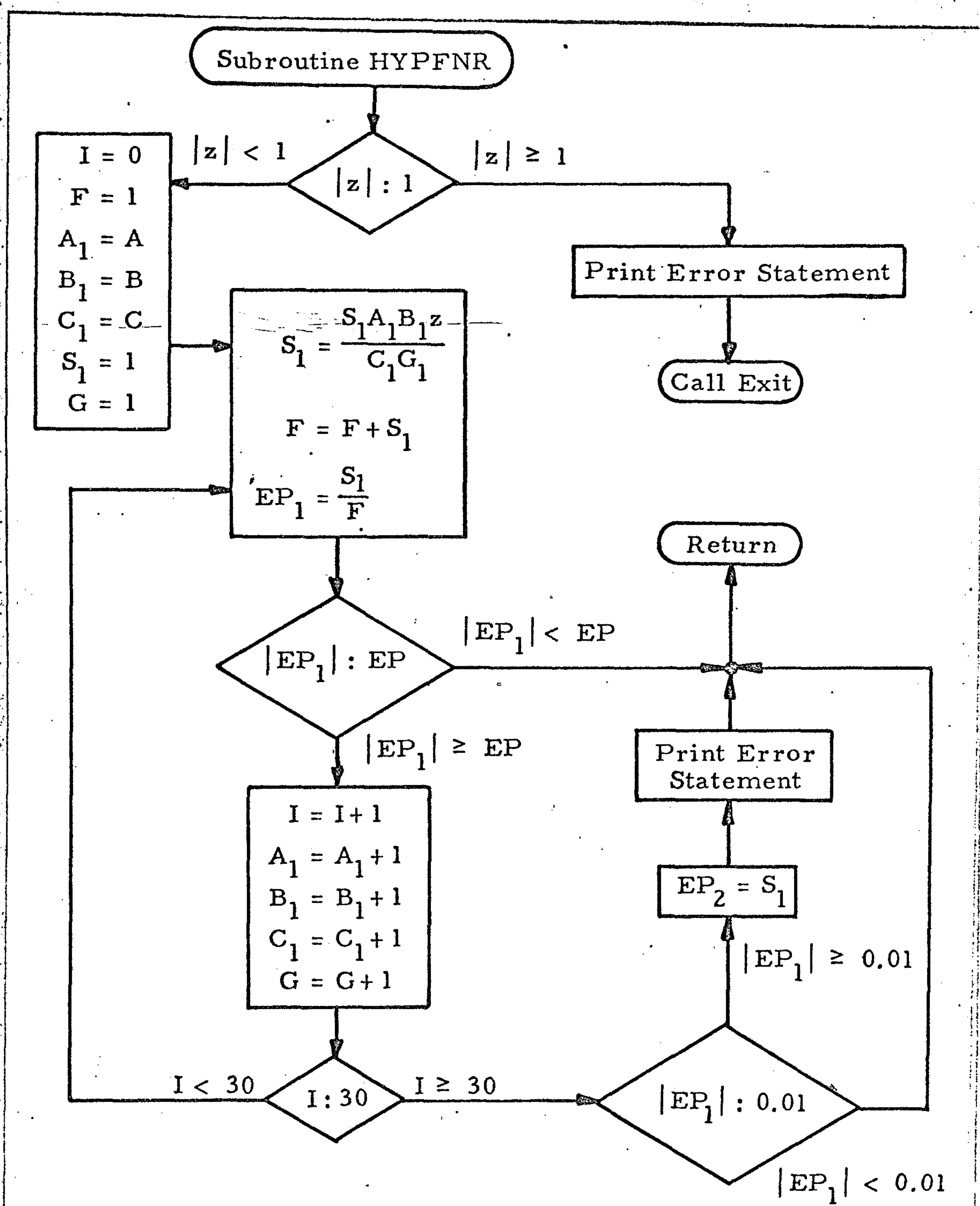

Figure 40. Flow chart--Subroutine HYPFNR

Figure 41. FORTRAN Listing--SIMPAC Program

```
C     PROGRAM TO COMPUTE LOAD AND DISPLACEMENT
C     DURING IMPACT OF A SPHERICAL SHELL ON AN ELASTIC SURFACE
C     MODAL MEMBRANE SOLUTION
C     PROGRAM NAME IS SIMPAC
      DIMENSION DLOADZ(200),DLOAD(30,200),BN(30),FMU(30),FOM(30),B1(30),
     1B2(30),INDATA(19)
      COMMON/MAIN/BETA,POI,RH,NMAX,DT,ERROR,BNZ,XJ,I,TI,N,BNT,XJS,FNT,
     1XL,DX,MM/MASTER/DLOADZ,DLOAD,BN,FMU,FOM,B1,B2
      INTEGER OUT
      DATA IN,OUT/2,3/,L1,L2/200,30/
C     INPUT DATA
C     CARD 1 - SPRING,BETA,POI,RH
C     CARD 2 - NMAX,TMAX,DT,ERROR
C     CARD 3 - E,RHO,H
C     CARD 4 - MONTH,DAY,YEAR
C     CARD 5 - RUN NUMBER
    1 READ(IN,51)SPRING,BETA,POI,RH,LL
   51 FORMAT(2E8.1,F8.6,F8.2,I4)
      READ(IN,52)NMAX,TMAX,DT,ERROR,DX
   52 FORMAT(4X,I4,F8.3,F8.5,E8.1,F8.5)
      READ(IN,120)E,RHO,H
  120 FORMAT(E8.1,2F8.5)
      READ(IN,53)MONTH,KDAY,KYEAR
   53 FORMAT(3I2)
      READ(IN,54)KRUN
   54 FORMAT(I4)
      STIFF=E*SPRING/H
      CVEL=SQRT (E*386./(RHO*(1.-POI*POI)))
      RADIUS=RH*H
      VZERO=BETA*CVEL
      TIME=RADIUS/CVEL
```

```
      WRITE(OUT,55)MONTH,KDAY,KYEAR,KRUN
   55 FORMAT(1H1,49HIMPACT OF A SPHERICAL SHELL ON AN ELASTIC SURFACE/1H
     1 ,25HMODAL - MEMBRANE SOLUTION/1H ,15HPROGRAM SIMPAC ,I2,1H/,I2,
     21H/,I2,5H RUN ,I4//1H ,28HSHELL AND SURFACE PARAMETERS/)
      WRITE(OUT,56)SPRING,BETA,POI,RH
   56 FORMAT(1H ,7HSPRING=,E8.1/1H ,2X,5HBETA=,E8.1/1H ,3X,4HPOI=,F8.6/
     11H ,3X,4HR/H=,F8.2//)
      WRITE(OUT,121)E,RHO,H
  121 FORMAT(1H ,19HPHYSICAL PROPERTIES//1H ,22HMODULUS OF ELASTICITY=,
     1E8.1,8H LBS/IN2/1H ,14X,8HDENSITY=,F8.5,10H LBS/IN3/G/1H ,6X,
     216HSHELL THICKNESS=,F8.5,7H INCHES/)
      WRITE(OUT,122)STIFF,RADIUS
  122 FORMAT(1H ,4X,18HSURFACE STIFFNESS=,E14.7,11H LBS/IN/IN2/1H ,9X,
     113HSHELL RADIUS=,E14.7,7H INCHES/)
      WRITE(OUT,123)TIME,CVEL,VZERO
  123 FORMAT(1H ,2X,20HREAL TIME (SECONDS)=,E14.7,22H * NONDIMENSIONAL T
     1IME//1H ,7X,15HSOUND VELOCITY=,E14.7,14H INCHES/SECOND/1H ,5X,
     217HINITIAL VELOCITY=,E14.7,14H INCHES/SECOND//)
```

```
C     COMPUTE CONSTANTS
      G=SPRING*(1.-POI*POI)*RH*RH
      WRITE(OUT,8)
    8 FORMAT(1H ,19HANALYSIS PARAMETERS/)
      WRITE(OUT,10)NMAX,TMAX,DT,ERROR,DX,G
   10 FORMAT(1H ,2X,5HNMAX=,I4/1H ,2X,5HTMAX=,F8.3/1H ,4X,3HDT=,F8.5/1H
     1,1X,6HERROR=,E8.1/1H ,4X,3HDX=,F8.5/1H ,5X,2HG=,E14.7//)
      WRITE(OUT,250)
  250 FORMAT(1H ,9HCONSTANTS/)
      WRITE(OUT,2)
```

```
    2 FORMAT(1H ,1X,1HN,5X,6HAN(MU),9X,9HBN(OMEGA),7X,5HB1(N),10X,5HB2(N
     1)/)
      POI2=(1.-(POI*POI))
      DO 3 N=1,NMAX
      EN=N
      EN2=EN*(EN+1.)
      G4=EN2+1.+3.*POI
      G5=POI2*(EN2-2.)
      G6=SQRT (G4*G4-4.*G5)
      FMU(N)=SQRT ((G4-G6)/2.)
      FOM(N)=SQRT ((G4+G6)/2.)
      G12=EN2-1.+POI
      IF(N-1)4,4,5
    4 B1(N)=0.
      GO TO 6
    5 B1(N)=(G12/FMU(N)-FMU(N))/G6
    6 B2(N)=-(G12/FOM(N)-FOM(N))/G6
      WRITE(OUT,7)N,FMU(N),FOM(N),B1(N),B2(N)
    7 FORMAT(1H ,I3,2(2X,E14.7,1X,E14.7))
    3 CONTINUE
```

```
C     SOLUTION TO THE PROBLEM
C     ASSUME INITIAL VALUES
      DL=DX
      TI=DT
      XJ=1.-BETA*DT
      I=1
      XJS=1.
      PHIJS=0.
      W1=0.
      TAN=SQRT (1.-XJ*XJ)/XJ
      PHIJ=ATAN (TAN)
      WRITE(OUT,50)XJ,PHIJ
   50 FORMAT(1H0,14HINITIAL XZERO=,E14.7,10H, PHIZERO=,E14.7)
C     OPTION TO INPUT PRECOMPUTED DATA
      IF(LL.EQ.0)GO TO 18
      READ(IN,211)IDONE
  211 FORMAT(I4)
      DO 202 J=1,IDONE
      READ(IN,203)(INDATA(K),K=1,19)
  203 FORMAT(19I4)
      ISUM=0
      DO 204 K=1,19
  204 ISUM=ISUM+INDATA(K)
      IF(ISUM)205,206,205
  205 GO TO 19
  206 READ(IN,207)TI,XJ,XJS
  207 FORMAT(3E14.7)
      READ(IN,208)BNZ,DLOADZ(J)
  208 FORMAT(4X,2E14.7)
      DO 209 N=1,NMAX
  209 READ(IN,208)BN(N),DLOAD(N,J)
  202 CONTINUE
```

```
      I=IDONE+1
      TI=TI+DT
      READ(IN,216)W1
  216 FORMAT(28X,E14.7)
C     COMPUTE BN(T) (SUBROUTINE BNTAU)
      REWIND 5
   18 WRITE(OUT,20)TI
```

```
   20 FORMAT(1H1,18HSOLUTION FOR TIME=,F10.5/)
      N=0
      CALL BNTAU(DLOADZ,DLOAD,FMU,FOM,B1,B2,L1,L2)
      BNZ=BNT
      DO 11 N=1,NMAX
      CALL BNTAU(DLOADZ,DLOAD,FMU,FOM,B1,B2,L1,L2)
   11 BN(N)=BNT
C     COMPUTE XZERO(STAR) IF NONZERO (SUBROUTINE XJGEOM)
      IF(W1)62,63,63
   62 XL=XJS
      WRITE(OUT,64)
   64 FORMAT(1H0,32HCONVERGENCE DATA FOR XZERO(STAR))
      MM=1
      DX=DL
      CALL XJGEOM(BN,L2)
      XJS=XL
      TAN=SQRT (1.-XJS*XJS)/XJS
      PHIJS=ATAN (TAN)
C     COMPUTE XZERO (SUBROUTINE XJGEOM)
   63 XL=XJ
      WRITE(OUT,65)
   65 FORMAT(1H0,26HCONVERGENCE DATA FOR XZERO)
```

11-5

```
      MM=-1
      CALL XJGEOM(BN,L2)
      XJ=XL
      TAN=SQRT (1.-XJ*XJ)/XJ
      PHIJ=ATAN (TAN)
C     COMPUTE DN(T) USING SUBROUTINE FNTAU
      WRITE(OUT,21)
   21 FORMAT(1H0,46HSERIES EXPANSION TERMS FOR LOAD AND DEFLECTION/)
      WRITE(OUT,22)XJ,XJS,PHIJ,PHIJS
   22 FORMAT(1H ,2X,6HXZERO=,E14.7,3X,12HXZERO(STAR)=,E14.7/1H ,8HPHIZER
     1O=,E14.7,1X,14HPHIZERO(STAR)=,E14.7/)
      WRITE(OUT,23)
   23 FORMAT(1H ,2X,1HN,3X,5HBN(T),10X,5HDN(T),11X,5HFN(T),11X,1HM,4X,
     12HDX/)
      KKK=9999
      PUNCH 110,KKK
  110 FORMAT(76X,I4)
      PUNCH 24,TI,XJ,XJS,MONTH,KDAY,KYEAR,KRUN
   24 FORMAT(3E14.7,22X,6HSIMPAC,3I2,I4)
      N=0
      CALL FNTAU(BN,L2)
      DLOADZ(I)=G*(FNT-BNZ)
      WRITE(OUT,25)N,BNZ,DLOADZ(I),FNT,MM,DX
   25 FORMAT(1H ,I4,2(1X,E14.7),2X,E14.7,1X,I4,1X,E14.7)
      PUNCH 26,N,BNZ,DLOADZ(I),FNT,TI,MONTH,KDAY,KYEAR,KRUN
   26 FORMAT(I4,4E14.7,4X,6HSIMPAC,3I2,I4)
      DO 27 N=1,NMAX
      CALL FNTAU(BN,L2)
      DLOAD(N,I)=G*(FNT-BN(N))
      WRITE(OUT,25)N,BN(N),DLOAD(N,I),FNT,MM,DX
      PUNCH 26,N,BN(N),DLOAD(N,I),FNT,TI,MONTH,KDAY,KYEAR,KRUN
   27 CONTINUE
```

```
C     COMPUTE Q(1,I) AND W(1,I)
      XK=1.
      Q1=QLOAD(XK,  DLOADZ,DLOAD,L1,L2)
      W1=WDEFL(XK,BN,L2)
      IF(W1)30,30,31

   30 Q1=0.
   31 WRITE(OUT,28)Q1,W1
   28 FORMAT(1H0,8HQ(1,TI)=,E14.7,1X,8HW(1,TI)=,E14.7)
      PUNCH 29,TI,Q1,W1,MONTH,KDAY,KYEAR,KRUN
   29 FORMAT(3E14.7,15X,5HQANDX,2X,6HSIMPAC,3I2,I4)
C     RESOLVE PROBLEM FOR TIME T+DT
      I=I+1
      AI=I
      TI=AI*DT
      CALL SSWTCH(1,J)
      IF(J.EQ.1)GO TO 19
      IF(TI-TMAX)18,18,19
   19 CALL PUNCHR(5)
      GO TO 1
      END
```

Figure 42. FORTRAN Listing--Subroutine BNTAU

```
      SUBROUTINE BNTAU(DLOADZ,DLOAD,FMU,FOM,B1,B2,L1,L2)
C     SUBPROGRAM TO COMPUTE BN(TAU)
      DIMENSION DLOADZ(L1),DLOAD(L2,L1),       FMU(L2),FOM(L2),B1(L2),
     1B2(L2)
      COMMON/MAIN/BETA,POI,RH,NMAX,DT,ERROR,BNZ,XJ,I,TI,N,BNT,XJS,FNT,
     1XL,DX,MM
      IF(I-1)1,1,2
    1 IF(N-1)3,4,3
    3 BNT=0.
      RETURN
    4 BNT=RH*BETA*TI
      RETURN
    2 T1=DT
      I1=I-1
      IF(N-1)20,21,22
C     COMPUTE GENERAL ZERO ORDER TERM
   20 FOMZ=SQRT(2.*(1.+POI))
      F2=0.
      DO 8 J=1,I1
      F1=SIN (FOMZ*(TI-T1))*DLOADZ(J)
      F2=F1+F2
    8 T1=T1+DT
      BNT=DT*F2/FOMZ
      RETURN
```

```
C       COMPUTE GENERAL FIRST ORDER TERM
     21 E1=BETA*TI*RH
        F4=0.
        DO 6 J=1,I1
        F1=TI-T1
        F2=2.*SIN (FOM(1)*F1)/FOM(1)
        F3=(F1+F2)*DLOAD(1,J)
        F4=F4+F3
      6 T1=T1+DT
        BNT=(E1+DT*F4/3.)
        RETURN
C       COMPUTE GENERAL NTH ORDER TERM
     22 F2=0.
        DO 7 J=1,I1
        F1=(B1(N)*SIN (FMU(N)*(TI-T1))+B2(N)*SIN (FOM(N)*(TI-T1)))*DLOAD(N
       1,J)
        F2=F2+F1
      7 T1=T1+DT
        BNT=DT*F2
        RETURN
        END
```

Figure 43. FORTRAN Listing--Subroutine XJGEOM

```
      SUBROUTINE XJGEOM(BN,L2)
C     SUBPROGRAM TO DETERMINE XJ(T) USING GEOMETRICAL RELATIONS
C     USE METHOD OF SUCCESSIVE APPROXIMATIONS
      DIMENSION BN(L2)
      COMMON/MAIN/BETA,POI,RH,NMAX,DT,ERROR,BNZ,XJ,I,TI,N,BNT,XJS,FNT,
     1XL,DX,MM
      INTEGER OUT
      DATA OUT/3/
      L=0
      HR=1./RH
    5 IF(MM)15,16,16
   16 XLL=XL-DX
      WX=WDEFL(XL,BN,L2)
      FX=XL*WX-RH*(1.-XL)
      DFX=(WX-WDEFL(XLL,BN,L2))*XL/DX+WX+RH
      XK=XL-FX/DFX
      GO TO 17
   15 XK=1.-HR*XL*WDEFL(XL,BN,L2)
   17 IF(ABS ((XK-XL)/XK)-ERROR)1,1,2
```

```
C     MAXIMUM OF 30 TRYS FOR CONVERGENCE
    2 L=L+1
      IF(L-1)104,104,105
  104 WRITE(OUT,102)
  102 FORMAT(1H ,2X,1HL,3X,7HXL(OLD),8X,7HXL(NEW))
  105 WRITE(OUT,103)L,XL,XK
  103 FORMAT(1H ,I3,2(1X,E14.7))
      IF(L-30)3,4,4
    3 IF((XK)*(XK-1.))7,8,8
    7 XL=XK
      GO TO 5
    8 IF(XK)9,9,10
   10 XL=(1.+XL)/2.
      GO TO 5
    9 XL=XL/2.
      GO TO 5
    4 FXL=XK-XL
      WRITE(OUT,6)FXL,XL,XK
    6 FORMAT(1H0,20HERROR AFTER 30 TRYS=,E14.7/1H ,4X,7HXL(29)=,E14.7,1X
     1,7HXL(30)=,E14.7///)
    1 XL=XK
      IF(XL-1.)11,11,12
   12 XL=1.0
   11 IF(XL)20,20,21
   20 XL=0.001
   21 CONTINUE
      RETURN
      END
```

Figure 44. FORTRAN Listing--Subroutine FNTAU

```
      SUBROUTINE FNTAU(BN,L2)
C     SUBPROGRAM TO COMPUTE FN(T)
C     USE TRAPEZOIDAL RULE DURING INTEGRATION
      DIMENSION BN(L2)
      COMMON/MAIN/BETA,POI,RH,NMAX,DT,ERROR,BNZ,XJ,I,TI,N,BNT,XJS,FNT,
     1XL,DX,MM
C     DETERMINE INTEGRATION INTERVAL
      EN=N
      IF(N-7)1,1,2
    1 DX=0.05
      GO TO 3
    2 DX=1.25/(EN*EN)
C     CHECK FOR MINIMUM OF 5 INTEGRATION INTERVALS
    3 MM=(XJS-XJ)/DX
      IF(MM-5)4,5,5
    4 MM=5
C     COMPUTE EXACT INTEGRATION INTERVAL
    5 EM=MM
      DX=(XJS-XJ)/EM
```

```
C     PERFORM INTEGRATION
      M1=MM-1
      XK=XJS-DX
      F1=0.
      EN1=(2.*EN+1.)/2.
      DO 6 J=1,M1
      CALL LEGFNJ(N,XK,PN)
      F2=((RH*(1.-XK)/XK)-WDEFL(XK))*PN*EN1
      F1=F1+F2
    6 XK=XK-DX
      CALL LEGFNJ(N,XJS,P1)
      CALL LEGFNJ(N,XJ,P2)
      F3=((RH*(1.-XJS)/XJS)-WDEFL(XJS))*P1*EN1/2.
      F4=((RH*(1.-XJ)/XJ)-WDEFL(XJ))*P2*EN1/2.
      IF(N)7,7,8
    7 BNT=BNZ
      GO TO 9
    8 BNT=BN(N)
    9 FNT=BNT+(F1+F3+F4)*DX
      RETURN
      END
```

```
      FUNCTION QLOAD(XK,  DLOADZ,DLOAD,L1,L2)
C     SUBPROGRAM TO COMPUTE Q(X,T) AT THE POINT X=XK
      DIMENSION DLOADZ(L1),DLOAD(L2,L1)
      COMMON/MAIN/BETA,POI,RH,NMAX,DT,ERROR,BNZ,XJ,I,TI,N,BNT,XJS,FNT,
     1XL,DX,MM
      QNXT=DLOADZ(I)
      DO 1 J=1,NMAX
      CALL LEGFNJ(J,XK,PN)
      DQ=DLOAD(J,I)*PN
      QNXT=QNXT+DQ
      IF(ABS (DQ/QNXT)-ERROR)2,2,1
    1 CONTINUE
    2 QLOAD=QNXT
      RETURN
      END
```

Figure 45. FORTRAN Listing--Function QLOAD

```
      FUNCTION WDEFL(XK,BN,L2)
C     SUBPROGRAM TO COMPUTE W(X,T) AT THE POINT X=XK
      DIMENSION BN(L2)
      COMMON/MAIN/BETA,POI,RH,NMAX,DT,ERROR,BNZ,XJ,I,TI,N,BNT,XJS,FNT,
     1XL,DX,MM
      WNXT=BNZ
      DO 1 J=1,NMAX
      CALL LEGFNJ(J,XK,PN)
      DW=BN(J)*PN
      WNXT=WNXT+DW
      IF(ABS (DW/WNXT)-ERROR)2,2,1
    1 CONTINUE
    2 WDEFL=WNXT
      RETURN
      END
```

Figure 46. FORTRAN Listing--Function WDEFL

Figure 47. FORTRAN Listing--Subroutine LEGFNJ

```
C     SUBROUTINE TO COMPUTE LEGENDRE POLYNOMIALS
C     OF INTEGER ORDER AND ARGUMENT X=COS(PHI)
      SUBROUTINE LEGFNJ(N,X,PN)
      EP=1.0E-7
      EN=N
      IF(N-1)1,2,3
C     N=0
    1 PN=1.
      RETURN
C     N=1
    2 PN=X
      RETURN
C     N GREATER THAN ONE
    3 Y=ABS (X)
      H1=N/2
      H2=EN/2.
      IF(Y-0.8)5,4,4
    4 IF(Y-1.)7,8,7
C     Y NOT EQUAL TO ONE BUT GREATER THAN 0.8
    7 CALL HYPFNR(-EN,EN+1.,1.,(1.-Y)/2.,EP,PN)
      GO TO 15
C     Y LESS THAN 0.8
    5 A=1.
      L1=N/2
      A1=EN
      A2=L1
      DO 9 J=1,L1
      A=A*A1/(A2*4.)
      A1=A1-1.
    9 A2=A2-1.
```

```
      A2=L1
      G1=L1/2
      G2=A2/2.
      IF(G1-G2)10,11,10
   10 AA=-1.
      GO TO 12
   11 AA=1.
   12 IF(H1-H2)13,14,13
C     N IS ODD
   13 CALL HYPFNR((1.-EN)/2.,EN/2.+1.,1.5,Y**2,EP,PN)
      PN=AA*A*Y*PN*A1
      GO TO 15
C     N IS EVEN
   14 CALL HYPFNR(-EN/2.,(EN+1.)/2.,0.5,Y**2,EP,PN)
      PN=AA*A*PN
      GO TO 15
C     Y=1
    8 PN=1.
C     CHECK FOR NEGATIVE X
   15 IF(X)16,17,17
   16 IF(H1-H2)18,17,18
C     N IS ODD
   18 PN=-PN
   17 RETURN
      END
```

Figure 48. FORTRAN Listing--Subroutine HYPFNR

```
C     SUBROUTINE TO COMPUTE HYPERGEOMETRIC FUNCTION OF REAL ARGUMENT
      SUBROUTINE HYPFNR(A,B,C,Z,EP,F)
      INTEGER OUT
      DATA OUT/3/
      IF(ABS (Z)-1.)1,2,2
    2 WRITE(OUT,3)
    3 FORMAT(1H0,47HARGUMENT OF HYPFNR GREATER THAN OR EQUAL TO ONE)
      CALL EXIT
    1 I=0
      F=1.
      A1=A
      B1=B
      C1=C
      S1=1.
      G=1.
    4 S2=S1*A1
      S1=S2*B1
      S2=S1/C1
      S1=S2*(Z/G)
      F=F+S1
      EP1=S1/F
```

```
      IF(ABS (EP1)-EP)5,6,6
    6 I=I+1
      A1=A1+1.
      B1=B1+1.
      C1=C1+1.
      G=G+1.
      IF(I-30)4,9,9
    9 IF(ABS (EP1)-0.01)5,7,7
    7 EP2=S1
      WRITE(OUT,8)Z,EP1,EP2
    8 FORMAT(1H0,41HERROR IN HYPFNR ROUTINE (ARGUMENT EQUALS ,E14.7,1H)/
     11H ,22HRELATIVE ERROR EQUALS ,E14.7/1H ,22H ABSOLUTE ERROR EQUALS
     2,E14.7///)
    5 RETURN
      END
```

APPENDIX C

CHARACTERISTIC EQUATION DERIVATIONS

Eigenvalue Computations

The eigenvalues of the A matrix defined in equation 4.5 are determined here. The required eigenvalues are the roots λ_s of equation 4.7. This determinant equation may be written

$$|A-\lambda I| = -\begin{vmatrix} \lambda & 0 & 0 & 0 & 0 & 1 & 0 & 0 \\ 0 & \lambda & 0 & 0 & 0 & \upsilon & 0 & 0 \\ 0 & 0 & \lambda & 0 & 0 & 0 & 0 & 1 \\ 0 & 0 & 0 & \lambda & 0 & 0 & 0 & \upsilon \\ 0 & 0 & 0 & 0 & \lambda & 0 & K_s^2 & 0 \\ 1 & 0 & 0 & 0 & 0 & \lambda & 0 & 0 \\ 0 & 0 & 0 & 0 & 1 & 0 & \lambda & 0 \\ 0 & 0 & 1 & 0 & 0 & 0 & 0 & \lambda \end{vmatrix} = 0 \qquad \text{(C.1)}$$

Expanding equation C.1, it is seen that

$$|A-\lambda I| = \lambda^2(1-\lambda^2)^2(\lambda^2-K_s^2) = 0$$

Therefore, the required eigenvalues are

$$\lambda_s = 0,\ 0,\ \pm 1,\ \pm 1,\ \pm K_s \qquad \text{(C.2)}$$

Eigenvector Computations

The eigenvectors of the A matrix defined in equation 4.5 are determined here. The eigenvectors may be found from equation 4.6 when written in the form

$$l^s(A - \lambda_s I) = 0 \tag{C.3}$$

Each eigenvector is assumed to be a row matrix of the form

$$l^s = \left\{ l_1, l_2, l_3, l_4, l_5, l_6, l_7, l_8 \right\} \tag{C.4}$$

The components of each eigenvector are found by multiplying equation C.4 through equation C.3 once for each eigenvalue λ_s'.

If $\lambda_1 = 0$, the following equations are obtained by multiplying l^1 through equation C.3:

$$l_6 = l_7 = l_8 = 0$$
$$l_1 + \upsilon l_2 = 0 \quad \text{or} \quad l_1 = -\upsilon l_2$$
$$K_s^2 l_5 = 0$$
$$l_3 + \upsilon l_4 = 0 \quad \text{or} \quad l_3 = -\upsilon l_4$$

Therefore, the desired eigenvector is seen to be

$$l' = \left\{ -\upsilon l_2, l_2, -\upsilon l_4, l_4, 0, 0, 0, 0 \right\} \tag{C.5}$$

Assuming that the arbitrary coefficients $l_2 = 1$ and $l_4 = 0$, the eigenvector corresponding to λ_1 is seen to be

$$l' = \left\{ -\upsilon, 1, 0, 0, 0, 0, 0, 0 \right\} \tag{C.6}$$

It is noted that the eigenvalues λ_1 and λ_2 are both zero. An independent eigenvector corresponding to λ_2

may be found from equation C.5 if the arbitrary coefficients are defined as $l_2 = 0$ and $l_4 = 1$. This eigenvector may be written

$$l^2 = \left\{ 0, 0, -v, 1, 0, 0, 0, 0 \right\} \tag{C.7}$$

If $\lambda_3 = 1$, the following equations are obtained by multiplying l^3 through equation C.3:

$$l_1 + l_6 = 0$$
$$l_3 + l_8 = 0$$
$$l_2 = l_4 = 0$$
$$l_5 + l_7 = 0$$
$$l_1 + v l_2 + l_6 = 0$$
$$K_s^2 l_5 + l_7 = 0$$
$$l_3 + v l_4 + l_8 = 0$$

The solution of these equations leads to the relations

$$-l_1 = l_6$$
$$-l_3 = l_8$$
$$l_2 = l_4 = l_5 = l_7 = 0$$

Therefore, the desired eigenvector is seen to be

$$l^3 = \left\{ l_6, 0, l_8, 0, 0, -l_6, 0, -l_8 \right\} \tag{C.8}$$

Assuming that the arbitrary coefficients $l_6 = 1$ and $l_8 = 0$, the eigenvector corresponding to λ_3 is seen to be

$$l^3 = \left\{ 1, 0, 0, 0, 0, -1, 0, 0 \right\} \tag{C.9}$$

As with λ_1 and λ_2, it is seen that λ_3 and λ_5 are duplicate eigenvalues. An independent eigenvector corresponding to $\lambda_5 = 1$ may be found from equation C.8 if the arbitrary coefficients are defined as $l_6 = 0$ and $l_8 = 1$. This eigenvector may now be written

$$l^5 = \left\{ 0, 0, 1, 0, 0, 0, 0, -1 \right\} \quad \text{(C.10)}$$

If $\lambda_4 = -1$, the following equations are obtained by multiplying 1^4 through equation C.3:

$$-l_1 + l_6 = 0$$
$$-l_3 + l_8 = 0$$
$$l_2 = l_4 = 0$$
$$-l_5 + l_7 = 0$$
$$l_1 + \upsilon l_2 - l_6 = 0$$
$$K_5^2 l_5 - l_7 = 0$$
$$l_3 + \upsilon l_4 - l_8 = 0$$

The solution of these equations leads to the relations

$$l_1 = l_6$$
$$l_3 = l_8$$
$$l_2 = l_4 = l_5 = l_7 = 0$$

Therefore, this eigenvector is seen to be of the form

$$l^4 = \left\{ l_6, 0, l_8, 0, 0, l_6, 0, l_8 \right\} \quad \text{(C.11)}$$

Assuming the arbitrary coefficients $l_6 = 1$ and $l_8 = 0$, the eigenvector corresponding to λ_4 is seen to be

$$l^4 = \left\{ 1, 0, 0, 0, 0, 1, 0, 0 \right\} \quad \text{(C.12)}$$

Again, λ_4 and λ_6 are seen to be duplicate eigenvalues. An independent eigenvector corresponding to $\lambda_6 = -1$ may be found from equation C.11 if the arbitrary coefficients are defined as $l_6 = 0$ and $l_8 = 1$. This eigenvector may now be written

$$l^6 = \{0, 0, 1, 0, 0, 0, 0, 1\} \qquad \text{(C.13)}$$

If $\lambda_7 = K_s$, the following equations are obtained by multiplying l^7 through equation C.3:

$$K_s l_1 + l_6 = 0$$
$$K_s l_2 = 0$$
$$K_s l_3 + l_8 = 0$$
$$K_s l_4 = 0$$
$$K_s l_5 + l_7 = 0$$
$$l_1 + v l_2 + K_s l_6 = 0$$
$$K_s^2 l_5 + K_s l_7 = 0$$
$$l_3 + v l_4 + K_s l_8 = 0$$

The solution of these equations leads to the relations

$$l_7 = -K_s l_5$$
$$l_1 = l_2 = l_3 = l_4 = l_6 = l_8 = 0$$

Therefore, if the arbitrary coefficient is assumed to be $l_5 = 1$, the required eigenvector may be written

$$l^7 = \{0, 0, 0, 0, 1, 0, -K_s, 0\} \qquad \text{(C.14)}$$

If $\lambda_8 = -K_s$, the following relations are obtained by multiplying l^8 through equation C.3:

$$-K_s l_1 + l_6 = 0$$
$$-K_s l_2 = 0$$
$$-K_s l_3 + l_8 = 0$$
$$-K_s l_4 = 0$$
$$-K_s l_5 + l_7 = 0$$
$$l_1 + v l_2 - K_s l_6 = 0$$
$$K_s^2 l_5 - K_s l_7 = 0$$
$$l_3 + v l_4 - K_s l_8 = 0$$

The solution of these equations leads to the relations

$$l_7 = K_s l_5$$
$$l_1 = l_2 = l_3 = l_4 = l_6 = l_8 = 0$$

Therefore, if the arbitrary coefficient is assumed to be $l_5 = 1$, the required eigenvector may be written

$$l^8 = \{0, 0, 0, 0, 1, 0, K_s, 0\} \qquad (C.15)$$

The transformation matrix whose rows consist of the eigenvectors l^s may now be written

$$T = \begin{bmatrix} -v & 1 & 0 & 0 & 0 & 0 & 0 & 0 \\ 0 & 0 & -v & 1 & 0 & 0 & 0 & 0 \\ 1 & 0 & 0 & 0 & 0 & -1 & 0 & 0 \\ 1 & 0 & 0 & 0 & 0 & 1 & 0 & 0 \\ 0 & 0 & 1 & 0 & 0 & 0 & 0 & -1 \\ 0 & 0 & 1 & 0 & 0 & 0 & 0 & 1 \\ 0 & 0 & 0 & 0 & 1 & 0 & -K_s & 0 \\ 0 & 0 & 0 & 0 & 1 & 0 & K_s & 0 \end{bmatrix} \qquad (C.16)$$

Solution of Characteristic Equations for $\phi = 0$ and $\phi = \pi$

Along the boundaries $\phi = 0$ and $\phi = \pi$, the quantities Y_i defined by equations ~~4.2~~ become indeterminate. A solution for these quantities and the physical variables is determined below for points along these boundaries.

Since $(\mathrm{ctn}\,\phi)_{\phi=0} = \infty$ and $(\mathrm{ctn}\,\phi)_{\phi=\pi} = -\infty$, it is seen from equation 4.2 that

$$\begin{aligned} \dot{u} &\equiv 0 \\ n_\phi &\equiv n_\theta \\ \varepsilon\dot{\beta}_\phi &\equiv 0 \\ m_\phi &\equiv m_\theta \\ q_{b\phi} &\equiv 0 \end{aligned} \tag{C.17}$$

if the quantities Y_i are to remain bounded.

From equations C.17 it follows that

$$\begin{aligned} \dot{u}_{,\tau} &\equiv 0 \\ \dot{\beta}_{\phi,\tau} &\equiv 0 \\ q_{b\phi,\tau} &\equiv 0 \end{aligned} \tag{C.18}$$

at the points $\phi = 0$ and $\phi = \pi$.

Using the relations given by C.17 and C.18, equations 4.10 may be written in the form

$$\begin{aligned} n_{\phi,\tau} &= (1+\nu)(Y_1 + \dot{w}) \\ m_{\phi,\tau} &= (1+\nu)Y_3 \\ n_{\phi,\phi} - \dot{u}_{,\phi} + n_{\phi,\tau} &= \nu Y_1 - Y_2 + (1+\nu)\dot{w} - P \end{aligned} \tag{C.19}$$

$$-n_{\phi,\phi} - \dot{u}_{,\phi} + n_{\phi,\tau} = \nu Y_1 + Y_2 + (1+\nu)\dot{w} + P$$

$$m_{\phi,\phi} - \varepsilon\dot{\beta}_{\phi,\phi} + m_{\phi,\tau} = \nu Y_3 - Y_4$$

$$-m_{\phi,\phi} - \varepsilon\dot{\beta}_{\phi,\phi} + m_{\phi,\tau} = \nu Y_3 + Y_4$$

$$q_{b\phi,\phi} - K_s\dot{w}_{,\phi} - \dot{w}_{,\tau} = -Y_5 + 2n_\phi - Q$$

$$-q_{b\phi,\phi} - K_s\dot{w}_{,\phi} + \dot{w}_{,\tau} = Y_5 - 2n_\phi + Q$$

Assuming that the radial load is either prescribed or defined as a function of the physical variables, equations C.19 can be solved for the eight unknowns Y_1, Y_2, Y_3, Y_4, Y_5, n_ϕ, m_ϕ, and $\dot{w}$. On performing this solution, it is seen that

$$\begin{aligned}
Y_1 &= \dot{u}_{,\phi} \\
Y_2 &= -n_{\phi,\phi} - P \\
Y_3 &= \varepsilon\dot{\beta}_{\phi,\phi} \\
Y_4 &= -m_{\phi,\phi} \\
Y_5 &= 2n_\phi - Q - q_{b\phi,\phi} + \dot{w}_{,\tau} \\
\dot{w}_{,\phi} &= 0 \\
n_{\phi,\tau} &= (1+\nu)(Y_1 + \dot{w}) \\
m_{\phi,\tau} &= (1+\nu)Y_3
\end{aligned} \tag{C.20}$$

Using the last two of equations C.20, the various derivatives with respect to ϕ on the right side of equations C.20 can be determined.

APPENDIX D

MEMBRANE - CHARACTERISTIC COMPUTER PROGRAM

General

The detailed development and FORTRAN listings for the membrane-characteristic computer program are given in this appendix.

The program is written in the FORTRAN IV language and, as listed, can be run on the UNIVAC 1107 computer.

The main program is named SHLWAV. The subroutines NONE, NGEN, NLST, DISPLD, and OUTPUT are used to carry out repetitive operations in the main program.

Program Description

The program carries out the method of characteristics analysis for the response of a spherical shell impacting an elastic surface. The computational procedure is as described for the membrane theory solution in Chapter IV.

A detailed flow chart for the main program, SHLWAV, is given in Figure 49. The computation of the various problem variables is carried out with the use of the subroutines NONE, NGEN, NLST, and DISPLD. Detailed flow charts for these subroutines are given in Figures 50 to 53.

The desired results are written using the OUTPUT

Figure 49. Detailed Flow Chart--SHLWAV Program

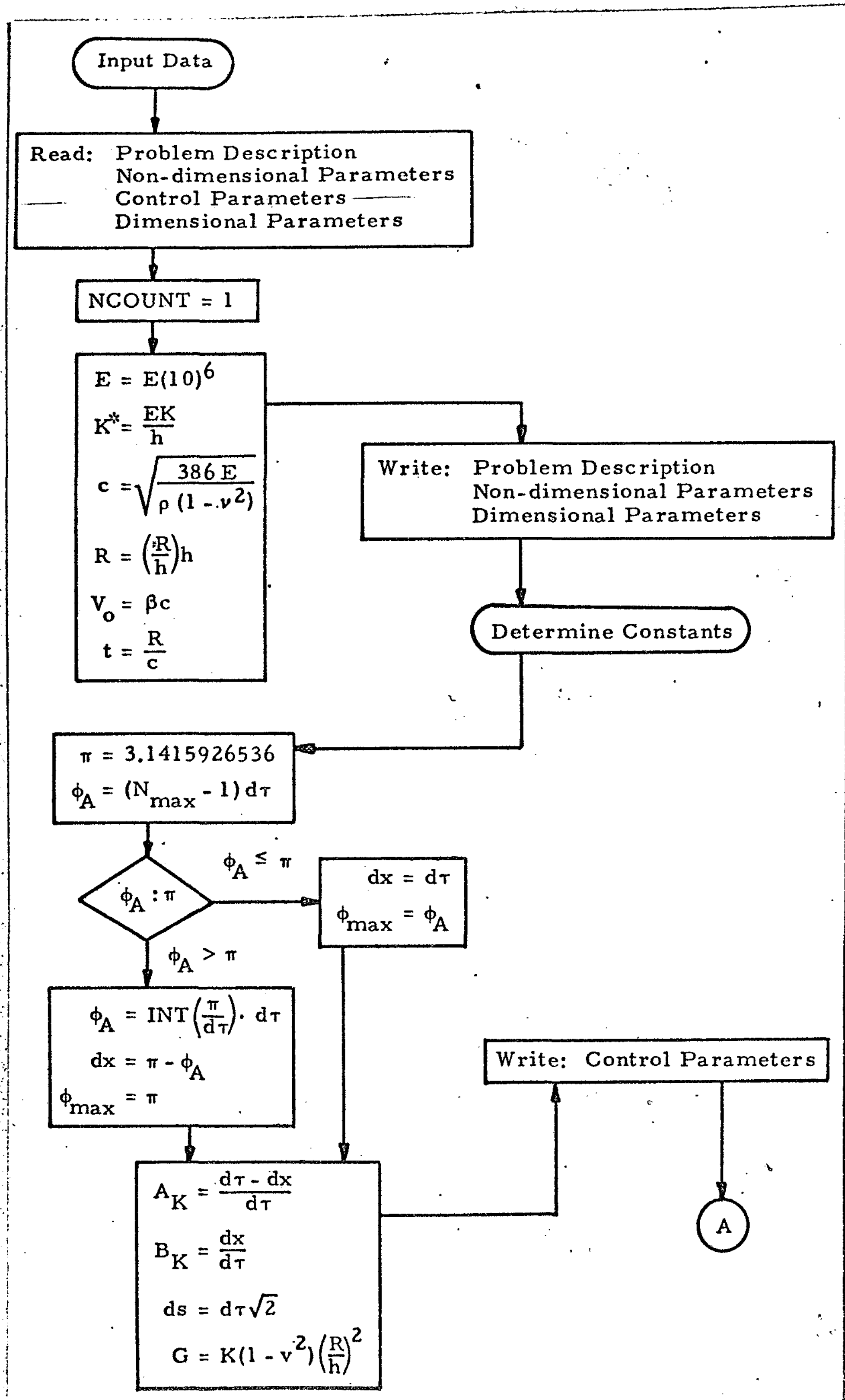

Input Data
Read: Problem Description
Non-dimensional Parameters
Control Parameters
Dimensional Parameters
NCOUNT = 1
$E = E(10)^6$
$K^* = \frac{EK}{h}$
$c = \sqrt{\frac{386\,E}{\rho\,(1-\nu^2)}}$
$R = \left(\frac{R}{h}\right)h$
$V_o = \beta c$
$t = \frac{R}{c}$
Write: Problem Description
Non-dimensional Parameters
Dimensional Parameters
Determine Constants
$\pi = 3.1415926536$
$\phi_A = (N_{max} - 1)\,d\tau$
$\phi_A : \pi$
$\phi_A \leq \pi$
$dx = d\tau$
$\phi_{max} = \phi_A$
$\phi_A > \pi$
$\phi_A = \mathrm{INT}\left(\frac{\pi}{d\tau}\right) \cdot d\tau$
$dx = \pi - \phi_A$
$\phi_{max} = \pi$
$A_K = \frac{d\tau - dx}{d\tau}$
$B_K = \frac{dx}{d\tau}$
$ds = d\tau\sqrt{2}$
$G = K(1 - \nu^2)\left(\frac{R}{h}\right)^2$
Write: Control Parameters
A

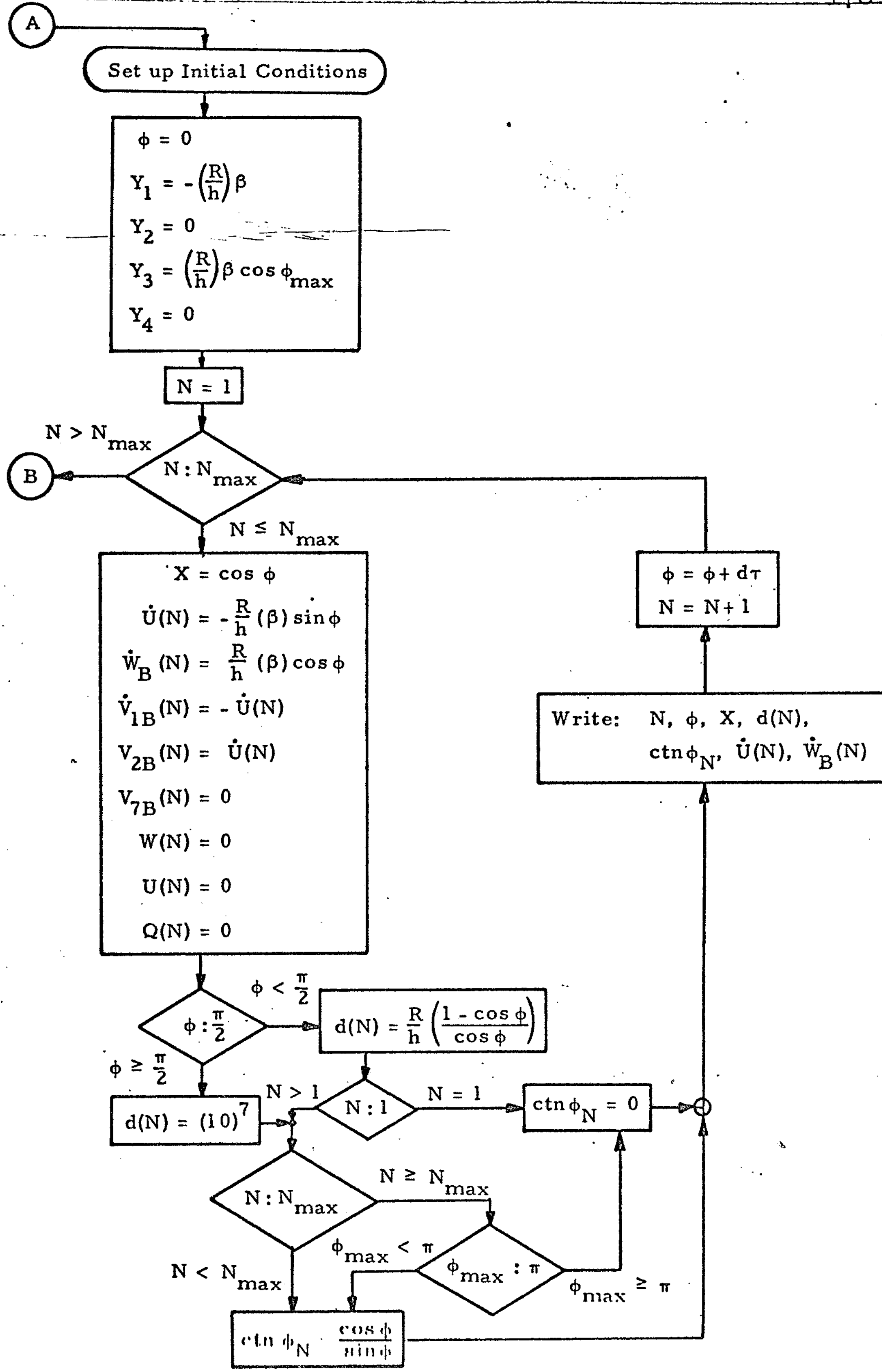
A
Set up Initial Conditions
$\phi = 0$
$Y_1 = -\left(\frac{R}{h}\right)\beta$
$Y_2 = 0$
$Y_3 = \left(\frac{R}{h}\right)\beta \cos\phi_{max}$
$Y_4 = 0$
$N = 1$
$N > N_{max}$
B
$N : N_{max}$
$N \leq N_{max}$
$X = \cos\phi$
$\dot{U}(N) = -\frac{R}{h}(\dot{\beta})\sin\phi$
$\dot{W}_B(N) = \frac{R}{h}(\beta)\cos\phi$
$\dot{V}_{1B}(N) = -\dot{U}(N)$
$V_{2B}(N) = \dot{U}(N)$
$V_{7B}(N) = 0$
$W(N) = 0$
$U(N) = 0$
$Q(N) = 0$
$\phi = \phi + d\tau$
$N = N + 1$
Write: $N, \phi, X, d(N),$
$\text{ctn}\,\phi_N, \dot{U}(N), \dot{W}_B(N)$
$\phi < \frac{\pi}{2}$
$\phi : \frac{\pi}{2}$
$d(N) = \frac{R}{h}\left(\frac{1-\cos\phi}{\cos\phi}\right)$
$\phi \geq \frac{\pi}{2}$
$N > 1$
$N : 1$
$N = 1$
$\text{ctn}\,\phi_N = 0$
$d(N) = (10)^7$
$N \geq N_{max}$
$N : N_{max}$
$\phi_{max} < \pi$
$\phi_{max} : \pi$
$N < N_{max}$
$\phi_{max} \geq \pi$
$\text{ctn}\,\phi_N = \frac{\cos\phi}{\sin\phi}$

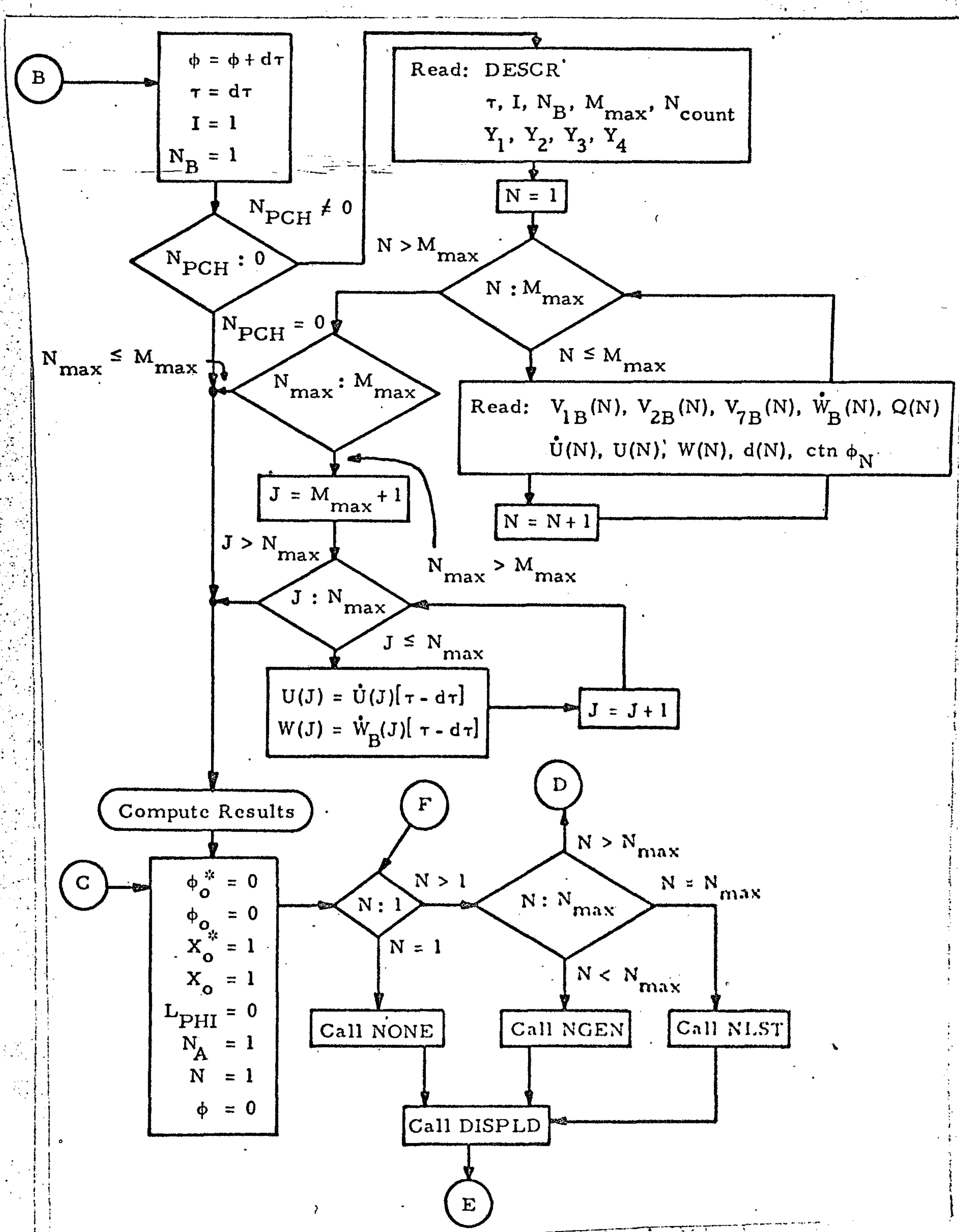

B
φ = φ + dτ
τ = dτ
I = 1
N_B = 1
N_PCH : 0
N_PCH ≠ 0
N_PCH = 0
Read: DESCR
τ, I, N_B, M_max, N_count
Y_1, Y_2, Y_3, Y_4
N = 1
N > M_max
N : M_max
N ≤ M_max
Read: V_1B(N), V_2B(N), V_7B(N), Ẇ_B(N), Q(N)
U̇(N), U(N), W(N), d(N), ctn φ_N
N = N + 1
N_max ≤ M_max
N_max : M_max
N_max > M_max
J = M_max + 1
J > N_max
J : N_max
J ≤ N_max
U(J) = U̇(J)[τ - dτ]
W(J) = Ẇ_B(J)[τ - dτ]
J = J + 1
Compute Results
C
φ_o* = 0
φ_o = 0
X_o* = 1
X_o = 1
L_PHI = 0
N_A = 1
N = 1
φ = 0
F
N : 1
N > 1
N = 1
D
N > N_max
N : N_max
N = N_max
N < N_max
Call NONE
Call NGEN
Call NLST
Call DISPLD
E

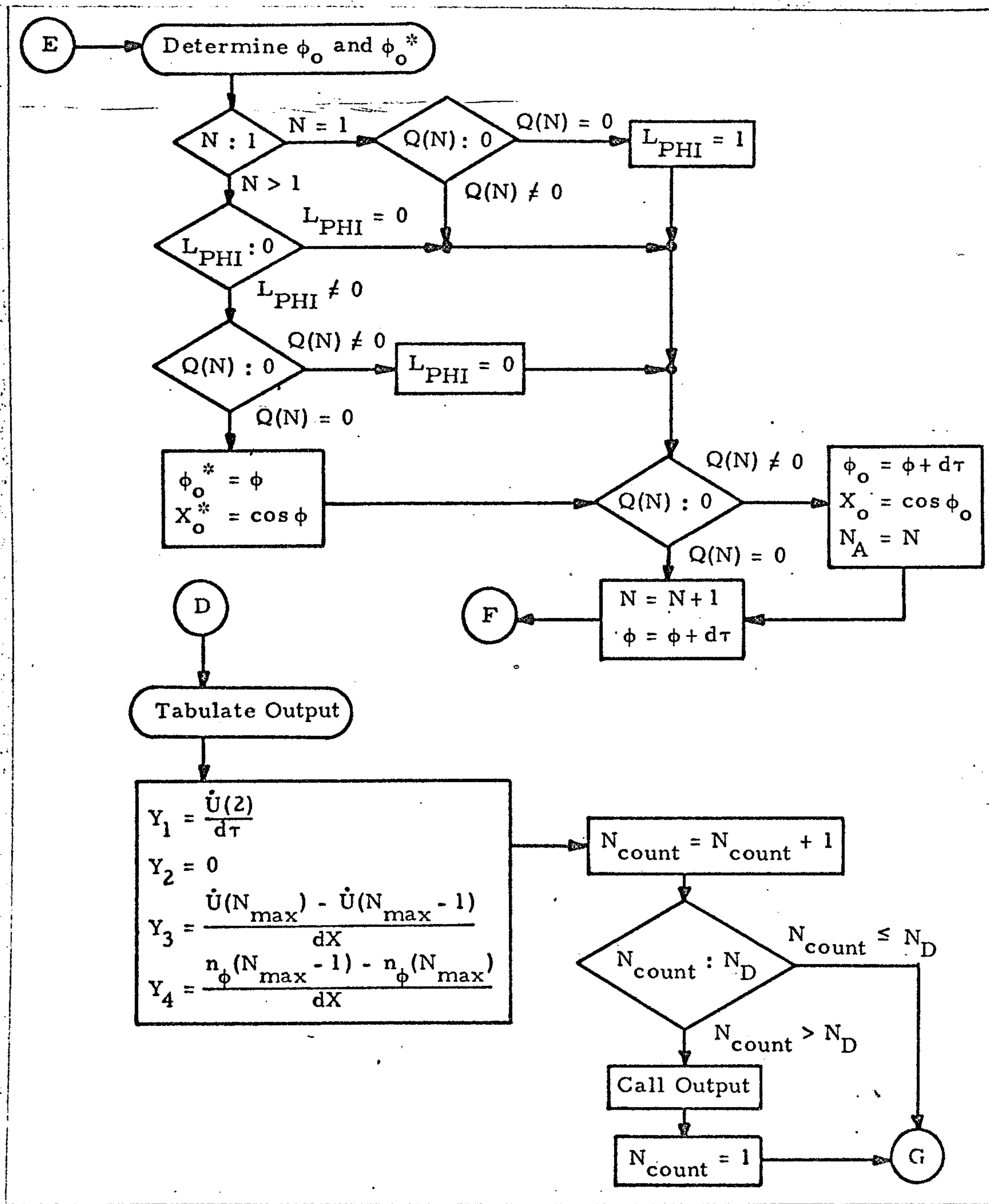
E
Determine ϕ_o and ϕ_o^*
N : 1
N = 1
N > 1
Q(N) : 0
Q(N) = 0
Q(N) ≠ 0
$L_{PHI} = 1$
$L_{PHI} : 0$
$L_{PHI} = 0$
$L_{PHI} \neq 0$
Q(N) : 0
Q(N) ≠ 0
$L_{PHI} = 0$
Q(N) = 0
$\phi_o^* = \phi$
$X_o^* = \cos\phi$
Q(N) : 0
Q(N) ≠ 0
$\phi_o = \phi + d\tau$
$X_o = \cos\phi_o$
$N_A = N$
Q(N) = 0
N = N + 1
$\phi = \phi + d\tau$
F
D
Tabulate Output
$Y_1 = \frac{\dot{U}(2)}{d\tau}$
$Y_2 = 0$
$Y_3 = \frac{\dot{U}(N_{max}) - \dot{U}(N_{max} - 1)}{dX}$
$Y_4 = \frac{n_\phi(N_{max} - 1) - n_\phi(N_{max})}{dX}$
$N_{count} = N_{count} + 1$
$N_{count} : N_D$
$N_{count} \le N_D$
$N_{count} > N_D$
Call Output
$N_{count} = 1$
G

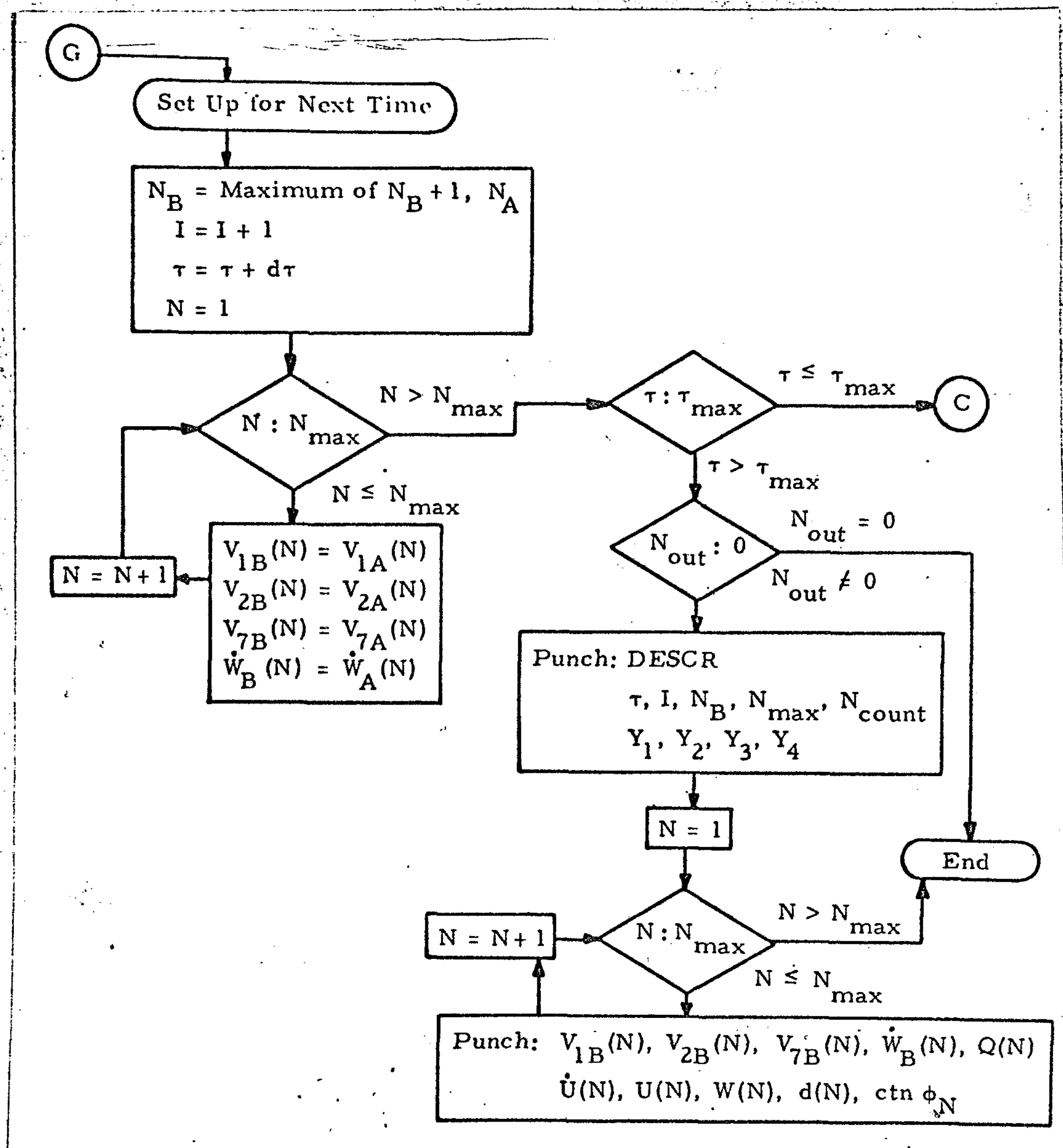
G
Set Up for Next Time
N_B = Maximum of $N_B + 1$, N_A
$I = I + 1$
$\tau = \tau + d\tau$
$N = 1$
$N : N_{max}$
$N > N_{max}$
$N \le N_{max}$
$V_{1B}(N) = V_{1A}(N)$
$V_{2B}(N) = V_{2A}(N)$
$V_{7B}(N) = V_{7A}(N)$
$\dot{W}_B(N) = \dot{W}_A(N)$
$N = N + 1$
$\tau : \tau_{max}$
$\tau \le \tau_{max}$
C
$\tau > \tau_{max}$
$N_{out} : 0$
$N_{out} = 0$
$N_{out} \ne 0$
Punch: DESCR
τ, I, N_B, N_{max}, N_{count}
Y_1, Y_2, Y_3, Y_4
$N = 1$
End
$N : N_{max}$
$N > N_{max}$
$N \le N_{max}$
$N = N + 1$
Punch: $V_{1B}(N)$, $V_{2B}(N)$, $V_{7B}(N)$, $\dot{W}_B(N)$, Q(N)
$\dot{U}(N)$, U(N), W(N), d(N), ctn ϕ_N

50

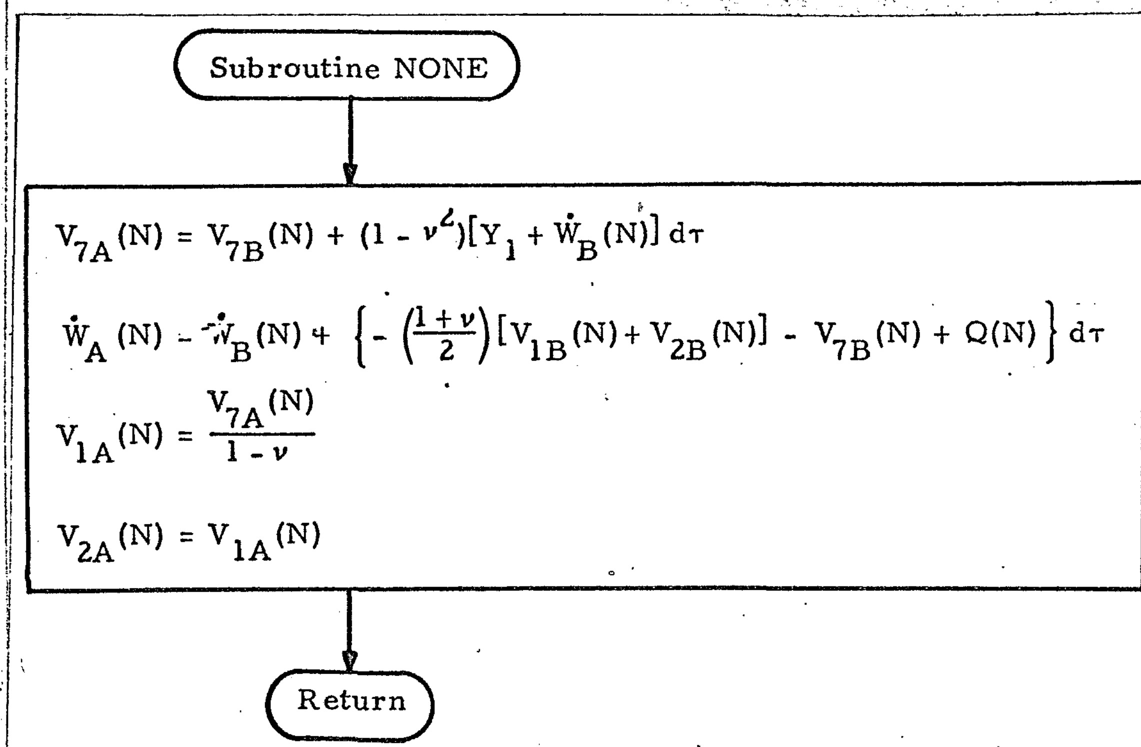

Figure 50. Flow Chart--Subroutine NONE

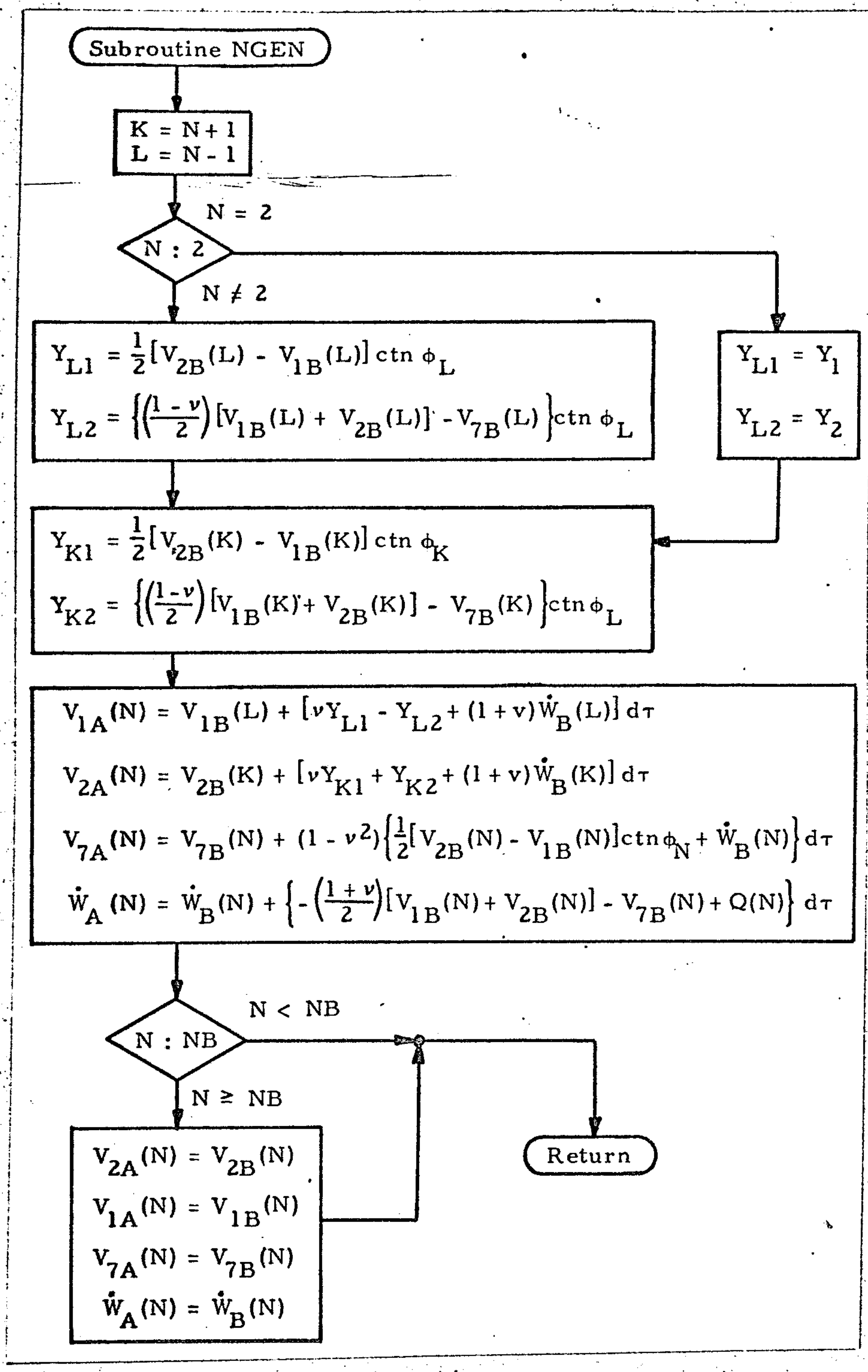

Figure 51. Flow Chart--Subroutine NGEN

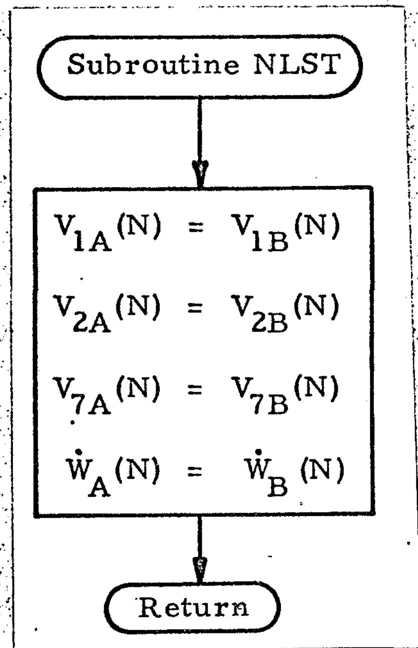

Figure 52. Flow Chart--Subroutine NLST

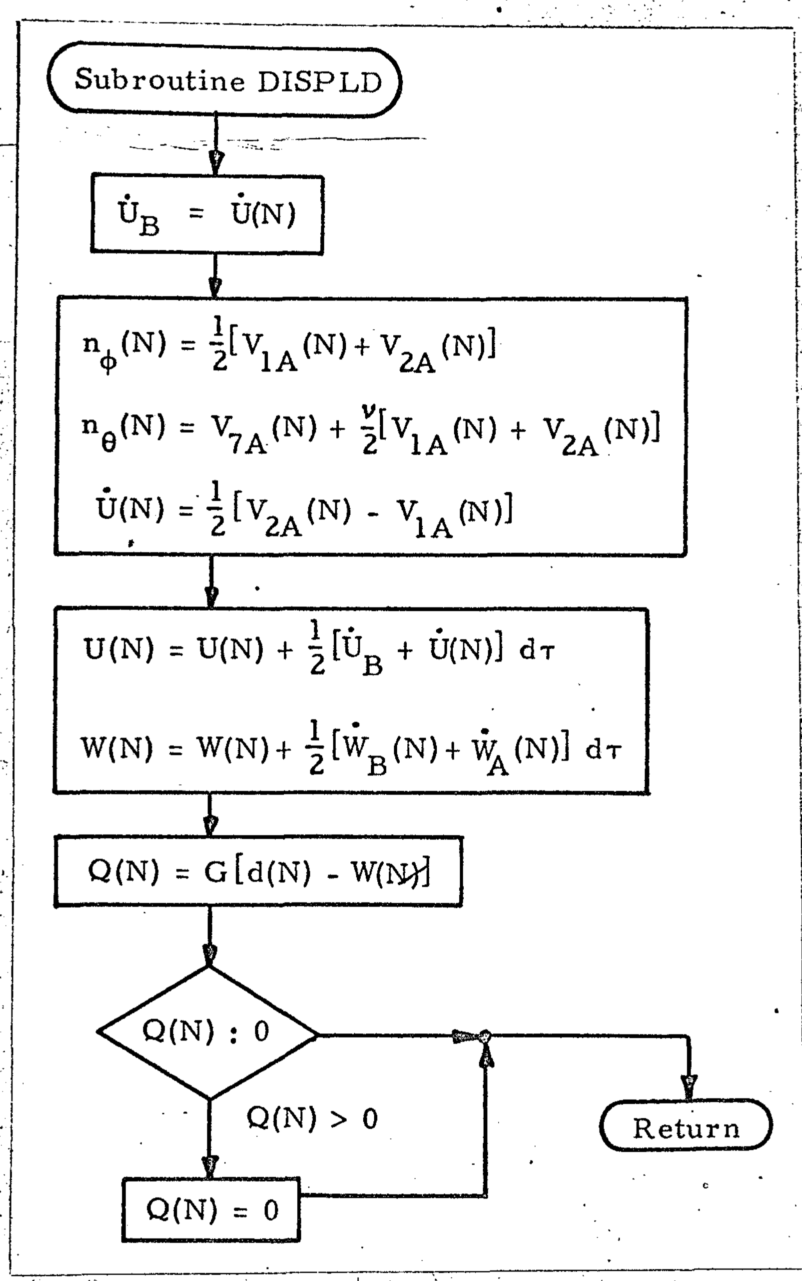

Figure 53. Flow Chart--Subroutine DISPLD

subroutine. This subroutine, whose flow chart is given in Figure 54, causes results to be written for only those grid points through which the initial stress wave has passed.

FORTRAN Listing.

The complete FORTRAN listing for the SHLWAV program and its subroutines is given in Figures 55 to 60.

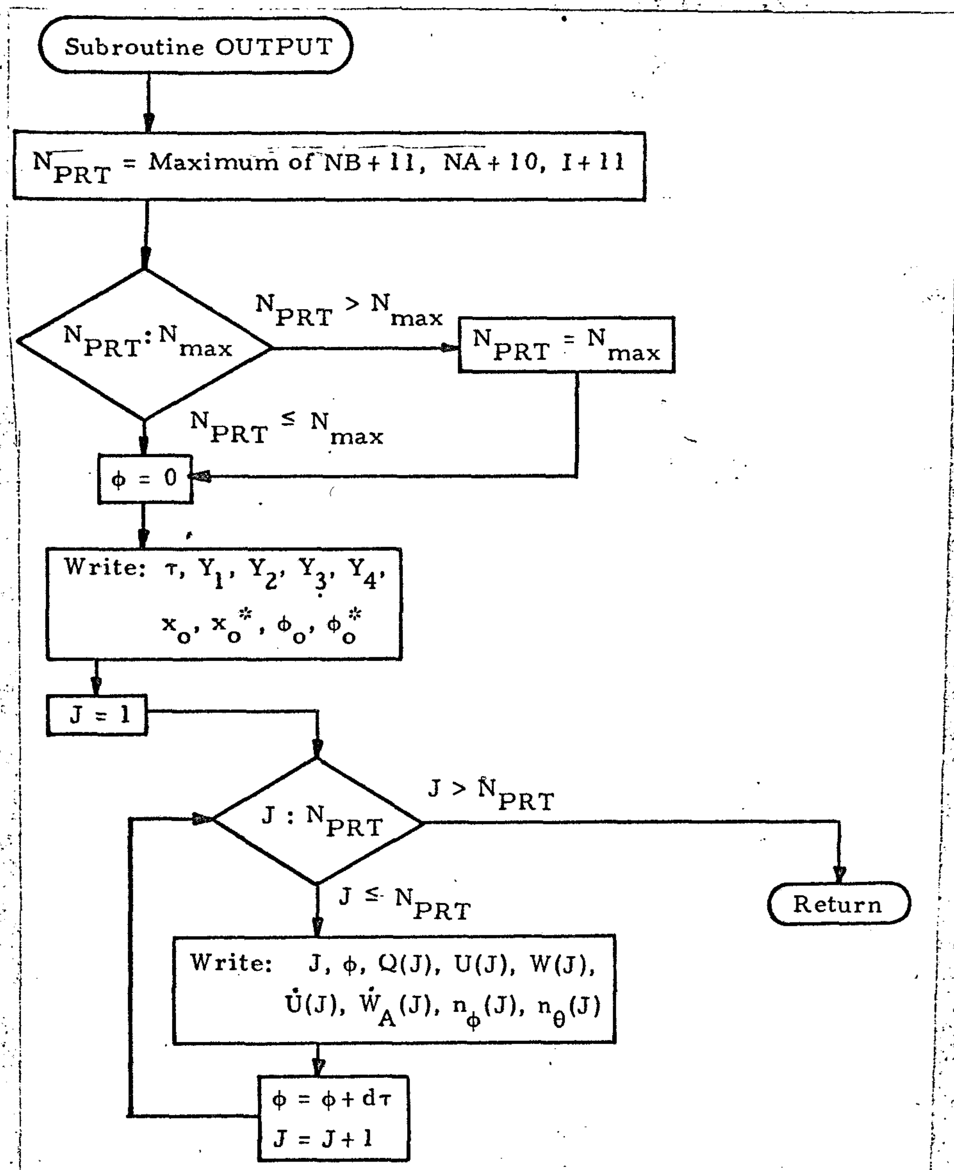

Figure 54. Flow Chart--Subroutine OUTPUT

Figure 55. FORTRAN Listing--SHLWAV Program

```
C     PROGRAM TO COMPUTE RESPONSE OF A
C     SPHERICAL SHELL ON AN ELASTIC SURFACE
C     CHARACTERISTIC - MEMBRANE SOLUTION
C     PROGRAM NAME IS SHLWAV
      DIMENSION V1A(500),V2A(500),V7A(500),WTA(500),V1B(500),V2B(500),
     1V7B(500),WTB(500),Q(500),CTN(500),FNP(500),FNT(500),U(500),W(500),
     2D(500),UT(500) ,DESCR(20)
      INTEGER OUT
      DATA IN,OUT/5,6/
C
C     INPUT DATA
C
C     CARD 1 - PROBLEM DESCRIPTION (COL. 1-80)
C     CARD 2 - NONDIMENSIONAL PARAMETERS (4E8.0)
C              SPRING= NONDIMENSIONAL SURFACE STIFFNESS
C                BETA= NONDIMENSIONAL IMPACT VELOCITY
C                 POI= POISSONS RATIO
C                  RH= SHELL RADIUS/SHELL THICKNESS
C     CARD 3 - CONTROL PARAMETERS (2E8.0,4I8)
C                TMAX= MAXIMUM TIME
C                  DT= TIME INCREMENT
C                NMAX= NODE POINT FOR MAXIMUM SHELL ANGLE
C                  ND= NUMBER OF TIME INCREMENTS BETWEEN PRINTOUTS
C                NPCH= 0 NO PREVIOUS DATA
C                      1 USE PREVIOUS DATA FOR INPUT
C                NOUT= 0 DO NOT PUNCH OUTPUT CARDS
C                      1 PUNCH OUTPUT CARDS
C     CARD 4 - DIMENSIONAL PARAMETERS (3E8.0)
C                   E= SHELL MODULUS OF ELASTICITY (PSI)
C                 RHO= SHELL DENSITY (LB/IN3)
C                   H= SHELL THICKNESS (INCHES)
```

```
 58 READ(IN,94)DESCR
 94 FORMAT(20A4)
    READ(IN,91)SPRING,BETA,POI,RH
 91 FORMAT(4E8.0)
    READ(IN,92)TMAX,DT,NMAX,ND,NPCH,NOUT
 92 FORMAT(2E8.0,4I8)
    READ(IN,120)E,RHO,H
120 FORMAT(3E8.0)
    NCOUNT=1
    E=E*1.E6
    STIFF=E*SPRING/H
    CVEL=SQRT (E*386./(RHO*(1.-POI*POI)))
    RADIUS=RH*H
    VZERO=BETA*CVEL
    TIME=RADIUS/CVEL
    WRITE(OUT,95)
 95 FORMAT(1H1,49HIMPACT OF A SPHERICAL SHELL ON AN ELASTIC SURFACE/1H
   1 ,34HCHARACTERISTIC - MEMBRANE SOLUTION/1H ,15HPROGRAM SHLWAV /)
    WRITE(OUT,97)DESCR
 97 FORMAT(1H ,20A4)
    WRITE(OUT,124)
124 FORMAT(1H0,28HSHELL AND SURFACE PARAMETERS/)
    WRITE(OUT,96)SPRING,BETA,POI,RH
 96 FORMAT(1H ,7HSPRING=,E8.1/1H ,2X,5HBETA=,E8.1/1H ,3X,4HPOI=,F8.6/
   11H ,3X,4HR/H=,F8.2//)
    WRITE(OUT,121)E,RHO,H
121 FORMAT(1H ,19HPHYSICAL PROPERTIES//1H ,22HMODULUS OF ELASTICITY=,
   1E8.1,8H LBS/IN2/1H ,14X,8HDENSITY=,F8.5,10H LBS/IN3/G/1H ,6X,
   216HSHELL THICKNESS=,F8.5,7H INCHES/)
    WRITE(OUT,122)STIFF,RADIUS
```

```
  122 FORMAT(1H ,4X,18HSURFACE STIFFNESS=,E14.7,11H LBS/IN/IN2/1H ,9X,
     113HSHELL RADIUS=,E14.7,7H INCHES/)
      WRITE(OUT,123)TIME,CVEL,VZERO
  123 FORMAT(1H ,2X,20HREAL TIME (SECONDS)=,E14.7,22H * NONDIMENSIONAL T
     1IME//1H ,7X,15HSOUND VELOCITY=,E14.7,14H INCHES/SECOND/1H ,5X,
     217HINITIAL VELOCITY=,E14.7,14H INCHES/SECOND//)
C
C     DETERMINE CONSTANTS
C
      PI=3.1415926536
      NMAX1=NMAX-1
      NMAX2=NMAX-2
      EN1=NMAX1
      PHIA=EN1*DT
      IF(PI-PHIA)30,31,31
   31 DX=DT
      PHIMAX=PHIA
      GO TO 32
   30 NMAX2=PI/DT
      EN2=NMAX2
      PHIA=EN2*DT
      DX=PI-PHIA
      PHIMAX=PI
      NMAX1=NMAX2+1
      NMAX=NMAX1+1
   32 AK=(DT-DX)/DT
      BK=DX/DT
      DS=DT*SQRT (2.)
      G=SPRING*(1.-POI*POI)*RH*RH
      WRITE(OUT,33)NMAX,TMAX,DT,DS,PHIMAX,DX,G
   33 FORMAT(1H ,19HANALYSIS PARAMETERS//1H ,2X,5HNMAX=,I4/1H ,2X,5HTMAX
     1=,F8.3/1H ,4X,3HDT=,F8.5/1H ,4X,3HDS=,F8.5//1H ,7HPHIMAX=,F10.7/1H
     2 ,4X,3HDX=,E14.7              //1H ,5X,2HG=,E14.7//)
```

```
C
C     SET UP INITIAL CONDITIONS
C
      WRITE(OUT,60)
   60 FORMAT(1H ,44HINITIAL CONDITIONS   N(PHI)=N(THETA)=U=W=Q=0//1H ,2X
     1,1HN,4X,3HPHI,7X,10HX=COS(PHI),5X,11HD=RH(1-X)/X,5X,8HCTN(PHI),7X,
     25HDU/DT,10X,5HDW/DT)
      PHI=0.
      Y1=-RH*BETA
      Y2=0.
      Y3=RH*BETA*COS(PHIMAX)
      Y4=0.
      DO 61 N=1,NMAX
      X=COS (PHI)
      UT(N)=-RH*BETA*SIN (PHI)
      WTB(N)=RH*BETA*COS (PHI)
      V1B(N)=-UT(N)
      V2B(N)=UT(N)
      V7B(N)=0.
      W(N)=0.
      U(N)=0.
      Q(N)=0.
      IF(PHI-PI/2.)40,41,41
   40 D(N)=RH*(1.-COS (PHI))/COS (PHI)
      IF(N-1)34,34,35
   34 CTN(N)=0.
      GO TO 36
   41 D(N)=1.E+07
   35 IF(N-NMAX)37,38,38
   38 IF(PHIMAX-PI)37,34,34
   37 CTN(N)=COS (PHI)/SIN (PHI)
```

```
   36 WRITE(OUT,62)N,PHI,X,D(N),CTN(N),UT(N),WTB(N)
   62 FORMAT(1H ,I4,1X,F10.7,5(1X,E14.7))
   61 PHI=PHI+DT
      T=DT
      I=1
      NB=1
  205 IF(NPCH.EQ.0)GO TO 1
      READ(IN,206)DESCR
  206 FORMAT(20A4)
      READ(IN,207)T,I,NB,MMAX,NCOUNT
  207 FORMAT(E13.8,4I4)
      READ(IN,208)Y1,Y2,Y3,Y4
  208 FORMAT(4E13.8)
      DO 209 N=1,MMAX
      READ(IN,210)V1B(N),V2B(N),V7B(N),WTB(N),Q(N)
  210 FORMAT(5E13.8)
  209 READ(IN,210)UT(N),U(N),W(N),D(N),CTN(N)
      IF(NMAX.LE.MMAX)GO TO 1
      N1=MMAX+1
      TT=T-DT
      DO 300 J=N1,NMAX
      U(J)=UT(J)*TT
  300 W(J)=WTB(J)*TT
```

```
C
C     COMPUTE RESULTS
C
    1 PHIJS=0.
      PHIJ=0.
      XJS=1.0
      XJ=1.0
      LPHI=0
      NA=1
      N=1
      PHI=0.
    2 IF(N-1)3,3,4
    4 IF(N-NMAX)5,6,7
    3 CALL NONE(V1A,V2A,V7A,WTA,V1B,V2B,V7B,WTB,Q,CTN,POI,DT,N,Y1)
      GO TO 8
    5 CALL NGEN(V1A,V2A,V7A,WTA,V1B,V2B,V7B,WTB,Q,CTN,POI,DT,DS,N,Y1,
     1Y2,Y3,Y4,I,NB)
      GO TO 8
    6 CALL NLST(V1A,V2A,V7A,WTA,V1B,V2B,V7B,WTB,N)
    8 CALL DISPLD(V1A,V2A,V7A,WTA,WTB,FNP,FNT,UT,U,W,D,Q,POI,G,DT,N)
C
C     DETERMINE PHIZERO AND PHIZERO(STAR)
C
      IF(N.GT.1) GO TO 9
      IF(Q(N).NE.0.) GO TO 10
      LPHI=1
      GO TO 10
    9 IF(LPHI.EQ.0) GO TO 10
```

```
      IF(Q(N).EQ.0.) GO TO 11
      LPHI=0
      GO TO 10
   11 PHIJS=PHI
      XJS=COS(PHI)
   10 IF(Q(N).EQ.0.) GO TO 12
      PHIJ=PHI+DT
      XJ=COS(PHIJ)
      NA=N
   12 N=N+1
      PHI=PHI+DT
      GO TO 2.
C
C     TABULATE OUTPUT
C
    7 Y1=UT(2)/DT
      Y2=0.
      K=NMAX-1
      Y3=(UT(NMAX)-UT(K))/DX
      Y4=(FNP(K)-FNP(NMAX))/DX
      NCOUNT=NCOUNT+1
      IF(NCOUNT.LE.ND)GO TO 70
      CALL OUTPUT(Q,U,W,UT,WTA,FNP,FNT,T,XJ,XJS,PHIJ,PHIJS,Y1,Y2,Y3,Y4,
     1I,NA,NB,DT,NMAX)
      NCOUNT =1
   70 CONTINUE
```

```
C
C     SET UP FOR NEXT TIME
C
      NB=MAX0(NB+1,NA)
      I=I+1
      T=T+DT
      DO 63 N=1,NMAX
      V1B(N)=V1A(N)
      V2B(N)=V2A(N)
      V7B(N)=V7A(N)
   63 WTB(N)=WTA(N)
      IF(T.LE.TMAX) GO TO 1
      IF(NOUT.EQ.0)GO TO 58
      PUNCH 199,DESCR
  199 FORMAT(20A4)
      PUNCH 200,T,I,NB,NMAX,NCOUNT,(DESCR(J),J=1,12)
  200 FORMAT(E13.8,4I4,12A4)
      PUNCH 201,Y1,Y2,Y3,Y4,(DESCR(J),J=1,5)
  201 FORMAT(4E13.8,5A4)
      DO 203 N=1,NMAX
      PUNCH 204,V1B(N),V2B(N),V7B(N),WTB(N),Q(N),(DESCR(J),J=1,3)
  204 FORMAT(5E13.8,3A4)
  203 PUNCH 204,UT(N),U(N),W(N),D(N),CTN(N),(DESCR(J),J=4,6)
      GO TO 58
      END
```

```
      SUBROUTINE NONE(V1A,V2A,V7A,WTA,V1B,V2B,V7B,WTB,Q,CTN,POI,DT,N,Y1)
C
C     COMPUTE RESULTS AT GRID POINT N=1
C
      DIMENSION V1A(1),V2A(1),V7A(1),WTA(1),V1B(1),V2B(1),V7B(1),WTB(1),
     1Q(1),CTN(1)
      V7A(N)=V7B(N)+(1.-POI*POI)*(Y1+WTB(N))*DT
      WTA(N)=WTB(N)+(-0.5*(1.+POI)*(V1B(N)+V2B(N))-V7B(N)+Q(N))*DT
      V1A(N)=V7A(N)/(1.-POI)
      V2A(N)=V1A(N)
      RETURN
      END
```

Figure 56. FORTRAN Listing--Subroutine NONE

```
      SUBROUTINE NGEN(V1A,V2A,V7A,WTA,V1B,V2B,V7B,WTB,Q,CTN,POI,DT,DS,N,
     1Y1,Y2,Y3,Y4,I,NB)
C
C     COMPUTE RESULTS AT GENERAL GRID POINT
C     INCLUDES SPECIAL CASE AT N=2
C
      DIMENSION V1A(1),V2A(1),V7A(1),WTA(1),V1B(1),V2B(1),V7B(1),WTB(1),
     1Q(1),CTN(1)
      K=N+1
      L=N-1
      IF(N.EQ.2)GO TO 1
      YL1=0.5*(V2B(L)-V1B(L))*CTN(L)
      YL2=(0.5*(1.-POI)*(V1B(L)+V2B(L))-V7B(L))*CTN(L)
      GO TO 2
    1 YL1=Y1
      YL2=Y2
    2 YK1=0.5*(V2B(K)-V1B(K))*CTN(K)
      YK2=(0.5*(1.-POI)*(V1B(K)+V2B(K))-V7B(K))*CTN(K)
      V1A(N)=V1B(L)+(POI*YL1-YL2+(1.+POI)*WTB(L))*DT
      V2A(N)=V2B(K)+(POI*YK1+YK2+(1.+POI)*WTB(K))*DT
      V7A(N)=V7B(N)+(1.-POI*POI)*(0.5*(V2B(N)-V1B(N))*CTN(N)+WTB(N))*DT
      WTA(N)=WTB(N)+(-0.5*(1.+POI)*(V1B(N)+V2B(N))-V7B(N)+Q(N))*DT
      IF(N-NB)3,5,5
    5 V2A(N)=V2B(N)
      V1A(N)=V1B(N)
      V7A(N)=V7B(N)
      WTA(N)=WTB(N)
    3 CONTINUE
      RETURN
      END
```

Figure 57. FORTRAN Listing--Subroutine NGEN

```
      SUBROUTINE NLST(V1A,V2A,V7A,WTA,V1B,V2B,V7B,WTB,N)
C
C     COMPUTE RESULTS AT INTERIOR GRID POINT NMAX
C
      DIMENSION V1A(1),V2A(1),V7A(1),WTA(1),V1B(1),V2B(1),V7B(1),WTB(1)
      V1A(N)=V1B(N)
      V2A(N)=V2B(N)
      V7A(N)=V7B(N)
      WTA(N)=WTB(N)
      RETURN
      END
```

Figure 58. FORTRAN Listing--Subroutine NLST

```
      SUBROUTINE DISPLD(V1A,V2A,V7A,WTA,WTB,FNP,FNT,UT,U,W,D,Q,POI,G,DT,
     1N)
C     SOLUTION FOR DISPLACEMENT, STRESS, AND LOAD
C
      DIMENSION V1A(1),V2A(1),V7A(1),WTA(1),WTB(1),FNP(1),FNT(1),UT(1),
     1U(1),W(1),D(1),Q(1)
      UTB=UT(N)
      FNP(N)=0.5*(V1A(N)+V2A(N))
      FNT(N)=V7A(N)+0.5*POI*(V1A(N)+V2A(N))
      UT(N)=0.5*(V2A(N)-V1A(N))
      U(N)=U(N)+(UTB+UT(N))*DT/2.
      W(N)=W(N)+(WTB(N)+WTA(N))*DT/2.
      Q(N)=G*(D(N)-W(N))
      IF(Q(N))1,1,2
    2 Q(N)=0.
    1 RETURN
      END
```

Figure 59. FORTRAN Listing--Subroutine DISPLD

Figure 60. FORTRAN Listing--Subroutine OUTPUT

```
      SUBROUTINE OUTPUT(Q,U,W,UT,WTA,FNP,FNT,T,XJ,XJS,PHIJ,PHIJS,Y1,Y2,
     1Y3,Y4,I,NA,NB,DT,NMAX)
C
C     PRINT SIGNIFICANT RESULTS
C
      DIMENSION Q(1),U(1),W(1),UT(1),WTA(1),FNP(1),FNT(1)
      INTEGER OUT
      DATA IN,OUT/5,6/
      NPRT=MAX0(NB+11,NA+10,I+11)
      IF(NPRT-NMAX)2,2,3
    3 NPRT=NMAX
    2 PHI=0.
      WRITE(OUT,200)T
      WRITE(OUT,201)Y1
      WRITE(OUT,202)Y2
      WRITE(OUT,203)Y3
      WRITE(OUT,204)Y4
      WRITE(OUT,205)XJ,XJS,PHIJ,PHIJS
      WRITE(OUT,206)
      DO 1 J=1,NPRT
      WRITE(OUT,207)J,PHI,Q(J),U(J),W(J),UT(J),WTA(J),FNP(J),FNT(J)
    1 PHI=PHI+DT
```

```
  200 FORMAT(1H1,20HSHELL RESPONSE AT T=,F12.8/)
  201 FORMAT(1H ,5X,21HY1= DUT(1)/DPHI      =,E14.8)
  202 FORMAT(1H ,5X,21HY2=-DNPHI(1)/DPHI    =,E14.8)
  203 FORMAT(1H ,5X,21HY3= DUT(NMAX)/DPHI   =,E14.8)
  204 FORMAT(1H ,5X,21HY4=-DNPHI(NMAX)/DPHI=,E14.8)
  205 FORMAT(1H0,2X,6HXZERO=,E14.7,3X,12HXZERO(STAR)=,E14.7/1H ,8HPHIZER
     1O=,E14.7,1X,14HPHIZERO(STAR)=,E14.7/)
  206 FORMAT(1H ,2X,1HN,4X,3HPHI,8X,7HQ(LOAD),7X,12HU(TANG DISP),3X,
     111HW(RAD DISP),4X,12HUT(TANG VEL),3X,11HWT(RAD VEL),4X,11HN(PHI)FO
     2RCE,3X,13HN(THETA)FORCE)
  207 FORMAT(1H ,I4,F11.8,7E15.8)
      RETURN
      END
```

APPENDIX E

DERIVATION OF SHELL EQUATIONS

General

The equations of motion and force- and moment-displacement relations for a complete, symmetrically loaded spherical shell are derived in this appendix.

The equations thus derived are based on a theory which assumes a thin shell and small deformations. With this theory, the applied loads are considered to be acting on the middle surface of the shell and the effect of transverse normal stress is neglected. Total displacements, including rigid body effects, may be large. However, changes in displacement with respect to shell angle ϕ are assumed to be small.

The equations can be made identical to those used by Naghdi (11) and Prasad (12) if the above assumptions are applied to their more complex theories.

Equations of Motion

The equations of motion for a symmetrically loaded spherical shell have been derived by many authors. However, the derivation is repeated here for completeness.

The infinitesimal element shown in Figure 2 will be used in this derivation. This element has a length $R\,d\phi$ in the meridional direction and $R \sin\phi \, d\theta$ in the circumferential direction.

The equation of motion for forces parallel to may be written as follows:

$$\begin{aligned} &-N_\phi R \sin\phi \, d\theta + \left(N_\phi + \frac{\partial N_\phi}{\partial \phi} d\phi\right)\left[R\sin\phi + \frac{\partial}{\partial\phi}(R\sin\phi)d\phi\right] d\theta \\ &\quad - N_\theta R \, d\phi \, d\theta \cos\phi + Q_\phi R \sin\phi \, d\theta \left(\frac{d\phi}{2}\right) \\ &\quad + \left(Q_\phi + \frac{\partial Q_\phi}{\partial\phi} d\phi\right)\left[R\sin\phi + \frac{\partial}{\partial\phi}(R\sin\phi)d\phi\right] d\theta \left(\frac{d\phi}{2}\right) \\ &\quad + p^* R \, d\phi \, R \sin\phi \, d\theta = \rho h R^2 \sin\phi \, d\phi \, d\theta \frac{\partial^2 u^*}{\partial t^2} \end{aligned} \tag{E.1}$$

Neglecting all terms in which $d\phi$ is of higher than first order and dividing through by $R \sin\phi \, d\phi \, d\theta$, equation E.1 may be written

$$N_{\phi,\phi} + (N_\phi - N_\theta) \operatorname{ctn}\phi + Q_\phi = \rho h R \frac{\partial^2 u^*}{\partial t^2} - R p^* \tag{E.2}$$

The equation of motion for forces parallel to q^* may be written as follows:

$$\begin{aligned} &-Q_\phi R \sin\phi \, d\theta + \left(Q_\phi + \frac{\partial Q_\phi}{\partial\phi} d\phi\right)\left[R\sin\phi + \frac{\partial}{\partial\phi}(R\sin\phi)d\phi\right] d\theta \\ &\quad - N_\theta R \, d\phi \, d\theta \sin\phi - N_\phi R \sin\phi \, d\theta \left(\frac{d\phi}{2}\right) \\ &\quad - \left(N_\phi + \frac{\partial N_\phi}{\partial\phi} d\phi\right)\left[R\sin\phi + \frac{\partial}{\partial\phi}(R\sin\phi)d\phi\right] d\theta \left(\frac{d\phi}{2}\right) \\ &\quad + q^* R \sin\phi \, d\theta \, R \, d\phi = \rho h R \sin\phi \, d\theta \, R \, d\phi \frac{\partial^2 w^*}{\partial t^2} \end{aligned} \tag{E.3}$$

Neglecting all terms in which $d\phi$ is of higher than first order and dividing through by $R \sin\phi \, d\phi \, d\theta$, equation E.3 may be written

$$Q_{\phi,\phi} + Q_\phi \operatorname{ctn}\phi - (N_\phi + N_\theta) = \rho h R \frac{\partial^2 w^*}{\partial t^2} - R q^* \qquad \text{(E.4)}$$

The equation of motion for moments about an axis orthogonal to p^* and q^* is as follows:

$$\begin{aligned} &-\left[Q_\phi R \sin\phi \, d\theta \left(\frac{R d\phi}{2}\right)\right] - \left(Q_\phi + \frac{\partial Q_\phi}{\partial \phi} d\phi\right)\left[R\sin\phi + \frac{\partial R \sin\phi}{\partial \phi} d\phi\right] d\theta \left(\frac{R d\phi}{2}\right) \\ &\quad - M_\theta R \, d\phi \cos\phi \, d\theta - M_\phi R \sin\phi \, d\theta \\ &\quad + \left(M_\phi + \frac{\partial M_\phi}{\partial \phi} d\phi\right)\left[R \sin\phi + \frac{\partial R \sin\phi}{\partial \phi} d\phi\right] d\theta \\ &\quad = \left(\frac{1}{12}\right) \rho R \sin\phi \, d\theta \, h^3 R \, d\phi \, \frac{\partial^2 \beta_\phi}{\partial t^2} \end{aligned} \qquad \text{(E.5)}$$

Neglecting all terms in which $d\phi$ is of higher than first order and dividing through by $R \sin\phi \, d\phi \, d\theta$, equation E.5 may be written

$$M_{\phi,\phi} + (M_\phi - M_\theta) \operatorname{ctn}\phi - R Q_\phi = \frac{1}{12} \rho h^3 R \frac{\partial^2 \beta_\phi}{\partial t^2} \qquad \text{(E.6)}$$

Equations E.2, E.4, and E.6 are seen to be identical to equations 2.1.

Middle Surface Strain-Displacement Relations

The strain-displacement relations for a symmetrically loaded spherical shell may be derived in two steps. First, in this section, strain-displacement relations are determined for elements on the middle surface of the shell.

Second, strain-displacement relations for an arbitrary point, located a distance z from the middle surface, are determined in the next section.

The derivation presented here generally follows that given by Flugge (4:85).

Using quantities shown in Figure 61, the meridional strain is defined as

$$\varepsilon_\phi = \frac{dL_{A'B'} - dL_{AB}}{dL_{AB}} \tag{E.6}$$

where

$$dL_{AB} = R\,d\phi$$

$$dL_{A'B'} = \left\{\left[\left(dL_{AB} + u^*_{,\phi}\,d\phi\right)\left(\frac{R+w^*}{R}\right)\right]^2 + \left(w^*_{,\phi}\,d\phi\right)^2\right\}^{1/2}$$

$$\approx \left(dL_{AB} + u^*_{,\phi}\,d\phi\right)\left(\frac{R+w^*}{R}\right)\left\{1 + \frac{1}{2}\left(\frac{R}{R+w}\right)^2\left(w^*_{,\phi}\right)^2\left(\frac{d\phi}{dL_{AB} + u^*_{,\phi}\,d\phi}\right)^2\right\}$$

Expanding equation E.6,

$$\varepsilon_\phi = \left[1 + \left(\frac{w^* + u^*_{,\phi}}{R}\right) + \frac{w^* u^*_{,\phi}}{R^2}\right]\left(1 + \frac{1}{2}\psi^2\right) - 1 \tag{E.7}$$

where $\psi = \left(\frac{R}{R+w}\right)\left(\frac{w^*_{,\phi}}{R + u^*_{,\phi}}\right)$

If the displacements and rotations are small, it can be assumed that

$$\frac{w^* u^*_{,\phi}}{R^2} \approx 0$$

$$\left(\frac{w^*_{,\phi}}{R}\right)^2 \approx 0 \tag{E.8}$$

Using relations E.8, equation E.7 may be written

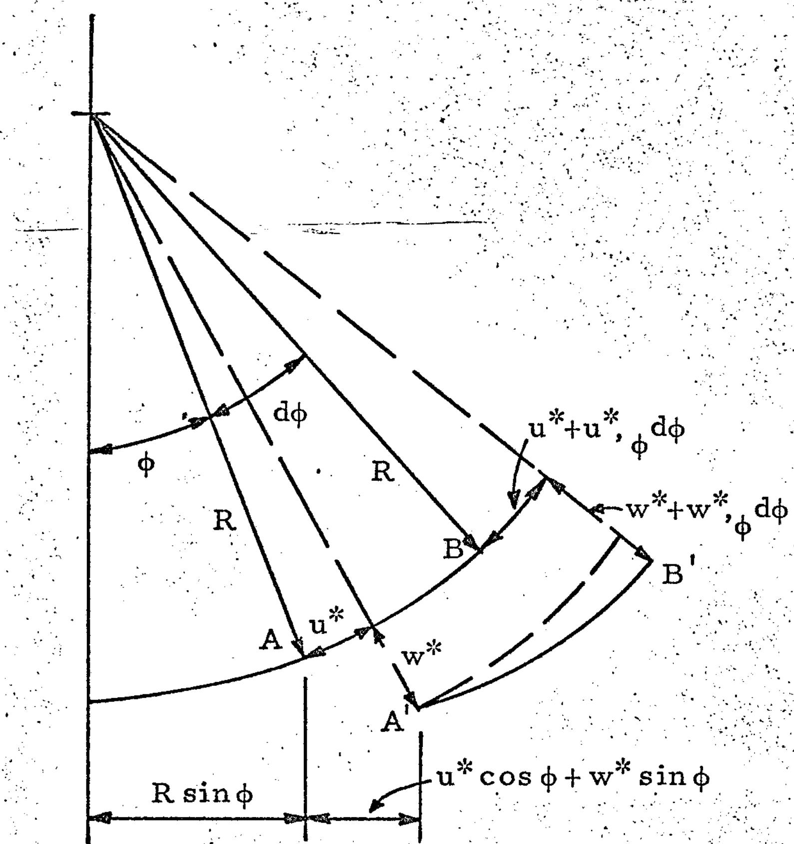

Figure 61. Middle surface deformation along meridian

$$\varepsilon_\phi = \frac{1}{R}\left(w^* + u^*_{,\phi} \right) \tag{E.9}$$

Using quantities shown in Figure 62, the hoop strain is defined as

$$\varepsilon_\theta = \frac{dL_{A'C'} - dL_{AC}}{dL_{AC}} \tag{E.10}$$

where

$$dL_{AC} = R \sin\phi \; d\theta$$

$$dL_{A'C'} = \left(1 + \frac{u^* \cos\phi + w^* \sin\phi}{R \sin\phi} \right) dL_{AC}$$

Expanding equation E.10,

$$\varepsilon_\theta = \frac{1}{R}\left(u^* \operatorname{ctn}\phi + w^* \right) \tag{E.11}$$

The shear strain $\gamma_{\phi\theta} = 0$ due to the symmetry of the system.

General Strain-Displacement Relations

The strain-displacement relations for an arbitrary point located a radial distance z from the middle surface of the shell are now determined. This derivation uses the previously computed middle surface strain-displacement relations and generally follows the procedure given by Flugge (4:315).

The desired strain-displacement relations can be written in the form of equations E.9 and E.11 if u^*, w^*, and R are replaced by u_A, w_A and $R+z$, respectively.

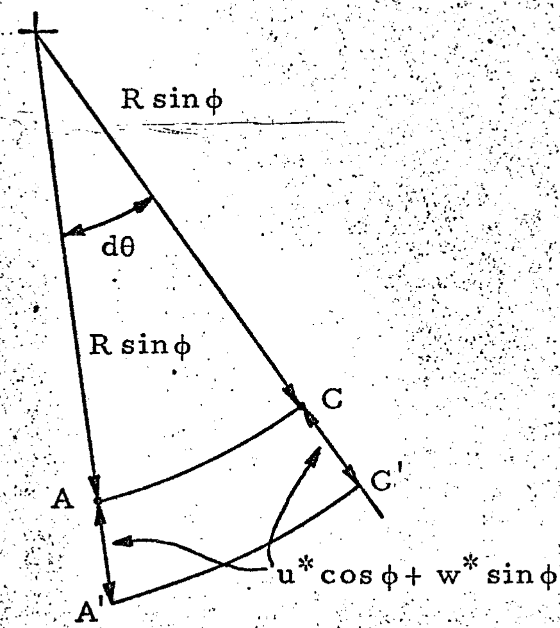

Figure 62. Middle surface deformation along parallel circle

Therefore,

$$\varepsilon_\phi = \frac{w_A + u_{A,\phi}}{R+z}$$

$$\varepsilon_\theta = \frac{u_A \operatorname{ctn}\phi + w_A}{R+z} \qquad \text{(E.12)}$$

$$\gamma_{\phi\theta} = 0$$

In order to use equations E.12, u_A and w_A must be written in terms of the middle surface displacements u^* and w^* and the element rotation β_ϕ. Two assumptions are made when performing this operation.

First, normals to the middle surface before deformation are assumed to remain normal to the middle surface after deformation. In doing this, deformations due to the shear force Q_ϕ are neglected.

Second, the distance z of the arbitrary point from the middle surface of the shell is assumed constant during the deformation. This assumption infers that stresses and strains in the z direction are zero and is valid if the shell is sufficiently thin.

The desired relations between u_A and w_A and u^*, w^*, and β_ϕ are seen from Figure 63 to be

$$u_A = u^*\left(\frac{R+z}{R}\right) + z\beta_\phi$$

$$w_A = w^* \qquad \text{(E.13)}$$

if β_ϕ is assumed to be a small angle.

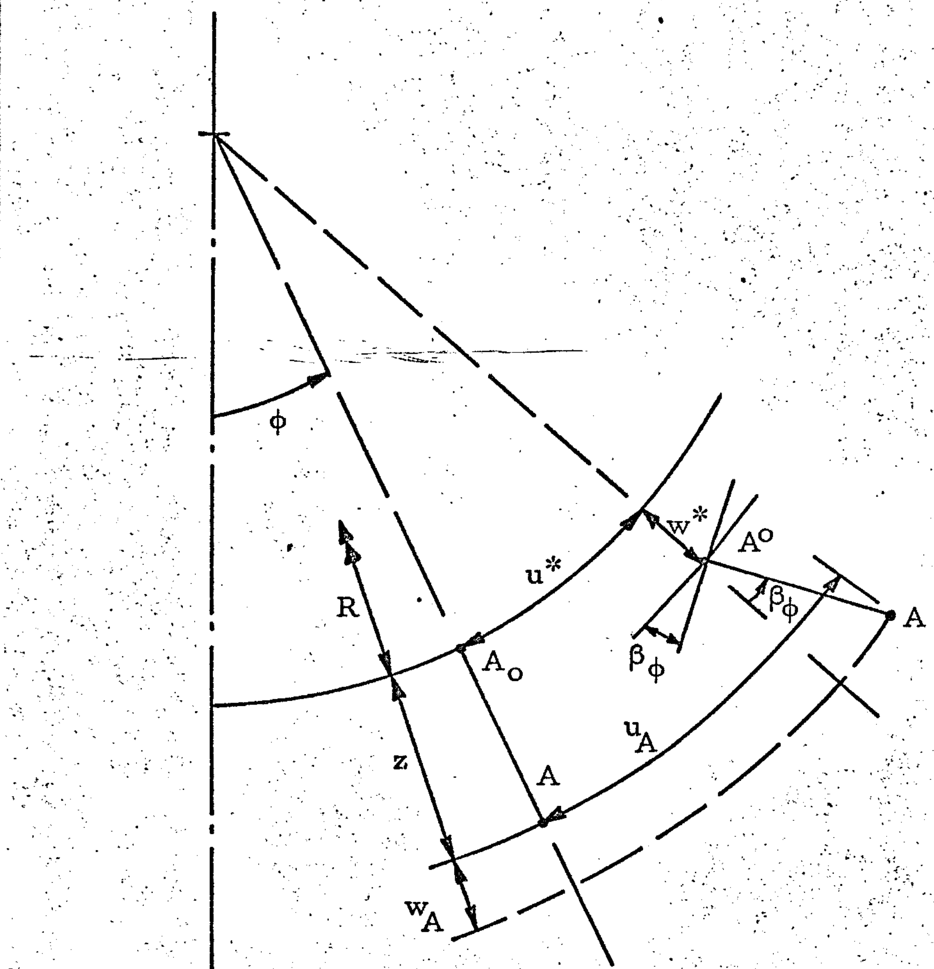

Figure 63. Deformation of arbitrary point along meridian

Substituting equations E.13 into E.12, the desired strain-displacement relations become

$$\varepsilon_\phi = \frac{u^*_{,\phi}}{R} + \frac{w^*}{R+z} + \frac{z\beta_{\phi,\phi}}{R+z}$$

$$\varepsilon_\theta = \frac{u^* \operatorname{ctn}\phi}{R} + \frac{w^*}{R+z} + \frac{z\beta_\phi \operatorname{ctn}\phi}{R+z} \qquad \text{(E.14)}$$

$$\gamma_{\phi\theta} = 0$$

Force- and Moment-Displacement Relations

The force- and moment-displacement relations for a symmetrically loaded spherical shell are now determined. The shell is assumed to be a homogeneous, isotropic body such that the stress-strain relations may be written

$$\sigma_\phi = \left(\frac{E}{1-\upsilon^2}\right)(\varepsilon_\phi + \upsilon\varepsilon_\theta)$$

$$\sigma_\theta = \left(\frac{E}{1-\upsilon^2}\right)(\varepsilon_\theta + \upsilon\varepsilon_\phi) \qquad \text{(E.15)}$$

$$\tau_{\phi\theta} = \frac{E\gamma_{\phi\theta}}{2(1+\upsilon)} = 0$$

Assuming the shell thickness to be h, the normal forces N_ϕ and N_θ can be found from the relations

$$N_\phi R \sin\phi \, d\theta = \int_{-\frac{h}{2}}^{\frac{h}{2}} \sigma_\phi \, dz \, (R+z) \sin\phi \, d\theta$$

$$N_\theta R \, d\phi = \int_{-\frac{h}{2}}^{\frac{h}{2}} \sigma_\theta \, dz \, (R+z) \, d\phi \qquad \text{(E.16)}$$

The shell geometry relations used in these relations can be seen from Figure 64. Substituting equations E.14 and E.15 into equations E.16, the desired normal force-displacement relations are seen to be

$$N_\phi = \left(\frac{Eh}{1-\nu^2}\right)\left(\frac{1}{R}\right)\left[u^*_{,\phi} + \nu u^* \operatorname{ctn}\phi + (1+\nu)w^*\right]$$

$$N_\theta = \left(\frac{Eh}{1-\nu^2}\right)\left(\frac{1}{R}\right)\left[u^* \operatorname{ctn}\phi + \nu u^*_{,\phi} + (1+\nu)w^*\right] \qquad \text{(E.17)}$$

The bending moments M_ϕ and M_θ can be found from the relations

$$M_\phi R \sin\phi \, d\theta = \int_{-\frac{h}{2}}^{\frac{h}{2}} \sigma_\phi \, z \, dz \, (R+z) \sin\phi \, d\theta$$

$$M_\theta R d\phi = \int_{-\frac{h}{2}}^{\frac{h}{2}} \sigma_\theta \, z \, dz \, (R+z) \, d\phi \qquad \text{(E.18)}$$

Substituting equations E.14 and E.15 into equations E.18, the desired moment-displacement relations are seen to be

$$M_\phi = \frac{D}{R}\left\{\beta_{\phi,\phi} + \nu\beta_\phi \operatorname{ctn}\phi + \frac{1}{R}\left(u^*_{,\phi} + \nu u^* \operatorname{ctn}\phi\right)\right\}$$

$$M_\theta = \frac{D}{R}\left\{\beta_\phi \operatorname{ctn}\phi + \nu\beta_{\phi,\phi} + \frac{1}{R}\left(u^* \operatorname{ctn}\phi + \nu u^*_{,\phi}\right)\right\} \qquad \text{(E.19)}$$

where $D = \dfrac{Eh^3}{12(1-\nu^2)}$

If R is large relative to $u^*_{,\phi}$ and $u^* \operatorname{ctn}\phi$, equations E.19 can be written in the form

$$M_\phi = \frac{D}{R}\left(\beta_{\phi,\phi} + \nu\beta_\phi \operatorname{ctn}\phi\right) \qquad \text{(E.20)}$$

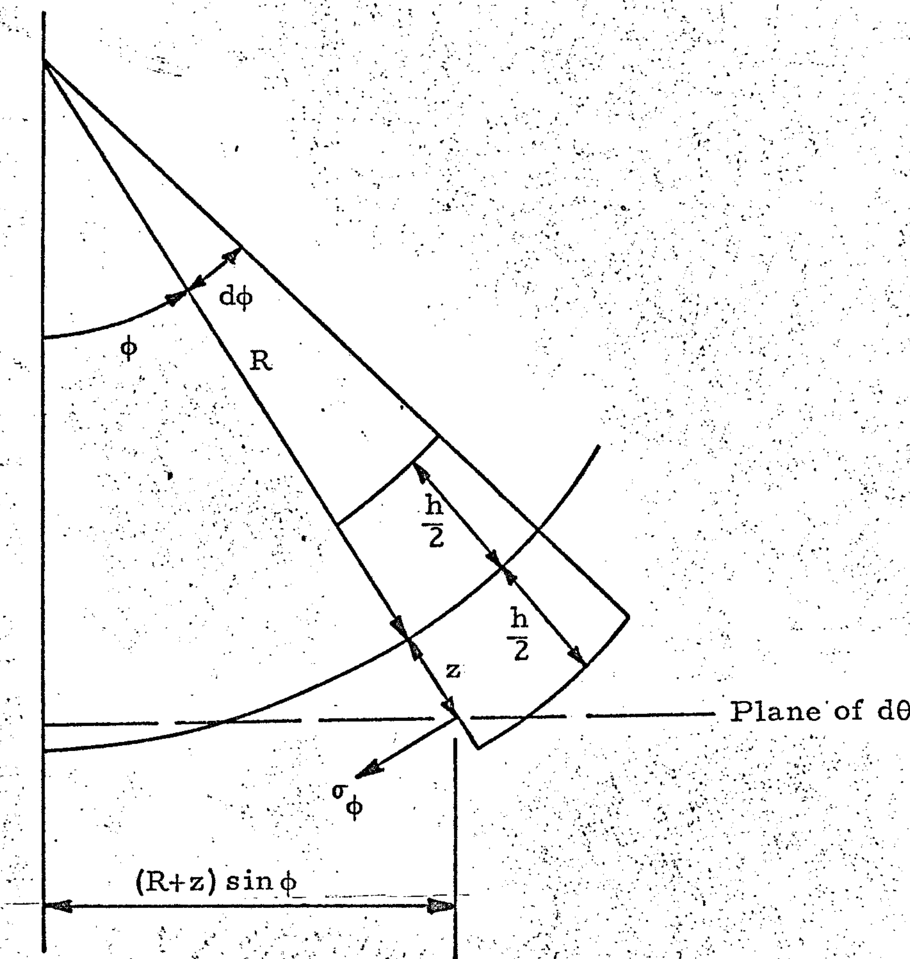

Figure 64. Orientation of σ_ϕ stress

$$M_\theta = \frac{D}{R}\left(\beta_\phi \operatorname{ctn}\phi + \nu\beta_{\phi,\phi}\right)$$

The relation between the shear force Q_ϕ and the shell displacements can be found as follows. As seen from Figure 65, the shear strain due to Q_ϕ is approximately

$$\gamma_{r\phi} = \frac{w^*_{,\phi}}{R} + \beta_\phi \qquad \text{(E.21)}$$

Assuming the shell to be a homogeneous, isotropic body, the shear stress-strain relation may be written

$$\tau_{r\phi} = \frac{E\gamma'_{r\phi}}{2(1+\nu)} \qquad \text{(E.22)}$$

On integrating this shear stress over the thickness of the shell, the desired force-displacement relation is seen to be

$$Q_\phi = \int_{-\frac{h}{2}}^{\frac{h}{2}} \left[\frac{E}{2(1+\nu)}\right]\gamma_{r\phi}\,dz = \left[\frac{Eh}{2(1+\nu)k_s}\right]\left(\frac{w^*_{,\phi}}{R} + \beta_\phi\right) \qquad \text{(E.23)}$$

where k_s = averaging coefficient for non-uniform shear stress distribution.

It is noted that a value of $k_s = \frac{6}{5}$ is used by Prasad (12).

Equations E.17, E.20, and E.23 are seen to be identical to those given in equations 2.3.

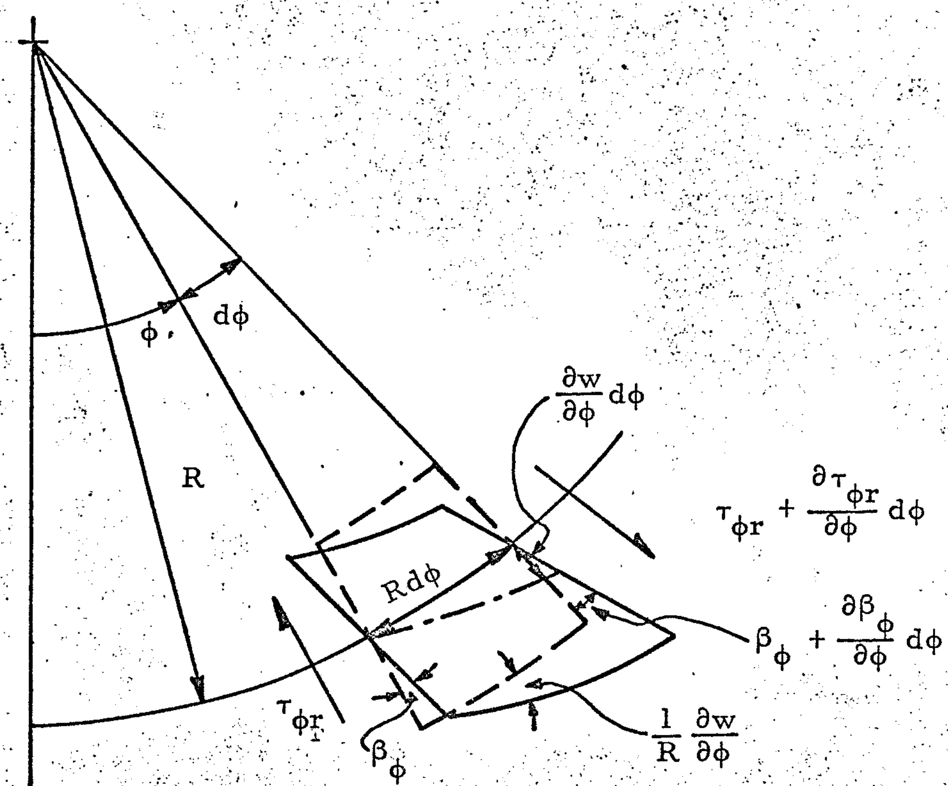

Figure 65. Shear deformation along meridian